MSc. Project

Development of a Satellite Communication System for the Submarines of the Royal Netherlands Navy

G.P. Bouten

Delft University of Technology

TU Delft

Development of a Satellite Communication System for the Submarines of the Royal Netherlands Navy

by

G.P. Bouten

Master thesis submitted to Delft University of Technology
in partial fulfilment of the requirements for the degree of

Master of Science in Aerospace Engineering

Student number:	5177375	
Project duration:	May 2021 - December 2021	
Chair:	Dr. A. Cervone	TU Delft
External examiner:	Dr. B.C. Root	TU Delft
Supervisor:	Dr. S. Speretta	TU Delft
Daily Supervisor:	Ir. B.J.J Stijnen	RNLAF

Cover Image: Royal Netherlands Navy Submarine of the Walrusklasse [12]

TU Delft

Preface

The thesis project that lies before you marks the end of my studies, as I will be graduating from the TU Delft. My studying career starts with a bachelors degree in Mechanical Engineering. After completion I felt indecisive about my future studies. During the subsequent gap year, I was fortunate enough to witness a number of rocket launches from Cape Canaveral Air Force Station in Florida. The events revived an old fascination for rockets and space in general, leading to the decision to study Spaceflight.

Now that I have achieved this milestone it evokes a feeling of satisfaction and accomplishment. However, I want to be careful not to attribute this accomplishment solely to my own abilities, as I have been lucky for most my life. As a true engineer I would like to quantify the role luck plays in my, and everybody's lives:

In 2017 more than 18,300 people applied for NASA's astronaut class, with only 11 positions available [49]. During the selection procedure both skill and luck will play a role. If the assumption is made that the selection is 95% based on skill and 5% on luck, an analysis can be performed to see how much luck the applicants need to become an astronaut. Both the skill and luck level of each applicant get a percentage between 0% and 100%. Simulating the selection procedure 100,000 times yields that the average level of luck required to secure a position as astronaut is 94.79%. To make the role that luck plays even more evident, the average number of astronauts out of the 11 currently selected, that would still become an astronaut when only skill would be considered is 1.59.

For me, this shows the role that luck plays in our lives. When things go right we tend to attribute it to personal skill, and it is hard to acknowledge where we have been lucky. Thus, I have realised, that the wind has been in my back for most of my life. I would, therefore like to thank some people that made me so lucky.

Starting with my family, I would like to thank them for their strong, never ending, support and encouragement during my studies. I am grateful for my girlfriend, Renée, who has always been a great source of enthusiasm and motivation. Furthermore, I would like to thank my RNLAF supervisor Bas Stijnen, especially for his extensive explanations of all matter related to the Ministery of Defence. Last I would like to thank Stefano Speretta for the continues input and guidance during the project.

Gèmo Bouten
Delft, December 2021

Contents

List of Figures v

List of Tables ix

List of Abbreviations 1

Abstract 3

1 Introduction 5
- 1.1 Objective, Questions & Approach . . . 5
- 1.2 Thesis structure. . . . 6

2 Frame of Reference: Netherlands Ministry of Defence 7
- 2.1 The Royal Netherlands Air Force . . . 7
  - 2.1.1 Sectie Space . . . 8
  - 2.1.2 Brik-II Satellite . . . 9
  - 2.1.3 Remote Radio Station . . . 12
- 2.2 The Royal Netherlands Navy . . . 15
  - 2.2.1 Submarines . . . 16

3 Requirements 21
- 3.1 Mission Concept . . . 21
- 3.2 System requirements . . . 22
  - 3.2.1 Similarities Remote Radio Station . . . 24
  - 3.2.2 Prototype Requirements . . . 24

4 Antenna design 27
- 4.1 Link Analysis . . . 27
  - 4.1.1 Signal to Noise Ratio . . . 27
  - 4.1.2 Modulation scheme. . . . 29
  - 4.1.3 Satellite Antenna Gain . . . 30
- 4.2 Orbital Characteristics . . . 31
  - 4.2.1 Standard General Perturbations Satellite Orbit Model 4 . . . 31
  - 4.2.2 Integration Step. . . . 33
  - 4.2.3 Propagation time . . . 33
  - 4.2.4 Ground Segment Location . . . 34
- 4.3 Submarine Antenna . . . 35
- 4.4 Simulation Model . . . 39
- 4.5 Optimisation . . . 40
  - 4.5.1 Results . . . 44
- 4.6 Performance . . . 46

5 Antenna Manufacturing 51
- 5.1 3D Design. . . . 51
- 5.2 Antenna Assembly . . . 53
- 5.3 Impedance Matching . . . 54
  - 5.3.1 L-Network . . . 56

6 Measurements **63**
6.1 Test set-up . . . 63
6.1.1 Radiation Pattern verification . . . 63
6.1.2 Link Strength Verification . . . 64
6.2 Measurement execution . . . 65
6.2.1 Radiation pattern test . . . 65
6.2.2 Link strength measurement . . . 67
6.3 Results . . . 70
6.3.1 Radiation Pattern Measurements Results . . . 70
6.4 Discussion . . . 77
6.5 Leading Requirements Verification . . . 78

7 Conclusion and Recommendations **81**
7.1 Recap . . . 81
7.2 Answer to Sub-Questions . . . 81
7.3 Conclusion . . . 82
7.4 Recommendations and Future Work . . . 83

Appendix 1 **85**

Bibliography **87**

List of Figures

2.1 Position of Sectie Space in the Armed Forces . . . 8
2.2 The Brik-II satellite . . . 10
2.3 Principle of phase difference that enables localisation of radio signals . . . 11
2.4 Store and Forward Payload . . . 11
2.5 Brik-II development consortium . . . 12
2.6 Render of the Remote Radio Station . . . 13
2.7 Remote Radio Station (RRS) system overview . . . 14
2.8 The four Dutch submarines of the Walrus class . . . 16

3.1 Sail of the Walrus submarine . . . 21

4.1 Specific attenuation due to atmospheric gases (Pressure $= 1013.25hPa$, Temperature $= 15°C$, Water Vapour Density $= 7.5g/m^3$) . . . 28
4.2 Advanced Coding and Modulation (ACM) modes $\frac{E_b}{N_0}$ for set Bit Error Rate (BER) . . . 30
4.3 ACM modes $\frac{E_b}{N_0}$ for BER $= 10^{-6}$ . . . 30
4.4 Antennas on Brik-II . . . 30
4.5 Satellite radiation pattern uplink and downlink antenna . . . 30
4.6 Graphical User Interface (GUI) of Standard General Perturbations Satellite Orbit Model 4 (SGP4) propagator in MATLAB . . . 31
4.7 Rotations of reference frame necessary . . . 32
4.8 1 month propagation . . . 34
4.9 4 months propagation . . . 34
4.10 8 months propagation . . . 34
4.11 Data transfer for different latitudes . . . 34
4.12 Yagi-Uda Antenna . . . 35
4.13 Phased Array antenna . . . 36
4.14 Egg-Beater antenna . . . 37
4.15 Helical Antenna . . . 38
4.16 Simulation model flowchart . . . 39
4.17 Basic helical antenna used as basic design . . . 40
4.18 Spacing between turns . . . 41
4.19 Number of turns . . . 41
4.20 Feed-height of antenna . . . 41
4.21 Diameter of antenna . . . 41
4.22 Four variables helical antenna . . . 41
4.23 Data throughput for different ground plane radii . . . 42
4.24 Resulting data throughput for passes with different maximum elevation angles . . . 43
4.25 General scan antenna designs between boundary values . . . 44
4.26 The four best antenna designs . . . 45
4.27 Final helical antenna design . . . 45
4.28 3D radiation pattern . . . 46
4.29 Vertical cut radiation pattern . . . 46
4.30 Average data throughput passes for maximum elevation angles . . . 47
4.31 3D radiation pattern uplink . . . 47
4.32 Vertical cut radiation pattern downlink and uplink . . . 47
4.33 Average data throughput passes for maximum elevation angles . . . 48

4.34 Data transfer rate for fixed and variable ACM mode along with elevation angle 48
4.35 Signal to Noise Ratio (SNR), antennas gain and elevation angle over time 49
4.36 Pass 1 and 4 as seen from the ground segment 49

5.1 3D model helical antenna mold 51
5.2 Female N chassis connector 52
5.3 Arm to connect submarine antenna to Remote Radio Station (RRS) rotor 53
5.4 The four 3D printed parts submarine antenna 53
5.5 Submarine antenna assembled 53
5.6 Connector hole in antenna base plate 53
5.7 Assembled antenna on RRS stand 54
5.8 Connector on underside ground plane 54
5.9 Schematic of antenna system 54
5.10 Smith Chart antenna before impedance match 55
5.11 Voltage Standing Wave Ratio (VSWR) antenna before impedance match 56
5.12 Moving in Smith chart 57
5.13 Section of Smith chart that can be match L-network 57
5.14 L-network used for impedance matching 57
5.15 X_c and X_l impedance matching 58
5.16 Coil used as inductor 59
5.17 Trimmer capacitor 59
5.18 Estimation impedance antenna 60
5.19 Impedance of antenna with tuned L-network 60
5.20 VSWR Antenna with L-network 61
5.21 VSWR Antenna with L-network magnified around the downlink frequency 61

6.1 Radiation pattern test set-up 63
6.2 Schematic representation of submarine antenna orientation variation 64
6.3 Main transmitting antenna measurement 1 65
6.4 Reference antenna measurement 1 65
6.5 Submarine antenna 65
6.6 Anechoic chamber measurement 1 66
6.7 Submarine antenna during measurement 66
6.8 Transmitting antenna measurement 1 66
6.9 Main transmitting antenna measurement 2 67
6.10 Reference antenna measurement 2 67
6.11 Submarine antenna 67
6.12 Radiation pattern measurement set-up outdoor 67
6.13 Radiation pattern measurement set-up outdoor 67
6.14 Transmitting antenna radiation pattern measurement outdoor 67
6.15 Outdoor measurement set-up for link strength testing 68
6.16 FieldFox receiver outdoor measurement 68
6.17 FieldFox receiver indoor measurement set-up test 69
6.18 Radiation pattern slice 0°-180° 70
6.19 Radiation pattern slice 90°-270° 70
6.20 Radiation pattern manufactured antenna 71
6.21 Radiation pattern slice 0°-180° 71
6.22 Radiation pattern slice 90°-270° 71
6.23 Radiation pattern slice 0°-180° 72
6.24 Radiation pattern slice 90°-270° 72
6.25 Schematic L-network to simulate losses 72
6.26 L-network simulated output 73
6.27 Radiation pattern slice 0°-180° 74
6.28 Radiation pattern slice 90°-270° 74

6.29 Data rate with fixed ACM mode for predicted and measured radiation pattern 75
6.30 SNR and antenna gain for predicted and measured radiation pattern 75
6.31 Data rate variable ACM mode for predicted and measured radiation pattern 75
6.32 Average data throughput pass for different maximum elevation angles 76
6.33 L-network location on submarine antenna 77
6.34 Average data throughput for passes with different maximum elevation angles 78

List of Tables

2.1 General Brik-II characteristics 9
2.2 Characteristics Store and Forward Payload 12
2.3 General characteristics of the Royal Netherlands Navy submarines 16

3.1 System requirements total system 23
3.2 Leading requirements during the project 25

4.1 Integration step size results 33
4.2 Boundary values for the variables in the helical antenna optimisation 42
4.3 Final design properties and performance 46

5.1 Characteristics 3D print submarine antenna 52
5.2 Ideal and minimal values mismatch loss and VSWR 55
5.3 Capacitance and inductance values 58
5.4 Predicted and measured component parameters 59

6.1 Measurement parameters 70

7.1 System requirements prototype 85

List of Abbreviations

ABS Acrylonitrile Butadiene Styrene

ACINT Acoustic Intelligence

ACM Advanced Coding and Modulation

AEHF Advanced Extreme High Frequency

BER Bit Error Rate

BPSK Binary phase-shift keying

COMINT Communications Intelligence

CU Compute Unit

EIRP Effective Isotropic Radiated Power

ELINT Electronic Intelligence

EOV Electronic Warfare

ESM Electronic Support Measures

ESR Equivalent Series Resistance

EU European Union

FSPL Free Space Path Loss

FTE Full Time Employee

GNSS Global Navigation Satellite System

GPS Global Positioning System

GUI Graphical User Interface

HMI Human Machine Interface

HPBW Half Power Beam Width

IMINT Imagery Intelligence

LEO Low Earth Orbit

LNA Low-Noise Amplifier

MOD Ministery of Defence

NATO North Atlantic Treaty Organisation

NLR Netherlands Aerospace Centre

PoE Power over Ethernet

RF Radio Frequency

RNLAF Royal Netherlands Air Force

RRS Remote Radio Station

SA Spectrum Analyser

SATCOM Satellite Communication

SDR Software Defined Radio

SFP Store and Forward Payload

SGP4 Standard General Perturbations Satellite Orbit Model 4

SMD Surface Mount Device

SNR Signal to Noise Ratio

SSA Space Situational Awareness

STS Satellite Tracking System

TLE Two-Line Element Method

UHF Ultra High Frequency

UiO University of Oslo

USA United States of America

VHF Very High Frequency

VLF Very Low Frequency

VNA Vector Network Analyser

VSWR Voltage Standing Wave Ratio

WGS Wideband Global Satcom

WGS84 World Geodetic System 1984

Abstract

The Brik-II satellite is a Nano-Satellite which has the main objective to be a technology demonstrator and prove the use of self owned military satellites. One of the payloads onboard the Brik-II satellite is called the Store and Forward Payload. It has the capability to Store and Forward messages from and to different military assets. To demonstrate this capability it has been purposed to design and install a communication system onboard the Royal Netherlands Navy submarines enabling communication with Brik-II. Subsequently, this would be a good way to demonstrate the performance and operational relevance of such system.

The first step was to identify the problem that should be solved. The main objective of this MSc thesis was to design, manufacture and test an operationally deployable communication system for the submarines operated by the Royal Netherlands Navy. Based on the main objective and consultation with the Navy the requirements of the system were compiled. From the requirements it was concluded that there are a number of similarities between the Remote Radio Station (RRS) and the submarine communication system. However, the antenna system installed on the RRS cannot meet the size requirements. Therefore a new antenna systems had to be design that would comply with the requirements. This has been the main focus of this MSc thesis.

To find the optimal design for the antenna, a simulation tool for the communication between the submarine and Brik-II was developed. In the model different antennas were tested to identify the optimal design. The type of antenna used in the optimisation is a helical antenna. Once the optimal design was identified it was manufactured used the 3D printing facilities at the 982 Squadron in Dongen. Hereafter, measurements were conducted to verify that the radiation pattern of the antenna corresponds with the predicted radiation pattern. The similarities in shape between the predicted and measured pattern were evident. However, the measured gain of the antenna was lower than the predicted gain. To meet the requirements the losses will have to be mitigated. Multiple solutions were purposed to reduce the losses. A communication test between the antenna and the satellite could not be conducted due to technical difficulties during testing.

Part of the main objective was to develop an operationally deployable system. This first prototype developed in this MSc thesis provides a basis for further iteration. The current design imposes two constraints on the deployability. First the antenna gain losses have to be mitigated since the lower gain results in less than required data throughput. The losses can be reduced by implementing the proposed solutions. Second, the choice of a helical antenna with an omnidirectional radiation pattern results in an increased chance of detection by possible adversaries. This functional constraint cannot be remedied due to the size requirements. In conclusion, the antenna design proposed in this thesis gives a basis for a system that can provide added value to the operations of the submarine.

1

Introduction

Multiple countries are developing military capabilities in space, such as the United States Space Forces and the French Space Command [32]. The Ministry of Defense in the Netherlands has now joined this movement. The Royal Netherlands Air Force (RNLAF) has launched the Brik-II satellite in June of 2021. The Brik-II satellite is a Nano-Satellite that will provide insight in the use of self-owned military satellites. The main objective of Brik-II is to demonstrate the usefulness of military capabilities in space, which will be achieved by the three payloads on board. During this MSc thesis the focus will be on an application of the Store and Forward Payload (SFP). The payload has the capability to store and forward messages between military assets. The use-case considered is the communication between the Royal Netherlands Navy's submarines and SFP on-board Brik-II. The submarines currently have Satellite Communication (SATCOM) capabilities. However, the systems are depended on allied partners, thus the use is limited since it is shared. Furthermore, the transmitted information is not private and can be received by allied partners. Due to these constraints it is still common practise to store gathered intelligence on-board and only unload upon arrival at the port [19]. It can be concluded that Dutch SATCOM capabilities can improve added value to the submarine operations. The Brik-II satellite fills this need since it is the first satellite capable of supporting the Dutch armed forces independent of other parties. The submarines have to be adjusted such that communication with Brik-II is possible. The development of such SATCOM system is the objective of this MSc thesis.

1.1. Objective, Questions & Approach

The main research objective of this thesis is:

> "**Research Objective:** *To enable communication between a submarine and the Store and Forward payload of the Brik-II satellite by means of designing, manufacturing and testing an operationally deployable communication system for the submarines operated by the Royal Netherlands Navy.*"

The first step in achieving the research objective is to gather the requirements for the system by consulting with the Navy. The requirements are based on how the system will be utilised during operations. Once the requirements have been gathered a system can be designed that meets the requirements. To do this, a tool will be developed that simulates the communication between the satellite and the submarine. To simulate the communication, the characteristics of the SATCOM system should be known. Therefore the following research question has to be answered:

> "**Sub-Question 1:** *What physical design characteristics does a satellite communication system have to meet to be deployable on-board the Dutch submarines?*"

Using the simulation tool, it is possible to characterise the performance of submarine antenna system. It will be used to optimise the system design based on the set requirements. Once an optimal design

is found, the antenna will be manufactured to the set specifications. Hereafter the antenna will be subjected to a number of tests that will determine if the performance of the antenna is as expected. The first test will provide insight in the antenna radiation pattern. The second test will attempt to communicate with Brik-II. The simulation tool along with the two tests will help to answer the last research question:

> "**Sub-Question 2:** *What are the performance characteristics of the submarine satellite communication system?*"

If the process is completed as mentioned above, the research questions should be answered. Furthermore the objective of this thesis should be achieved. The structure of this report is discussed in section 1.2 hereafter.

1.2. Thesis structure

The thesis is organised into 5 main chapters. *Chapter 2* provides a frame of reference regarding the Netherlands Ministery of Defence (MOD). Furthermore an elaboration on the military hardware of interest (e.g. Brik-II) is given. In *Chapter 3* the requirements for the system are covered and explained. *Chapter 4* covers the simulation of the communication between satellite and submarine. The simulation will be used to find the optimal design and the results are presented. Subsequently, *chapter 5* covers the manufacturing of the design obtained in the optimisation. In *chapter 6* the antenna is subjected to two measurements. The first is a radiation pattern test to verify the performance of the antenna. The second is a test in which the antenna attempts to communicate with the Brik-II satellite. Finally, *chapter 6* states the relevant conclusions and provides recommendations on future work.

2

Frame of Reference: Netherlands Ministry of Defence

The Netherlands MOD has the main responsibility to protect The Netherlands and it oversees territories. To be able to accomplish this goal, it has to have personnel, financial means, and material resources at its disposal. The ministry is politically led by the minister of Defense, which is Henk Kamp at this time [21]. The MOD has over 68000 employee and is one of the biggest employers in The Netherlands [24].

The Ministry of Defence is subdivided in to four main branches namely; The Royal Netherlands Air Force, The Royal Netherlands Navy, The Royal Netherlands Army, and The Royal Netherlands Military Police. The MSc thesis is conducted in cooperation between the The RNLAF and The Royal Netherlands Navy. In this chapter both are discussed in more detail to provide an elaborate frame of reference. Parts of information discussed is based on the literature study that precedes this MSc thesis [26]. A large part of the information presented in this section is provided with the courtesy of the RNLAF [51].

2.1. The Royal Netherlands Air Force

The RNLAF is the youngest of the four branches of the MOD. It is a high-tech organisation which supports the objectives of the The Netherlands MOD. The main capabilities are defending the Dutch airspace, providing support during operations, and deliver offensive and defensive capabilities in conflict situations. To achieve the objectives the RNLAF has 6450 people personnel [24].

In recent years Space became more affordable and accessible, this allows countries with a relatively small military budget, like the Netherlands, to explore this new warfare domain. Satellites provide valuable information which cannot be easily obtained otherwise. In 2013 the RNLAF decided that it was time to join this movement. As such the department of space was created, in Dutch named Sectie Space. The MSc. thesis has been conducted under the supervision of Sectie Space. Within the Air Force, Sectie Space is located in the Air and Space Warfare Centre, which is responsible for new developments concerning the Air and Space Domain. In Figure 2.1 a hierarchy map of the Netherlands MOD is shown, leading through the different organisational layers to the Defence Space Security Centre.

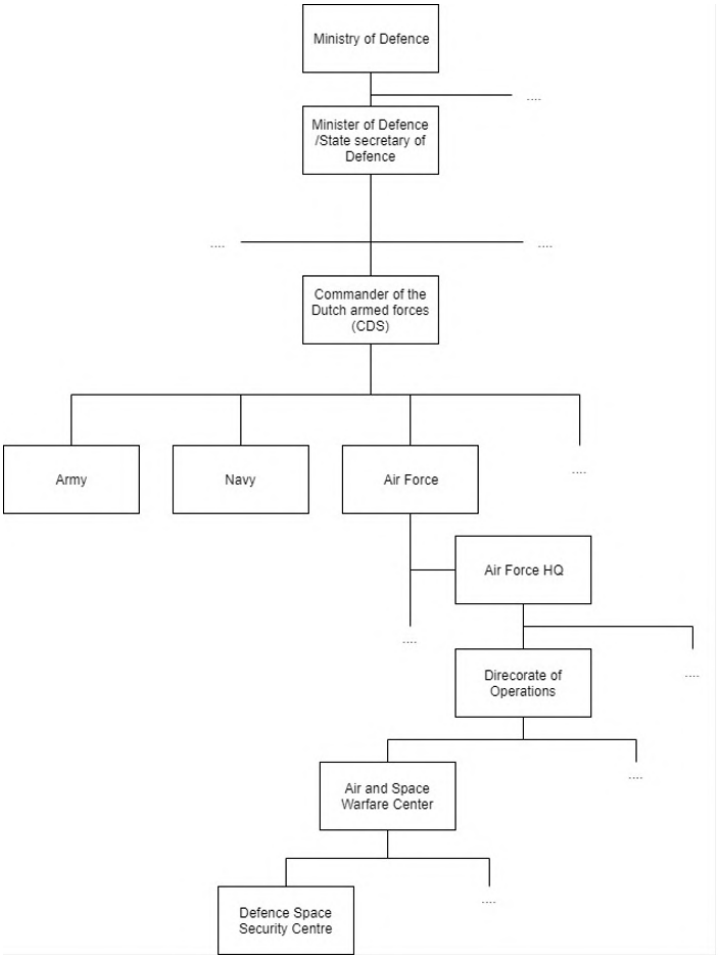

Figure 2.1: Position of Sectie Space in the Armed Forces

2.1.1. Sectie Space

The Sectie Space has multiple purposes for the RNLAF. The Sectie focuses on a number of projects such as international cooperation and coordination, the development of Space Situational Awareness (SSA) capabilities, obtain commercial satellite data, satellite communication, and the use of small satellite for military purposes.

The space department was stated in 2013 with only two people, two years later the Space Security Centre was established and the Sectie Space doubled in size. In 2019 the space department was renamed to the Defence Space Security Centre, and grown in personnel to ten FTE's. The space support to military operations can be divided in to six elements as defined by the North Atlantic Treaty Organisation (NATO).

1. **Satellite Communication:** Used to communicate data between different military assets. The data can be messages (voice or text), but also commands for autonomous vehicles etc.
2. **Intelligence Surveillance and Reconnaissance:** The objective is to gather information on potential adversaries. The intelligence can be obtained by analysing imagery, but also for example by intercepting transmissions or geo-locating radar systems based on their signal emission.
3. **Positioning, Navigation and Timing:** Currently there are four Global Navigation Satellite System (GNSS) systems; GPS (USA), Galileo (EU), GLONASS (Russia), and Beidou (China). These systems are used to determine the location of assets. Furthermore they have the ability to provide accurate timing, that can be used for synchronising systems. GNSS spoofing, the manipulation of the GNSS signal to confuse receiving devices, is a growing treat for military assets [54].

4. **Space Domain Awareness:** The objective is to ensure safety in space. Furthermore it provides overflights warning, and detects and monitors space debris [9].
5. **Shared Early Waring:** An early warning system to detect missiles launched by enemies.
6. **Meteorological:** Provide terrestrial and space weather forecast. Space weather is important ensure communication capabilities, as charged particles from space can cause disruption.

Apart from the 6 NATO space domains, the space department manages several high tech projects to develop technology and capabilities that can be injected into military operations. Concerning SSA there are two project on going, one called DISCOVER which is a project conducted with Thales Hengelo, the aim is to see if the new air surveillance radar can also look into low earth orbit. A second SSA project is FOTOS, this project is about optical observations from earth to space to track and categorise space objects. The RNLAF is working internationally with 11 countries to proof the military relevance of small satellites, called the responsive space capabilities MOU. Furthermore, the Air Force has two satellite development projects, MILSPACE-II a cooperation between the Norwegian MOD and the RNLAF. In MILSPACE-II two satellites are constructed that will fly in formation. Launch is planned for 2022 and the project is conducted by a consortium of Netherlands Aerospace Centre (NLR), TNO and FFI. Also, the space department has its own satellite program for the Brik-II satellite. Brik-II is the main system around which the design process in this MSc Thesis is conducted. In the next section a further elaboration on the Brik-II, its mission, and the capabilities is given.

2.1.2. Brik-II Satellite

As more countries are developing military capabilities in space, such as the United States Space Forces and the French Space Command [32], the Netherlands MOD decided to join this movement. The capabilities off a satellite can be of good value to the armed forces. From this incentive the Brik-II satellite project was created. Brik-II is the first military satellite launched by the Netherlands MOD. The satellite has been launched on 30^{th} of June 2021 on-board the Tubular Bells: Part One mission by Virgin Orbit [23]. The launch was successful and the satellite is in a 500 km orbit with a 60.7° inclination.

The main objective of the project is to be a technology demonstrator. The satellite can prove the usefulness of military owned satellites for the armed forces. The fact that it is a demonstrator implies that the armed forces are not operationally dependent on the satellite's capabilities. This does not imply that the satellite has no operational benefits. The relatively small 6U CubeSat has three payloads on-board, which each have different capabilities. The capabilities of the payloads will be discussed in the next section. To provide a good overview of the Brik-II satellite a number of characteristics are listed in table 2.1.

Characteristic	**Value**
Size	6U CubeSat
Mass	<10 [kg]
Orbital inclination	60.7 [°]
Eccentricity	0
Payloads	3
Minimal lifetime	2 years
Ground station location	Dongen (NL)
Active ACDS	Yes

Table 2.1: General Brik-II characteristics

Capabilities

The Brik-II satellite has three payloads on-board. The capabilities of the payloads, along with the operational added value, are listed below. To get a better understanding of the satellite structure, position of the payloads in the satellite are shown in figure 2.2.

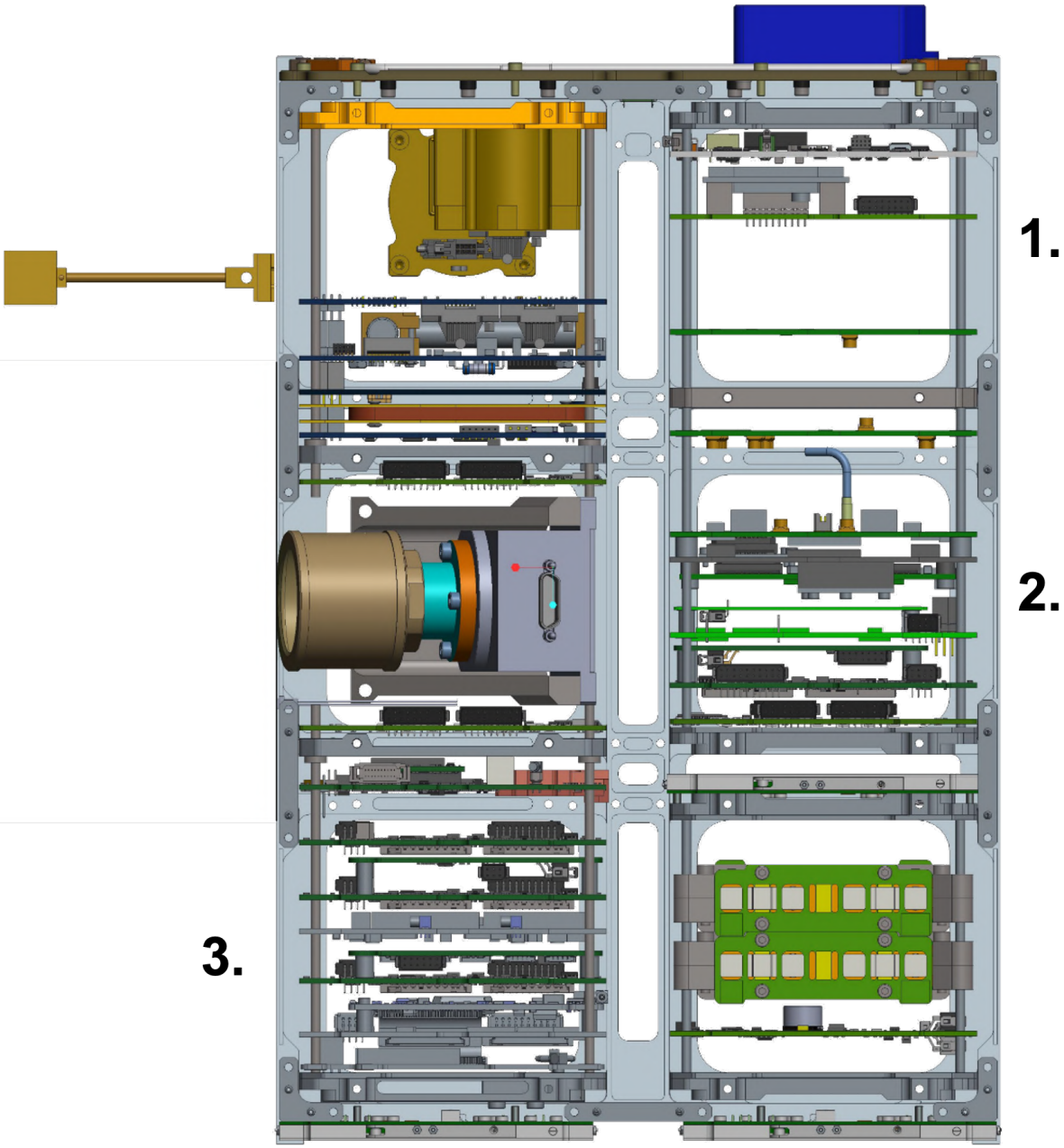

Figure 2.2: The Brik-II satellite

1. **ScinMon:** ScinMon is a scintillation monitor which uses Langmuir probes to measure space weather, density and temperature of electrons. The ScinMon payload has been develop by the University of Oslo (UiO). The scintillation monitor enables the Air Force to analyse if disturbances in GPS signals or radio traffic are caused by natural phenomena or potential adversaries. The data gathered by ScinMon will be used to develop a forecast model to better understand the disturbance caused by the interaction of solar particles with the earth's magnetic field [68]. The information gathered is the electron temperature and electron density. The payload consists of 4 multi needle Langmuir probes, along with an electron emitter to control the potential of the satellite.

2. **PHINO:** PHINO is an Electronic Support Measures (ESM) sensor that has the ability to measure radio signals. PHINO has been developed by the NLR. It allows the Air Force to detect and analyse the use of radio signals on earth. This can be provide valuable information of potential

adversaries, such as the location of ground radar systems. PHINO calculates the angle of arrival of a radio transmission from earth, to geolocate the source on the surface. The angle of arrival is determined by measuring the phase difference of the incoming signal. The principle can be seen in figure 2.3 below.

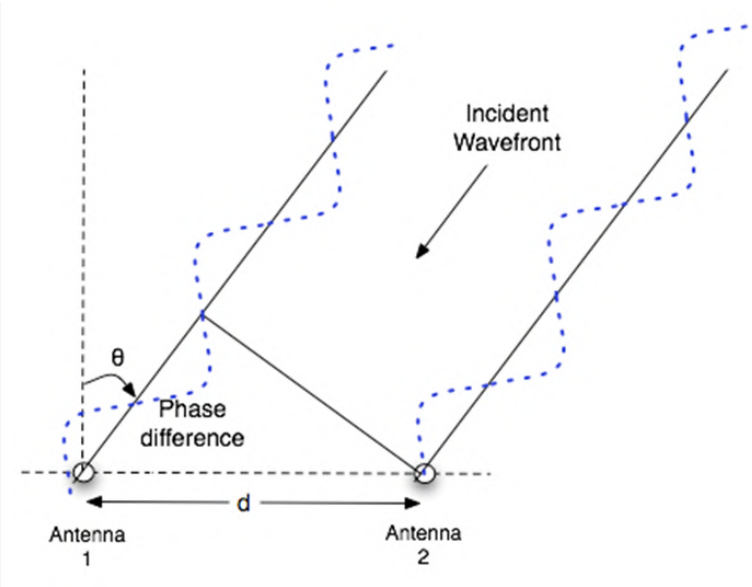

Figure 2.3: Principle of phase difference that enables localisation of radio signals

3. **Store and Forward Payload:** SFP has the capability to store messages and relay these at a different location on earth. The SFP is design and build by the 982 Squadron in Dongen (NL). The payload enables the armed forces to transmit secure messages between different assets. The payload consist of a small Software Defined Radio (SDR) that operates in the Ultra High Frequency (UHF) band. The antenna of the SFP is shared with the rest of the spacecraft (e.g. to transmit housekeeping data). The SFP before integration with the satellite can be in figure 2.4.

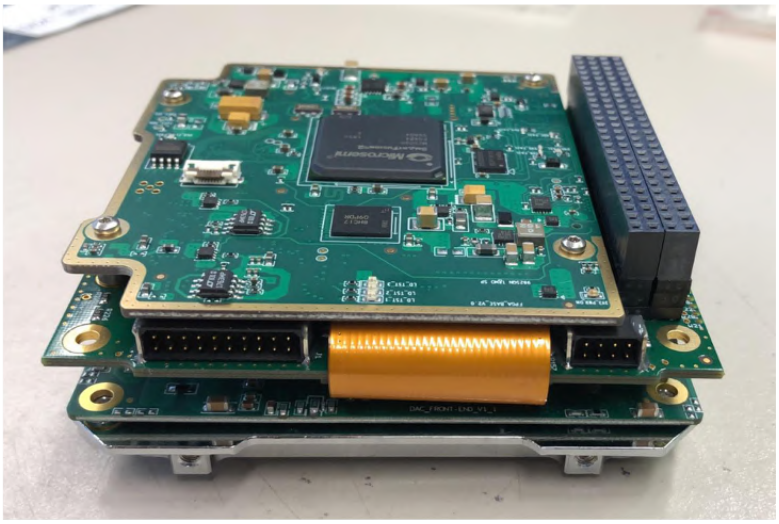

Figure 2.4: Store and Forward Payload [51]

In table 2.2 below a number of characteristics regarding the SFP are listed. It can be seen that the payload uses two separate frequencies for up- and downlink. Upon request of the RNLAF

the uplink and downlink frequency will not be disclosed in this project. A range of values can be seen in table 2.2, these provide an indication of the frequencies used.

Characteristic	Value
Uplink frequency	300-320 MHz
Downlink frequency	260-280 MHz
Bandwidth	25 KHz
Antenna 'temperature'	290 K
Electronics 'temperature'	550 K
Transmit power	2.5 W
Effective Isotropic Radiated Power (EIRP)	4 dBW
Modulation	Advanced Coding and Modulation (ACM) Default: Binary phase-shift keying (BPSK)

Table 2.2: Characteristics Store and Forward Payload [51]

Consortium

The Brik-II satellite was developed in with consortium of different partners, which each contributed in a different way. The structure in which the consortium operates can be seen in figure 2.5 below.

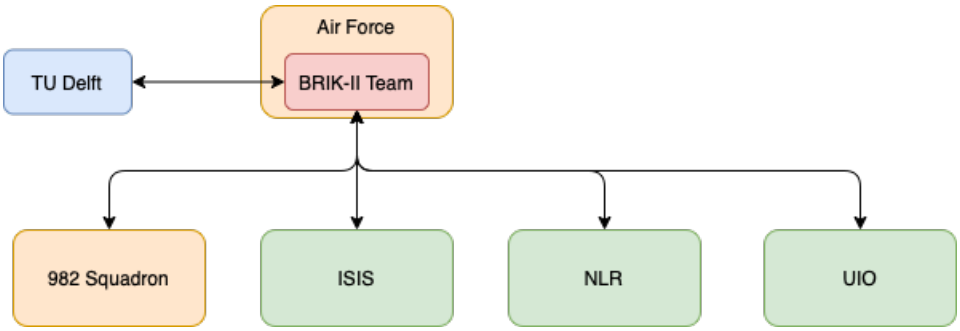

Figure 2.5: Brik-II development consortium

The satellite is the first satellite developed by and for the Air Force. Since this mission is a technology demonstrator the RNLAF decided they want to manage the project development themselves. The benefit of such set-up is that the RNLAF is close to the project team and has the opportunity to learn about a satellite project from within, by active participation. The structure chosen here is not common for defense contracts since the Air Force is usually the customer and does not actively participate in the development. The RNLAF Brik-II team is assisted by the TU Delft. The TU Delft has a lot of experience in various space activities amongst which building experimental satellites and assist the Air Force on a technical and programmatic level. ISIS is the platform integrator for the satellite along with being the launch broker. The 982 Squadron, NLR and UiO each deliver a payload, as mentioned in the previous section. The RNLAF is responsible for the development of the payloads and delivers those to ISIS for integration.

2.1.3. Remote Radio Station

Along with the development of the Brik-II satellite and the SFP. The Air Force has started with the implementation of the Brik-II capabilities into the Armed Forces operations. To enable the capabilities of the SFP forces in the field need a device that can communicate with the satellite. Using the device they can transfer message to other assets. The device which will enable this is the RRS. A 3D render of the RRS system can be seen in figure 2.6.

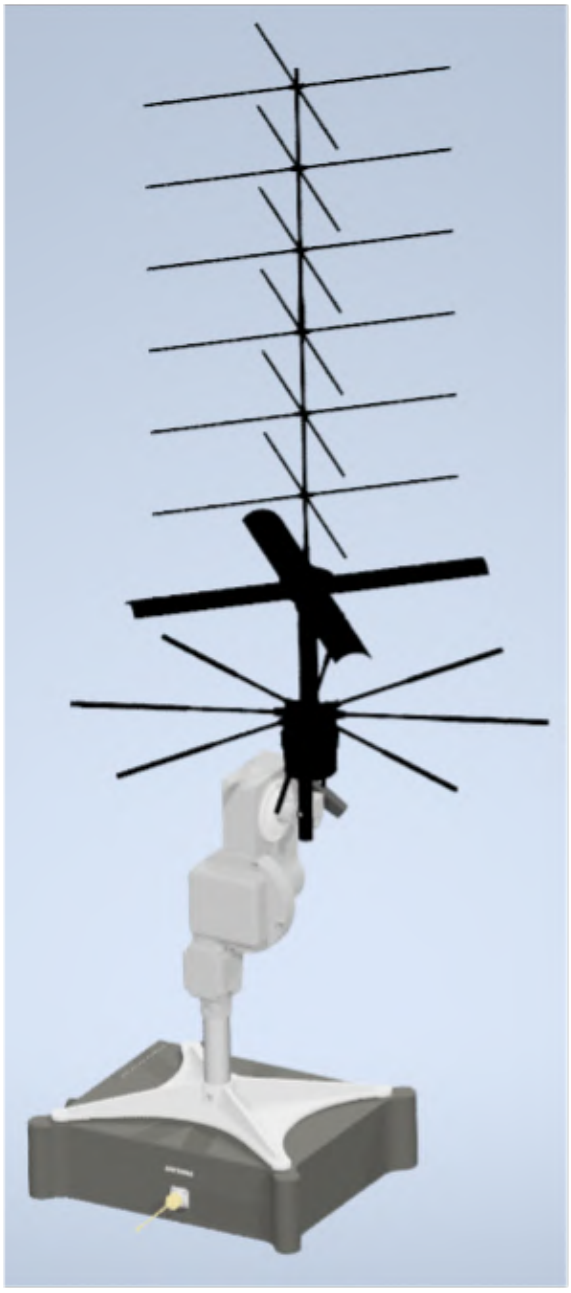

Figure 2.6: Render of the Remote Radio Station [64]

The RRS in build by the 982 Squadron in Dongen. The system consists out of three separate parts, namely; the antenna, rotor, and electronics box. The antenna is a TacSat UHF antenna, normally used to communicate with the TacSat-4 spacecraft. The TacSat antenna is design to operate in the frequency range of 240-420 MHz range, which is complied with the frequency range used by the SFP [18]. The rotor is an in-house design build by the 982 Squadron and can accurately point the antenna towards the satellite. The electronics box, shows as the grey box underneath the rotor in figure 2.6, houses a number of electronic components. A schematic of the internal electronics can be seen in figure 2.7.

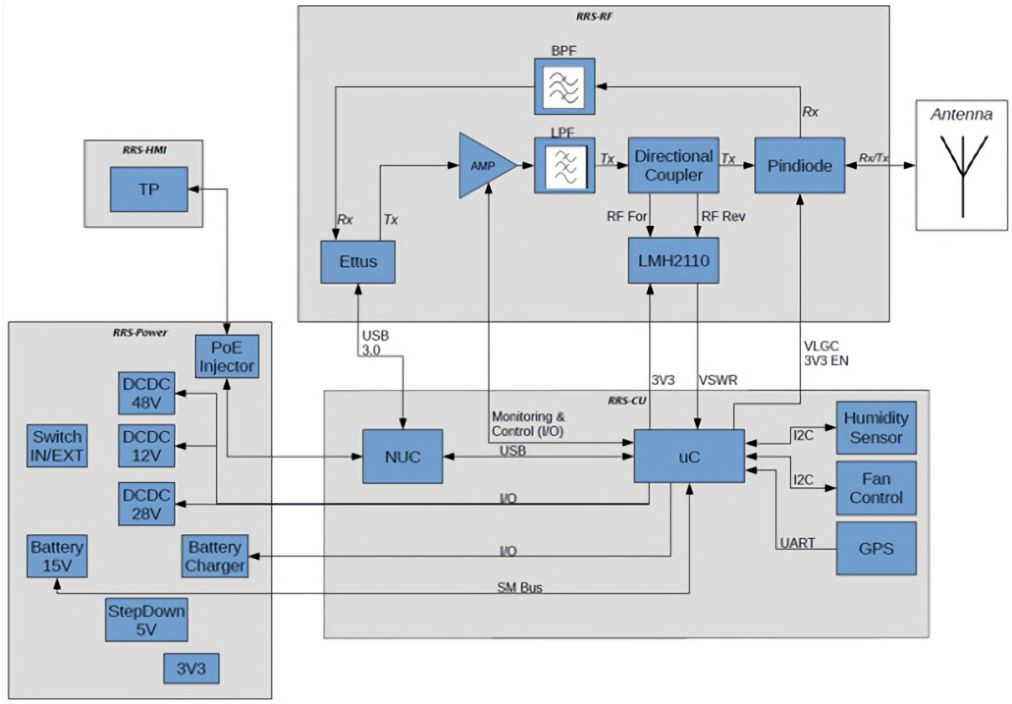

Figure 2.7: Remote Radio Station (RRS) system overview [64]

The grey rectangles in figure 2.7 are the subsystems of the RRS. The function of the subsystems is discussed hereafter;

- **Radio Frequency subsystem:** The main goal of the Radio Frequency (RF) subsystem is to covert input data to RF signals, apply a filter and amplify the signal before sending it to the antenna. It also filters and converts the incoming RF signals from the antenna to a digital signal which can be send to the Compute Unit (CU) subsystem. The RRS has one antenna which will be used for transmission and receiving. To be able to do both of these things, the receive (Rx) and transmit (Tx) path have to be switched. To facilitate this a pin diode is required. The diode does not mechanically switch between the Rx and Tx path but uses either one of the incoming signals. Using a pin diode ensures a low switching time and higher reliability compared to a mechanical switch. Next-to the pin diode is the directional coupler along with a LMH2110 power detector. Their main functionality is to measure the forward and reverse power of the Tx path. It enables the tuning of input power. If the reverse power is very high this can be detected and prevent damage to the signal amplifier. The amplifier itself can increase the signal coming from the Ettus b205 mini-i SDR with 45 dB. The Ettus is a SDR, meaning it uses software for modulation and demodulation of radio signals [36]. The Ettus is powered via USB, which is also used for data transfer to and from the Ettus [1].
- **Compute Unit (CU) subsystem:** The CU is the brain of the system. It monitors all the subsystems and their components. It is also the connection for the user interface, which shows the status of the system. Furthermore, it handles the messages that are entered into the RRS by the user. Part of the CU is the Intel NUC, is a small computer which has a large amount op processing power. It monitors the system handles all the data, provides the connection with the user interface, and communicates with the Ettus SDR. Much of the communication from the NUC runs through the micro controller. The components are controller by, or provide information to the micro controller are the following:
  - Determine Global Positioning System (GPS) coordinates
  - Measure temperature and humidity
  - Control cooling fan

  - Measure Rx and Tx power
  - Control and monitor the amplifier
  - Control power converters
  - Monitoring of the battery and charging
  - Control Pin Diode

- **Power subsystem:** The power subsystem for the RRS is different from the power supply onboard the submarine. It will most likely not operate on battery power and have a different input voltage. However, the subsystem does indicate the voltages which are required to run the system. The voltages specified for the subsystems will presumably be very similar to the voltages characteristics required by the system design in this MSc thesis. Therefore, it does provide a good overview of what typical system requirements are from components.

  - **48V:** Human Machine Interface via Power over Ethernet (PoE).
  - **28V:** Amplifier and battery
  - **12V:** NUC and rotor for antenna steering
  - **5/3.3V:** 5V for the pin diode. 3.3V for the micro-controller, humidity sensor, fan controller, GPS sensor, and the directional coupler

- **Satellite Tracking and Antenna subsystem:** The tracking system consists of a X/Y-rotor construction with two worm-wheel transmissions driven by two stepper motors. The antenna connected to the Satellite Tracking System (STS) is attached by one bolt and is power by a CLO connector. The connector delivers power to the antenna and handles the data transfer to and from the antenna. The system can calibrate itself automatically using the external BNO055 position sensor providing the current angel at which the antenna is pointing and the geomagnetic north sensor. The antenna is a TacSat antenna, as shown in figure 2.6.

- **Human Machine Interface subsystem:** The Human Machine Interface (HMI) subsystem is made to be portable and easy to use with a touchscreen, such that no mouse or keyboard is required. The touchscreen allows for interaction with the system, and displays information the following information regarding the system:

  - Show satellite passes schedule and information
  - A timer to indicate when passes starts
  - A way to upload a message
  - See GPS information, and position lock
  - Control Antenna pointing mechanism
  - Display transmission information
  - Display RRS system status

2.2. The Royal Netherlands Navy

The Royal Netherlands Navy is the oldest of the four branches of the MOD. The organisation supports the objectives of the The Netherlands MOD. The main objectives are defending the Netherlands. Furthermore it strives for safety on and from the sea. In The Netherlands and abroad, the Navy helps with crisis management, humanitarian relief operations and, natural disasters. To achieve the objectives, the Navy has 11289 people personnel [24]. One of the important pieces of equipment used are the Dutch submarines. The submarines are one of the main systems around which the design process in this MSc Thesis is conducted. In the next section an elaboration on the Dutch Submarines, their missions, and technical capabilities is given.

2.2.1. Submarines

In this section of the report a number of aspects of the submarines will be discussed. First some general characteristics and operational objectives will be discussed. Secondly, there will be further investigation to the communication systems on-board. A general problem encountered in writing this section is that a lot of the information is not publicly available and has a certain security level. Therefore, some parts are focused on general submarine communication instead of specific information of the Royal Netherlands Navy submarines. The submarines can be seen in figure 2.8.

Figure 2.8: The four Dutch submarines of the Walrus class [12]

Characteristics

The Royal Netherlands Navy currently has 4 operational submarines of the Walrus class. The submarines were build by Rotterdamsche Droogdok Maatschappij and taken into service between 1990 en 1994. Two submarines have recently received life-extending upgrades, the other two are currently being upgraded. The submarines are scheduled be retired between 2028 en 2031 [13]. Some general characteristics of this class of submarines can be found in table 2.3.

Specification	**Value**
Length	68 m
Width	8.5 m
Draft	7.5 m
Dive depth	>300 m
Water displacement	2450 ton
Propulsion type	Diesel-electric
Propulsion power	Diesel 4.63 MW, Electric 5.1 MW
Speed	20 knots submerged, 11 knots afloat
Staff	55
Weapons	20 Mark 48-torpedo's

Table 2.3: General characteristics of the Royal Netherlands Navy submarines [13]

The Walrus class submarine differentiates itself by its relatively small size. The propulsion on-board is a diesel-electric combination. This means that the power will be generated by the diesel motor while

the submarine is afloat, while the power will come from the internal battery while when submerged. Therefore the submarine is very quiet during an operation which makes it, along with its small size, less likely to be detected. The downside is that the submarine can only stay submerged for a relatively short amount of time compared to nuclear powered submarines. Since the power on-board is not as abundant as a nuclear submarine, the maximum speed is also relatively low. The advantage of battery powered submarines is that the don't need constant cooling like a nuclear submarine therefore they can be quieter and even harder to detect [13].

General Mission Objectives

The Dutch submarines can be used for many different purposes. A submarine is one of the most powerful assets of the Navy, since it is dangerous and hard to detect. An example of this was demonstrated by the Royal Netherlands Navy during the Kosovo conflict in 1999 [44]. For five weeks the Hr.Ms. Dolfijn, which was part of the Operation Allied Force by the NATO, and patrolled the coastal city of Bar and the bay of Kotor. For the first time the Dolfijn had all four torpedo tubes open and loaded in a active war situation. The commander in charge had the order to sink any military ship that would leave the port of Bar. The submarine was positioned at periscope depths such that it could monitor the missiles posted on the coast. It was also able to monitor shipping vessels via sonar and be on the lookout for enemy submarines. At the end none of the military ships left the harbor. This demonstrates the power of a submarine in a warfare situation, the threat it poses to the enemy by being hard to find and very lethal. The concern for a submarine attack is so high that no risk can be taken.

The situation mentioned above provides an overview of the most important tasks of a submarine namely, the deterring an enemy, gather intelligence, and possess large amounts of firepower. The deterring of and enemy is based on the large amount of firepower and the stealth of a submarine. The gathering of intelligence also very important during times of peace. The Dutch submarines are very suited for this task since they are silent, and due to their smaller size can come very close to shore [43]. Multiple forms of information gathering are used [20], each of which is explained below:

- **Imagery Intelligence (IMINT)**
  Imagery Intelligence (IMINT) is the gathering of intelligence through analysis of imagery. The imagery can be obtain using different sensors. In the submarine the periscope is used to capture video and images. The Dutch submarines have the capability to do this is in the visible and infrared spectrum. Apart from general intelligence gathering the periscope is also used for navigation and executing possible attacks [20].

- **Acoustic Intelligence (ACINT)**
  Acoustic Intelligence (ACINT) is the gathering of intelligence through the analysis of acoustic emissions. ACINT is essential in recognising and localising maritime vessels. To identify and recognise individual vessels the Navy uses fingerprinting, which is based on the sound emissions coming from a vessel. The emissions are received via Long- and Medium Range Sonar (LRS/MRS). The fingerprints are saved in a database such that maritime vessels can be recognised quickly [44].

- **Electronic Intelligence (ELINT)**
  Electronic Intelligence (ELINT) is the gathering of intelligence through analysis of electromagnetic emissions other than communication signals. With the Electronic Warfare (EOV) mast the Dutch submarines are able to accurately pinpoint the location of radar signals. This is used for two purposes. First is the avoidance of counter detection since it can warn for search radars. Second it can identify each radar system by their fingerprints which might provide valuable insight in moving radar systems. The information is stored in a database like the ACINT [20].

- **Communications Intelligence (COMINT)**
  Communications Intelligence (COMINT) is the gathering of intelligence through interception and analysis of communication signals. Since the Dutch submarines are capable of operating close to shore this capability can also be used to gather intelligence on coastal settlements. Intercepted messages are often heavily encrypted therefore they cannot be deciphered on-board, since the

submarine does not have the required computational power on-board [20]. The Brik-II satellite might solve this problem since the message can be transmitted to onshore systems which can potentially decipher the encryption.

The tasks mentioned above show the importance of the submarines to the Royal Netherlands Navy. However these are not the only capabilities of the submarine. They facilitate in a number of side tasks, which are itemized below [43].

- *Special Forces*: The submarine can facilitate in the drop-off and pick-up of special forces from the royal marines. Via a hatch in the bow of the ship the marines can be deploy.
- *Training*: The submarines can be used to train other Defense branches how to handle submarines.
- *Mines*: As a defense mechanism submarines lay mines in the ocean to protect against enemy submarines.

It can be concluded that all these capabilities make the submarine a very valuable asset. They can be deployed in a large range of different situations.

Communication Capabilities

During a mission it is important that the submarine can communicate. The intelligence gathered during a mission can be time sensitive and should be communicated with the armed forces. Furthermore, the submarine should be able to receive information from the outside world (e.g. news, change in mission, etc.). To make this possible, the submarine has a number of communication systems on board. Each of these have their own pros and cons, and are used in different situations. Sending information can be dangerous since the signal can be used to pinpoint the location of a submarine. Therefore a large amount of the information is classified. This includes the frequencies at which the systems operate. Because of the restrictions the information in this section will be less in depth. The Dutch submarines have three different communication systems available.

- **Very Low Frequency (VLF):** The frequency range is between 3-30 KHz for a Very Low Frequency (VLF) signal. The VLF frequency is used for over-the-horizon communication with the submarine [19]. Because of the large wavelength the signal is also able to penetrate water and can therefore be used to send messages to the submarine while submerged. The downside of this communication method is that the data rate is very low, so it is only used for navigation, Morse code, and to ask the submarine to surface [19]. Another downside is that the transmitter antenna needs to be huge and require a lot of power. Therefore it can only be placed on land, which means that the submarine cannot send messages via VLF, thus the submarine is only able to receive messages via Very High Frequency (VHF). Furthermore, the antenna required to transmit a message are very big, so big that the Dutch armed forces have not build one. To send a message they rely on other nations (e.g. Germany, France, Sweden) to transmit a message [22]. The dependence on other countries is a risk for the Navy.
- **Very High Frequency (VHF):** The frequency range is between 30-300 MHz for a VHF signal. The VHF signal cannot travel far over the horizon and is therefore often limited to 10/20 nautical miles, depending on weather and height of the antennae. The VHF antenna is mounted on top of the optical mast for maximum range capabilities [44]. Because of the range limitations the VHF is mainly used for communication with ships, airplanes and shore-stations. It is mostly used for telephone contact and general data transfer.
- **Satellite Communication (SATCOM):** The frequencies range used for SATCOM is classified. However a publicly available source shows that Royal Netherlands Navy uses the Ka-band (26.5–40 GHz) and Q-band (33-50 GHz) for the Advanced Extreme High Frequency (AEHF) program [62]. They also use the Ka-band and X-band (8.0–12.0 GHz) for the Wideband Global Satcom (WGS) program [62]. The connection can be used for the same information as the VHF connection. However, since the data rate can be higher it is also possible to send video's, photo's,

databases, etc. A downside of the current SATCOM capabilities is the dependence on other countries. Apart from the Brik-II, the Dutch Armed Force do not operate their own satellites and are there dependent on capabilities from allies. Therefore, other countries have knowledge about the Navy's activities. Furthermore the availability of SATCOM is not constantly available since the service is shared. Thus information is often still taken back to the harbor for analysis [19].

Each of the communications systems has their own pros and cons. They can be used in different situations and provide their benefit in different situation. It is clear that SATCOM is most useful for a submarine. The Brik-II satellite fill this need, it will be the first satellite capable of supporting the Dutch armed forces without dependence on other parties. The submarines have to be adjusted such that communication with Brik-II is possible. The development of such system is the objective of this MSc thesis.

3

Requirements

To satisfy the wishes from the Navy and deliver a product which has the correct characteristics, it is important to compile a detailed list of requirements for the project. The requirements are compiled in consideration with the Navy and the Air Force. Furthermore they are dictated by external limitations and the capabilities of the Brik-II satellite. To have a good understanding of how the system should function the potential role of the communication system in the submarine is described. Afterwards, the requirements the system shall meet are listed. These are important since they will ensure maximum deployability during missions.

3.1. Mission Concept

The submarine is a very versatile machine, it has large amounts of fire power, is hard to detect, and has a large amount of observation sensors on-board. Therefore, the submarine is a very effective deterrence against enemies. During times of peace, a submarine is still very useful for gathering information. Currently, the information on-board is not transferred to land. To improve the information distribution, the submarine will be equipped with a experimental communication system capable of communicating with Brik-II.

The communication system which will be designed in this thesis has to meet a number of requirements, such that it can be used during missions. In the initial design, the system will be installed on top of the submarine's sail since antenna has to be above water to communicate. The UHF frequency does not propagate far through water [26]. To protect the system from the sea water it will be installed inside a communication mast. The mast is a closed tube that houses the antennas of all communication systems onboard. The sail of the submarine is indicated by the white arrow in figure 3.1.

Figure 3.1: Sail of the Walrus submarine [12]

From the sail it can communicate with the Brik-II satellite. The communication will consist of two-way communication, i.e. transmitting and receiving message. The system will be controlled from inside the submarine using a computer. Here a message or file which has to be transferred can be selected. The system will also provide information regarding the satellite, such as when a satellite pass will occur, and the expected amount of data which can be transferred. During a mission it is important for the operator of the submarine to know when the satellite will pass. Since the satellite is in a Low Earth Orbit (LEO), communication will not always be possible because Brik-II will be over the horizon. When a satellite will pass is based on a prediction, that is the orbital elements of the satellite. If the orbital elements are not updated over a longer period of time the accuracy of this prediction degrades. Therefore, the elevation and azimuth angle of the satellite deviate from the real position, thus the time when the satellite passes over will not be accurately predictable. For safety reasons the submarine should be afloat only when the satellite passes over the submarine location. Therefore, it is important to provide an indication of when a satellite pass occurs. This might consist of a time-frame in which the pass will start along with a chance that the satellite will be there (e.g. 80% chance of contact between 9:34 and 9:52). Based on this information the operator can decide if it is worth the risk to float to the surface to communicate information. Another important aspect which determines the usability during a mission is how it influences the stealthiness of the submarine. The communication antenna has to be above the water to communicate since the UHF signal does not propagate well through water [26]. Surfacing increases the chance of visual detection by other parties. To limit the detectability, it would be preferred that the submarine only transmits a signal when necessary. A transmitted signal can be detected by other parties and be used to determine the submarine's position. Therefore, the Navy would like to have to capability to receive a message without the need to make initial contact with the Brik-II satellite (i.e. no transmission from the submarine to Brik-II). This should limit chance of the submarine being detected by potential adversaries, while it can still receive information transmitted by the Brik-II. Furthermore, if a transmission from the submarine is necessary, it is preferred that the system limits the transmission signals in directions other than that of the satellite. This means that the system will only transmit a signal with low power in other directions than that of the satellite. The purpose is again to limit the chance of detection since the signal will be weaker and therefore harder to detect, thus decreasing the likelihood of localisation. Concluding, the communication system should provide an adequate link budget, be integrated with the submarine, have a minimum detectability, and keep time afloat to a minimum. If the system meets these requirements, it will have added value during missions.

3.2. System requirements

From the mission concept and elaborate contact with both the Navy and the Air Force it was possible to gather a list of requirements for the communication system. These system requirements can be found in table 3.1. It should be mentioned that the cost of the system has not been taken into account as one of the requirements. The intended solution will probably be custom made by the Air Force and/or Navy and the costs will be relatively low. A detailed cost consideration is not included in this study.

ID	Requirement	Explanation
RQ-1	The system shall be able to transmit and receive messages from the Brik-II satellite using the UHF band	
RQ-1.1	The system shall provide a minimum link budget of >1 Mb during a single pass	The 1 Mb is set as a value which will provide enough reason for the submarine to surface
RQ-1.2	The system shall provide an estimation of the link budget during pass	
RQ-1.3	The system shall predict the chance of establishing contact during a certain period afloat (based on; The duration of submerging, the latest Two-Line Element Method (TLE) information, and the time the submarine can stay afloat)	Since the submarine can be submerged for a long time the accuracy of the prediction can vary. To enable the submarine personnel to make an informed decisions if they want to surface, this information should be provided
RQ-1.4	The system shall be able to maintain communication capabilities for at least 3 months after last contact	The system should still be usable after being submerged for a relatively long period
RQ-1.5	The system shall be able to receive and send messages when afloat	
RQ-1.6	The system shall be able to operate within 2 minutes after surfacing	To ensure a short duration of surfacing as this is a vulnerable situation for the submarine
RQ-1.7	The system shall be able to contact the Brik-II satellite under swaying conditions of less then 10 °/s	
RQ-1.8	The system shall be able to operate in a frequency range of 250 to 340 MHz	The extra frequency range is required to provide flexibility.
RQ-1.9	The system shall be able to operate in all weather conditions	
RQ-1.10	The system shall only transmit high power signals in the direction of the satellite to limit detectability	The submarine can be located by the interception of transmitted signal. Therefore the system should limit the necessities of transmission
RQ-2	The system shall be designed such that it can be integrated with the submarine	
RQ-2.1	The antenna system shall have a diameter <0.4 m and a height of <1 m such that it can be installed within the communication mast	
RQ-2.2	The cables shall pass through the pressure hull of the submarine according to the MIL-STD standards	The communication mast is not inside the pressure hull, therefore the cable have to pass through the pressure hull of the submarine
RQ-2.3	The system shall be powered by the 110 V system according to the MIL-STD-1399	
RQ-2.4	The system shall have a 19 inch server rack form factor with a limited depth of 40 cm	
RQ-2.5	The system shall consume less than 250 W of power while operating	
RQ-2.6	The system shall be secured in the communication mast	
RQ-2.7	The system shall be integrated into the communication suit of the submarine	The communication suit is the central system that controls the communication systems
RQ-2.8	The system shall be integrated without the removal or reduction in operational functionality of other systems on-board	Multiple communication systems can be located within the communication mast. The current systems have to remain functional
RQ-2.9	The system shall not interfere with other communication systems installed	If other systems operate in the same frequency domain, they cannot communicate simultaneously
RQ-3	The system shall be water and shock proof according to MIL-STD standards	
RQ-4	The system shall have a HMI	
RQ-4.1	The system shall have a screen to display information	
RQ-4.2	The system shall provide the satellite position, system status, GPS information, orbit information, possible system warnings, and contact status	
RQ-4.3	The system shall provide an interface from which a file can be selected for transmission	
RQ-4.4	The system shall consume less than 20 W of power during standby	
RQ-4.5	The interface shall be set-up such that it can be operated by an employee without an engineering background	
RQ-4.6	The system shall be rebootable within 5 minutes	
RQ-4.7	The system shall be able to store orbit parameters, file for transmission, error messages	
RQ-5	The system shall have an operational lifetime of 10 years	Expected time till the submarines are replaced
RQ-6	The system shall have service intervals of longer than 1 year	Maximum service interval submarines
RQ-7	The system shall have a mass of less than 30 kg	
RQ-8	The system shall be able to operate between a temperature of 0° to 45° Celsius	
RQ-9	The system shall be able to perform in all sea conditions	

Table 3.1: System requirements total system

Not all the requirements stated in table 3.1 can be met during this project. This has a number of reasons that have been listed below. The main focus of the project is to design and build a prototype system which can be used on-board the submarine. The main difference is that the system will not be integrated with the submarine. This means that the system has to be deployed outside by hand and taken inside before submerging. Also the computer system cannot communicate with other hardware on-board the submarine. The design of this first product has been discussed with the Navy, and the prototype requirements can be found in table 7.1 in appendix 1.

1. **Time**: A number of the requirements can be time consuming and meticulous to solve. These requirements often have to meet a certain military standard (MIL-STD), which would require large amounts of verification testing. Therefore it has been chosen to not focus on these requirements. The main focus is to overcome all the technical challenges related to the communication capabilities. Furthermore the operational deployability and usability aspects, such as the data throughput (RQ-1.1), will be focused on.

2. **Risk management**: During a project it is often beneficial to make a prototype. The prototype can be used for testing and validation. Making intermediate steps limits the risk of developing a system which would not be able to meet the requirements. Furthermore, it provides the opportunity for the Navy to provide feedback before the product is implemented in the submarine.

3. **Classification**: The submarine is a critical part of the Navy's operations. Therefore much of the information regarding the submarines inner workings are classified. This classification level is not given to non-military personnel. Therefore the exact documentation which would allow for a more detailed design, including the integration with the submarine, is not available.

4. **Necessity**: The submarines currently in service by the Navy are scheduled for replacement in 2027 [35]. Since this is relatively soon it could be decided to not develop a full integrated system. However, the feedback received on the current prototype would be an excellent basis for integration from the ground-up in the new submarines. In a new submarine design, the communication systems could be adjusted to integrate seamlessly with the submarine.

3.2.1. Similarities Remote Radio Station

The RRS is a portable ground station which can be used in any location on earth. The system has the capability to communicate with Brik-II. Therefore, the RRS has many similarities with the system that will be designed in this project. Since the system will be developed in the short duration of this MSc thesis, it was chosen to use the RRS as a basis for the design. The electronic hardware is adequate for a first iteration, as it has already been developed and tested. The software on the RRS systems is flexible and can be adapted to fit the Navy's requirements. The submarine communication system cannot be a copy the hardware of RRS because of the size constraints that are imposed by the communication mast of the submarine. The rotor in combination with the antenna are too large to meet requirement RQ-2.1. Thus the antenna system has to be redesigned to fit the requirement from the Navy, and is therefore the main focus of this project.

3.2.2. Prototype Requirements

The list of requirements for the prototype SATCOM system can be seen in table 7.1 in appendix 1. Since the functionality that should be achieved has not changed, a large part of the requirements have not changed compared to the full system requirements. Most of the requirements that have changed are regarding the integration with the submarine. During the design process of the antenna system a number of requirements can be regarded as the leading requirements. These requirements can be seen in table 3.2. The three leading requirements are related to the antenna of the system. The design of the antenna can be seen as the main focus of the project. The rest of the hardware used in the system (e.g. HMI) will not be implemented during the project. These parts can be based largely on the hardware that has been developed for the RRS.

ID	Requirement	Explanation
RQ-P-1.1	The system shall provide a minimum link budget of >1 Mb during a single pass under ideal conditions	The 1 Mb is set as a value which provide enough reason for the submarine to surface
RQ-P-1.8	The system shall only transmit high power signals in the direction of the satellite to limit detectability	The submarine can be located by the interception of transmitted signal. Therefore the system should limit the necessities of transmission
RQ-P-2.1	The system shall have a diameter <0.4 m and length of <1 m	The system should be carried up through the stairwell and hatch

Table 3.2: Leading requirements during the project

The three leading requirements each impose a trade-off on the design of the communication system. The detectability should be limited by only transmitting a high power signal in the direction of the satellite (RQ-P-1.8). Furthermore, in section 3.1 it has been indicated that the Navy prefers to limit transmissions from the submarine. During the project it will become clear these two points impose a trade-off with set link budget requirement (RQ-P-1.1). The third leading requirement is the size constraints for the design (RQ-P-2.1). This will limit the choice of different types of antennas (e.g. RRS Yagi-Uda) that can be implemented.

4

Antenna design

The RRS is designed by the Sectie Space together with 982 Squadron and serves as a good basis for the submarine communication system. However the system cannot be fully identical due to the differences in requirements. The system in the submarine has strict space requirements which makes the Yagi-Uda antenna used in the RRS too large, therefore a new antenna design is needed. The process of designing the antenna will be discussed in this chapter, and will be the main focus of the project. First, the theory used in the link analysis will be discussed. Second, it will be explained how the orbital characteristics have been implemented. Lastly it will be shown how the optimal antenna is found, along with the end result of the link budget for the submarine.

4.1. Link Analysis

The link analysis is used to determine the link strength at a point during the pass of the satellite. With the link strength the instantaneous data transfer rate can be calculated. If the link strength is calculated for the whole pass and integrated over time, the total mount of data transferred can be determined. The link strength is expressed in the form of the SNR. The section below shows how the instantaneous SNR is determined.

4.1.1. Signal to Noise Ratio

The SNR is influenced by a number of phenomena, such as the Free Space Path Loss (FSPL) or the atmospheric attenuation of the signal. Each of these factors have to be calculated to determine the SNR of the signal between the submarine and the satellite. The SNR can be expressed by the equation below.

$$SNR = EIRP - 10log(B) - FSPL - L + \frac{G}{T} + 10log(\frac{1}{k}) \tag{4.1}$$

Where:

- $EIRP$ | Effective Isotropic Radiated Power
- B | Bandwidth of the signal
- $FSPL$ | Free Space Path Loss
- L| Atmospheric attenuation loss
- $\frac{G}{T}$ | Gain Temperature Ratio
- k| Boltzmann constant

The following parts of equation 4.1 can already be determined, since the bandwidth is set for 25 KHz and the Boltzmann constant is a physical constant which does not vary.

$$10log(\frac{1}{k}) = 228.60[dBJ/K] \quad (4.2) \qquad 10log(B) = 43.9794[dB] \quad (4.3)$$

The other parts of SNR equation 4.1 are explained below.

Effective Isotropic Radiated Power

The Effective Isotropic Radiated Power (EIRP) is a combination of the transmit power and transmit gain. It can be described using equation 4.4 below:

$$EIRP = 10log(P) + G \quad (4.4)$$

Where:

- P | Transmit power [W]
- G | Gain transmitting antenna [dB]

The antenna gain is from the transmitting system. Therefore during downlink transmission the satellite antenna is used to calculate the EIRP. For the uplink transmission the ground station antenna will be used.

Free Space Path Loss

FSPL is the loss which occurs because the signal propagates as a spherical wave with constant power flux density but with the surface increasing with the second power of the distance from the transmitter. The effect of this can be calculated using the following equation 4.5:

$$FSPL = 20log(\frac{4\pi * D}{\lambda}) \quad (4.5)$$

Where:

- λ | The wavelength [m], which is calculated using the speed of light (c) and the communication frequency used: $\lambda = \frac{c}{f}$
- D | Distance between the satellite and the ground station

Atmospheric losses

The UHF signal that is used to communicate is not at such a high frequency that it experiences strong attenuation in the atmosphere. Weather circumstances don't have a large influence on the signal. The attenuation of a signal over different frequency can be seen in figure 4.1 below. Figure 4.1 has been recorded above land. The water vapor density is around 11.5 g/m^3 at sea [42].

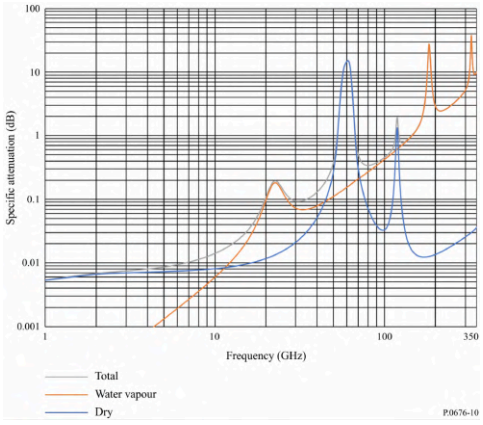

Figure 4.1: Specific attenuation due to atmospheric gases (Pressure = $1013.25hPa$, Temperature = $15°C$, Water Vapour Density = $7.5g/m^3$) [41]

The attenuation due to atmospheric gases is nearly not noticeable according to the figure. Since the water vapor density is higher at sea, a low attenuation value of 0.3 dB has been chosen such that minor attenuations are accounted for.

Gain-Temperature Ratio
The last part of the SNR equation is the gain-temperature (G/T) ratio of the receiving system. Therefore the temperature and antenna gain should be from the receiving system. The temperatures have been provided in the Interface Control Document supplied by the Air Force. From the document, the antenna noise temperature is 290 K and the electronics have a noise temperature of 800 K for downlink and 550 K for the uplink electronics. The G/T ratio can be calculated as shown in equation 4.6 below.

$$\frac{G}{T} = G - 10log(T) \tag{4.6}$$

Where:

- G | Gain of receiving system [dB]
- T | Total equivalent noise temperature of receiving system [K]

The GT-ratio in equation(4.6), as well as in the EIRP (4.4), the gain of the antennae is based on the orbital position. Meaning that the direction of the ground segment with respect to the radiation pattern of the satellite's antenna is considered. The same is done for the gain of the ground segment, in this case the antenna designed in this project. This makes sure that the model is not oversimplified by taking a fixed gain for the antennae.

4.1.2. Modulation scheme

When the SNR is determined using equation 4.1, the corresponding data rate should be calculated. The data rate is dependent on the modulation scheme and the coding rate [37]. The steps possible in modulation and coding rate are as predefined by the ACM modes. A higher SNR makes a higher ACM mode possible, which yields a higher data rate. The ACM modes are approximately 1 dB apart, meaning that when the SNR increases with 1 dB a higher ACM mode can be used, as can be seen in figure 4.2. The selected ACM mode depends on the SNR margin as received by the ground segment. When a high enough SNR margin is detected, it will inform the transmitter that a higher ACM mode can be used. To do this the receiver has to send a signal to the transmitter. In submarine operations it often not desired to transmit a signal since this can give away your location. This is also mentioned in requirement RQ-P-1.8. Therefore downlink will be fixed in ACM mode 1, when no ACM mode update can be transmitted. To see if ACM mode 1 or higher is possible, the $\frac{E_b}{N_0}$, the normalized SNR per bit, needs to be calculated. This is done using the equation 4.7 below [27]. For this calculation a BER of 10^{-6} has been set [37]. BER $= 10^{-6}$ should be good enough for the relatively low UHF frequency used [40]. During a pass in which 1 MB is send, only 1 bit would be wrong on average, which is acceptable.

$$SNR = \frac{E_b}{N_0}\eta \tag{4.7}$$

Where η is the coding efficiency of the ACM mode. For each of the coding rates, corresponding to the SNR modes, the data rate (DR) can be calculated using the following equation 4.8.

$$DR = B * \eta \tag{4.8}$$

Where B is the bandwidth used, which is set for 25 KHz. When the ACM mode is variable, the SNR calculated in equation 4.7 should be lower than the SNR determined by the link strength calculation. To make sure this is always the case, a safety factor is added. The safety factor is necessary since the model will not provide a perfect simulation of reality and there are always small and fast changing fluctuations in a transmission signal. The safety factor is applied such that the SNR should be double compared to what would be minimal, hence a safety factor of 3 dB [47]. If a constantly varying ACM protocol would be implemented the safety factor can be reduced 0.8 dB [29]. Currently this is not

supported by the Brik-II satellite. With the safety factor, transmission is possible when the following condition is met 4.9.

$$SNR \geq \frac{E_b}{N_0}\eta + S_{margin} \tag{4.9}$$

The $\frac{E_b}{N_0}$ and η are the two parameters which are varied when the ACM mode changes, with lower ACM mode condition 4.9 is easier met. The $\frac{E_b}{N_0}$ and η accompanying the ACM modes are found in the CCSDS [27] manual. These are visualised in the figure 4.2, with the selected value of BER $= 10^{-6}$ in table 4.3.

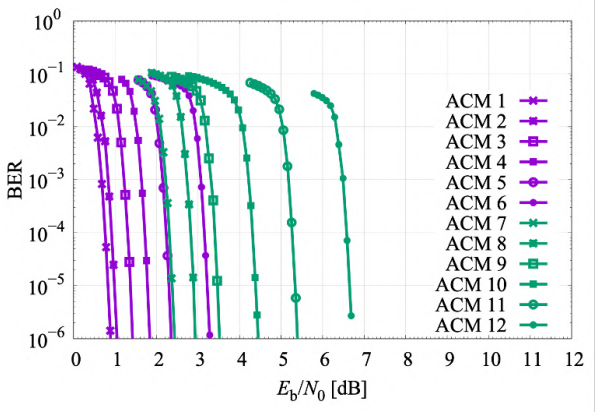

Figure 4.2: ACM modes $\frac{E_b}{N_0}$ for set BER [27]

	ACM	E_s/N_0 [dB]	E_b/N_0 [dB]	Efficiency
QPSK	1	-0.58	0.90	0.71
	2	0.42	1.08	0.86
	3	1.60	1.44	1.04
	4	2.71	1.87	1.21
	5	3.83	2.39	1.39
	6	5.42	3.30	1.63
8PSK	7	3.91	2.41	1.39
	8	5.10	3.00	1.63
	9	6.25	3.63	1.84
	10	7.75	4.53	2.10
	11	9.21	5.46	2.37
	12	10.90	6.69	2.64

Figure 4.3: ACM modes $\frac{E_b}{N_0}$ for BER = 10^{-6} [27]

4.1.3. Satellite Antenna Gain

The antenna gain of the satellite is used during for the link budget calculation. In case of downlink it is used in the EIRP calculation, while for uplink it is used in the $\frac{G}{T}$ ratio. The satellite has two different antenna onboard, one for uplink and one for downlink, as can be seen in figure 4.4. Both have a different radiation pattern. To obtain the antenna gain that is required to calculate the EIRP and $\frac{G}{T}$ ratio, the orientation of the satellite with respect to the ground segment should be known. The orientation can be used to determine where the ground station is in the radiation pattern of the satellite. The satellite antennas radiation patterns have been measured by ISIS, and can be seen in figure 4.5. The associated data is used in the simulation of the link budget.

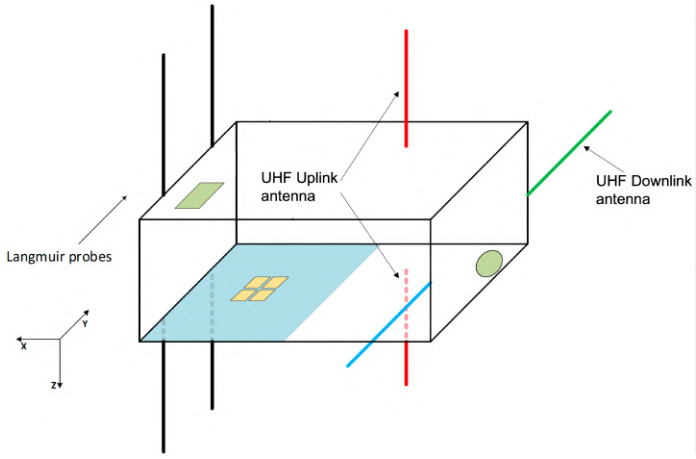

Figure 4.4: Antennas on Brik-II

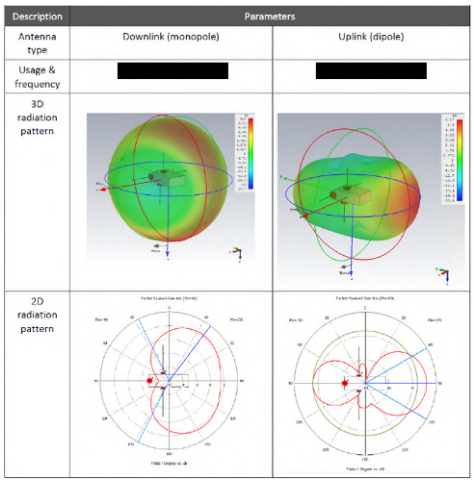

Figure 4.5: Satellite radiation pattern uplink and downlink antenna [50]

4.2. Orbital Characteristics

The instantaneous data rate of the pass can be calculated if the distance and antenna gain of the ground segment and satellite are known. To calculate these parameters, the orbit of the satellite should be modeled. This is done using a SGP4 propagator. How the propagator has been implemented will be explained in the section 4.2.1 below. Hereafter the required modifications to the propagator output data are discussed.

4.2.1. Standard General Perturbations Satellite Orbit Model 4

The SGP4 propagation model is widely used as a way to predict the future satellite position. The orbital characteristics which are used to predict the future position are supplied in the form of the TLE. The propagator has been built in MATLAB by D. Vallado, and has been sourced from CelesTrak [63]. The functioning of the propagator has been verified by comparisons with the implementation of the SGP4 model used in the Brik-II ground station. The delta between the two models is less than 5 s in pass. Since an average pass takes ±12 min, the deviation would be a maximum of 0.7%. Therefore the prediction was deemed adequate. Furthermore, the accuracy could not be verified in more detail since the prediction provided by the Air Force were not more accurate. On top of the CelesTrak propagator a GUI has been made which makes using it easier. The GUI is based on the design made by D. Deluca, which was taken as a basis [28]. The inputs of the GUI is explained below, along with a picture 4.6.

1. Here a TLE file can be selected from file. This has to be a .txt file but can be any TLE available
2. The start date and time of the propagation
3. The end date and time of the propagation
4. The step size used in the propagation. The influence on the accuracy is discussed further in this section
5. The latitude, longitude and altitude of the ground station location. Please note that this is a World Geodetic System 1984 (WGS84) model of the earth, so it is not the same as normal long/lat/altitude [17].

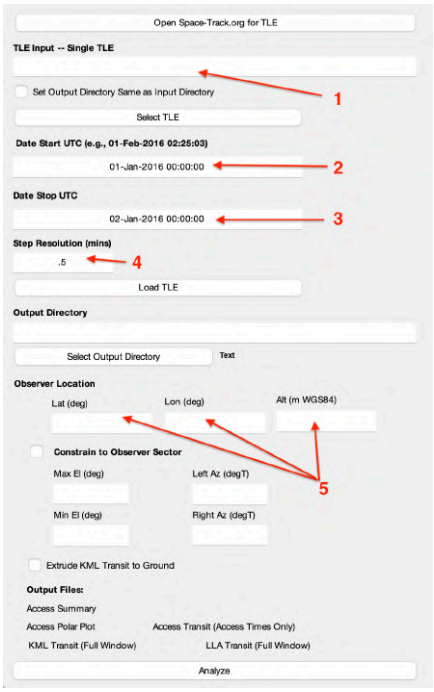

Figure 4.6: GUI of SGP4 propagator in MATLAB

The main output of the propagator is a text file containing the start, end, duration, and max elevation for all passes in the set time frame. Furthermore, propagator provides the elevation angle of the satellite at each time step during the passes (i.e. when visible above the horizon). This information is needed to perform the link budget analysis. The output from the propagator can also provide the orientation ground station with respect to the satellite. This is needed as the radiation pattern of the satellite antenna is taken into account. When the orientation of the ground station in the radiation pattern is known the satellite antenna gain is found. To obtain the orientation a number of calculations have to be performed. The propagator has been adjusted in such a way that the velocity vector of the satellite is extracted, which is then used to determined the orientation of the satellite with respect to the ground station. To calculate this, a number of reference frame translations and rotations are required. The actions required are simplified to 2D in figure 4.7 below.

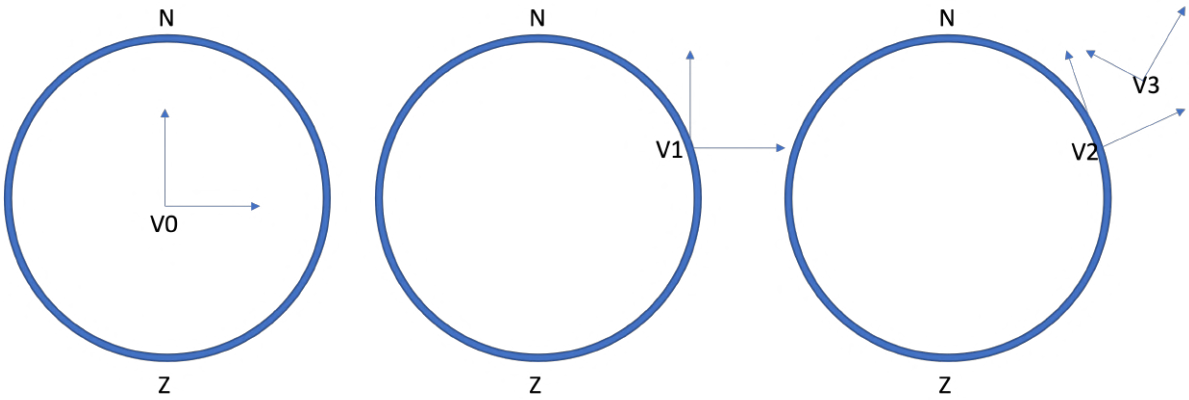

Figure 4.7: Rotations of reference frame necessary

The velocity vector obtained form the propagator is expressed in the V0 reference frame. V0 lies in the center of the earth according to the WGS84 model. The translation is done using the provided longitude, longitude, and altitude of the observer location. The V2 reference is achieved by rotating the frame such that one axis is perpendicular to the surface and one axis points to the WGS84 north pole. The V3 frame is the reference frame of the satellite. In this reference frame, the radiation patterns of the antennas are expressed. It is known that the direction of flight is in the -Z direction and the -X direction point to the center of the earth. If the velocity vector is known in the V2 coordinate frame, the rotational matrix between V2 and V3 can be calculated. Using the rotation matrix, along with the position vector of the satellite in the V2 reference frame, the position vector of the observer location in the V3 reference frame can determined. Since the orientation of the antenna radiation pattern with respect to the V3 reference frame is known, the antenna gain can be derived as the location of the observer in the V3 frame is known. Note that the rotation matrix has to be calculated for each step in the propagation since the orientation of V3 with respect to V2 changes constantly. Now the orientation of the satellite with respect to the ground segment is known at every location, therefore the antenna gain is found.

A number of extra adjustments are performed to the propagator output data. Since the propagator provides the information at all steps of the satellite's orbit, it does not remove indices when the satellite is below the horizon. As over the horizon communication is not possible, these will be removed. Furthermore, it will be useful to have the ability to remove passes that do not reach a certain elevation angle with respect to the observer. Since a pass with a low maximum elevation will not provide decent communication opportunity as the contact time is short. Another functionality that has been added is the ability to remove the propagation indices when the satellite is below a certain elevation angle. Thus the elevation angle from which communication is possible can be set. The functionally has been added since communication at low elevation angles can be unreliable due to link strength variation [34]. If the removal of certain passes and elevation angles is required, it will be discussed in the optimisation

section 4.5. The input parameters for the propagator are discussed in the sections hereafter.

4.2.2. Integration Step

The total data transferred over a certain period is calculated by integrating; The data rate is calculated for each point, hereafter it is multiplied with a small time step and summated to yield total data throughput. The time step which is used in the integration should be determined such that the integration produces accurate results. However, the time step cannot be made too small since the time step has a large influence on the computational time required. The step size is determined by running a small propagation of a time period, from 22-Sep-2021 18:40:00 till 23-Sep-2021 03:10:00, for multiple step sizes. Also the calculation duration has been recorded, to provide an indication of what the computational duration would be when propagation over a larger time frame. The large time frame is from Aug-2021 till Apr-2022, this time frame has been used to do the final antenna optimization. The recorded data can be seen in table 4.1. The **bold** line with an integration step of 0.1 min is the integration step chosen.

Step [min]	Step [s]	Data [MB]	Deviation	1/2 day propagation run time [s]	8 months propagation run time [h]
0,001	0,06	7,0349	0,000%	1524	225,21
0,005	0,3	7,0350	0,001%	305	45,04
0,01	0,6	7,0317	0,046%	152	22,52
0,05	3	7,0223	0,179%	30	4,50
0,075	4,5	7,0190	0,227%	20	3,00
0,1	**6**	**7,0157**	**0,274%**	**15**	**2,25**
0,125	7,5	7,0057	0,417%	12	1,80
0,25	15	6,9891	0,655%	6	0,90
0,5	30	7,0556	0,293%	3	0,45
0,75	45	6,8892	2,115%	2	0,30
1	60	6,6562	5,689%	2	0,23

Table 4.1: Integration step size results

The 0.1 min is chosen based on the trade-off between computational time and accuracy. The 0.274% deviation is relatively small. Going smaller would greatly increase the computational time as seen in the most right column of table 4.1. The 0.5 min time step could also be considered as an option since the deviation is smaller compared to the 0.1 min. However, the step sizes surrounding the 0.5 min show a larger deviation. The 0.5 min step size coincides just right with the start and end of the communication period. Therefore the deviation is less compared to the surrounding step sizes. A step size of 0.1 min, which is 6 s, along with the fact that a pass last around 10-12 minutes would yield around 100 to 120 steps. Over these steps the instantaneously data rate is integrated to obtain the total data throughput.

4.2.3. Propagation time

The design of the antenna should be based on real life situations. Such situation can be created using the SGP4 propagator, using the TLE information of Brik-II. How the satellite passes over the ground segment is an important parameter in the design process. The passes should include a good variety of passes, meaning that they should reach different maximum elevations during the pass. The orbital parameters of Brik-II cause the passes to cluster together in a roughly 11h window, in which passes are separated by the orbital period (98 min). The satellite passes over the main ground station in Dongen (NL) 6 or 7 times a day. Also the maximum elevations reached during the passes changes every day. To optimise the antenna as much as possible, it would be preferred to get a mix of different maximum elevation passes. Why Dongen was chosen a location is explained in section 4.2.4. To get an idea of what passes would happen over a certain time frame, the propagation has been done over the ground station in Dongen for 3 different time frames. How often a certain maximum elevation is achieved during a pass can be seen in the histograms below.

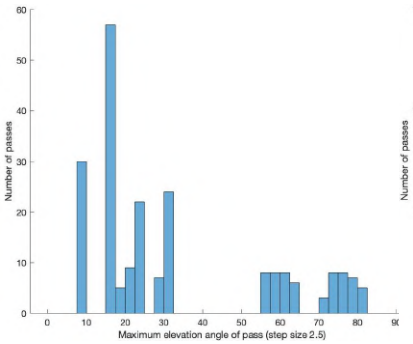

Figure 4.8: 1 month propagation

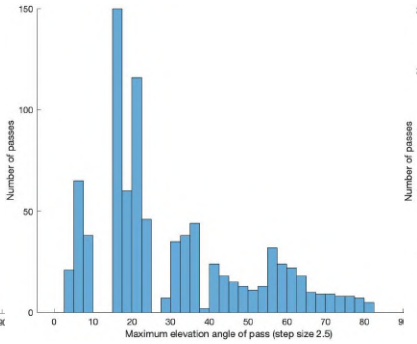

Figure 4.9: 4 months propagation

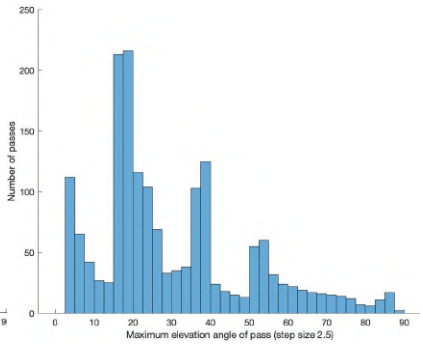

Figure 4.10: 8 months propagation

In figure 4.8 the propagation period is 1 month. It can be observed that the spread of different passes is relatively small since the duration is to0 short. In the short period no precession of the orbit has occurred. Therefore, the propagation needs to be longer such that more variation in pass in present in the data set. More variation will provide make sure that the antenna is optimised for a range of passes. In figure 4.9 the spread is much better, as it is over 4 months. However, there are still parts were there are no passes, especially between 10-15° and 25-30° elevation. In figure 4.10 the propagation has been run for 8 months. The data seems to be adequate to use as there is a good range of different passes. A longer propagation than 8 months might yield a better distribution of passes, however the computational time required to propagate satellite for 8 months is 7 days. Therefore it was chosen to not increase the propagation duration.

4.2.4. Ground Segment Location

The location of the ground segment as used in the propagator has an influence on the antenna design. The passes observed change for different locations on earth. The longitude has no influence on the passes observed. The latitude has a large influence on the passes as observed from the ground segment. It was investigated how the latitude influences the total amount of data which can be transferred. The propagation has been run from a number of latitudes for a period of one day (22-Sep-2021 00:00:00 till 23-Sep-2021 00:00:00), with a step size of 0.1 min as determined in section 4.2.2. The results can be seen in figure 4.11 below. The gain of the ground segment has been set at 0 dB, as an antenna radiation pattern might influence the results. The radiation pattern of the satellite's antenna has been taken into account. Furthermore the connection measured is the downlink from satellite to ground segment while using only ACM mode 1.

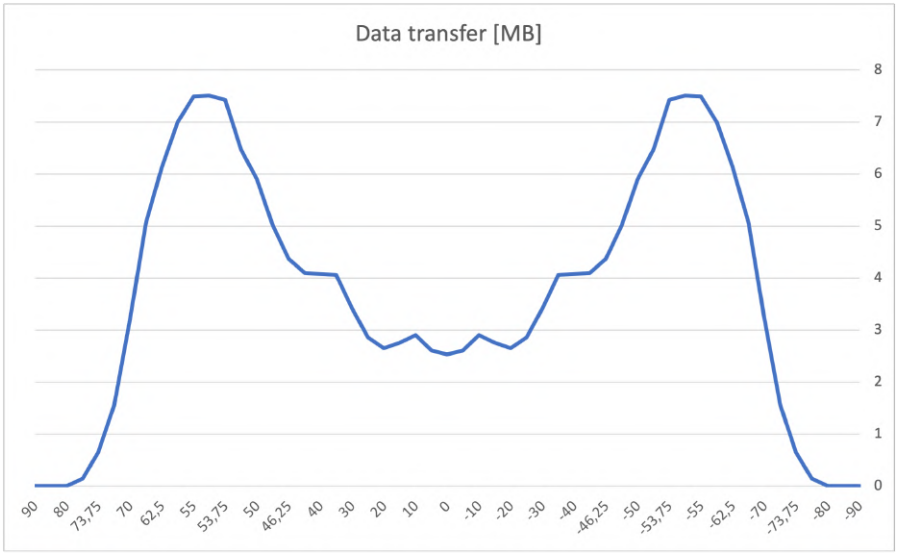

Figure 4.11: Data transfer for different latitudes

The main observation from figure 4.11 is that the latitude has a large influence on the total amount of data which can be transferred. Furthermore the lower and upper boundary of +/- 70° shows that there are places on earth where no communication is possible. The boundaries are caused by the 60.7° inclination orbit of Brik-II. The link budget is lower around the equator compared to the +/- 55° to 60° latitude. The contact time is lower compared to the higher latitudes, hence there is less time for communication. Because of this the choice for an optimisation location was not trivial. Since the primary objective of the Royal Netherlands Navy is to protect the Netherlands, it has been chosen to select a location at the same latitude. Because the Netherlands is relatively small and the latitude located at the peak in figure 4.11, the exact location does not have a large influence. Therefore, the military base where the 982 Squadron is stationed was chosen. So the location is in Dongen at latitude: 51.64° longitude: 4.96°. This location will also be used to conduct the tests that are discussed in section 6.

4.3. Submarine Antenna

The design of the submarine antenna is critical for the mission capabilities of the system. The radiation pattern should be designed such that the maximum amount of data can be transmitted while still adhering to all the requirements. There are many different antennae which have been considered. Each of these will be explained below, along with the benefits and downsides of this antenna within the environment set by the Navy.

1. **Yagi-Uda antenna** The Yagi-Uda antenna is a commonly used antenna. They can often be found on top of buildings and houses were it used to receive television. They work by sending a signal through the driving element, which is usually a folded dipole antenna. The driving element can be seen in figure 4.12 as the double wire. Behind the driving element there is a reflector. In front of the driving element are the directors, they focus the signal in the direction of the antenna. This results in an increased gain in the direction in the antenna, while at the same time make it less susceptible to signals from other directions.

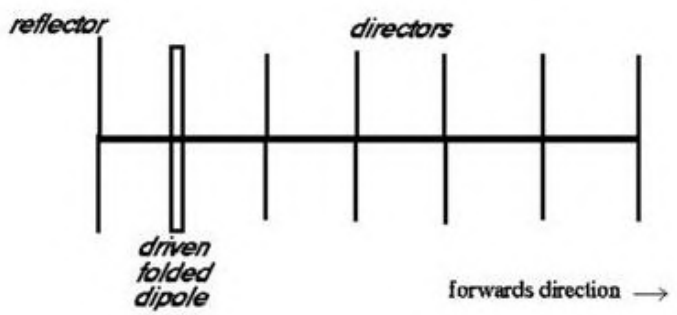

Figure 4.12: Yagi-Uda Antenna [58]

The directional high gain signal is useful for high data rate transmissions. However, the directional signal is also the downside of this design since it has to be pointed towards the satellite. Because the mast in which the antenna has to be installed has a relatively small diameter (40 cm) it would not be possible to point the antenna towards the satellite. The mast is not large enough to accommodate an antenna along with a rotor system used to track the satellite. Along with size constraints, a mechanical system with rotors used to track the satellite would not be suitable. As the submarine might be rocking due to waves and currents. Therefore the system is required to respond quickly to movement of the boat. Such system can probably be build, however it would complicate the system. So a Yagi-Uda antenna has multiple drawbacks, with the size constraints being the main one. Thus it is not chosen for further development in this project.

2. **Phased Array antenna** The next antenna which is considered is the Phased Array antenna. The antenna consists of a grid of antennae called elements, which can be controlled to add up in a certain direction and cancel each other out in other directions. Thus a number of low gain

omnidirectional antennae can form a directional high gain antenna if controlled correctly. The resulting antenna beam has a controllable direction. The beam is steered by commanding each element to transmit or receive with a small phase difference. The antenna does not have any moving parts therefore the steering can happen very fast, which is beneficial in rocky seas and increases reliability since moving parts can fail. A schematic view of a phased array antenna can be seen in figure 4.13.

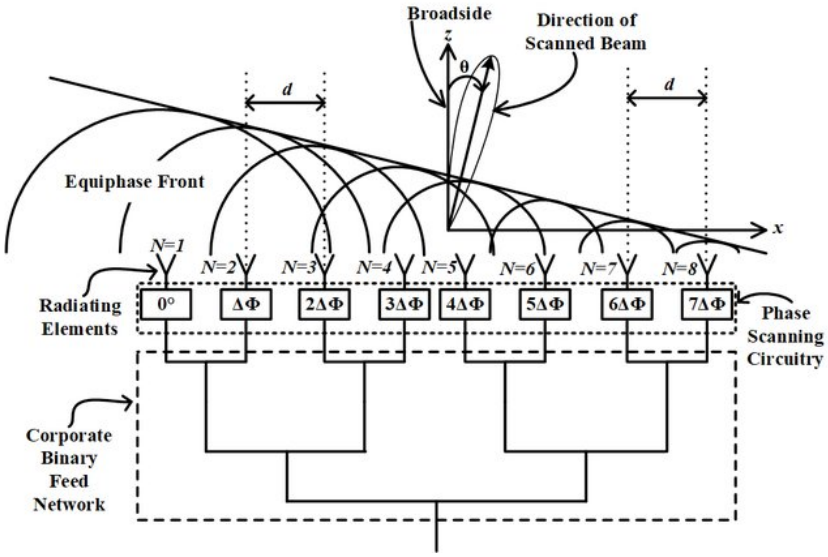

Figure 4.13: Phased Array antenna [57]

The elements which form the array can be arranged in different ways. Commonly used is a grid of elements which are spaced a constant distance apart. Complex form-factors are possible but would require an extensive control system. When considering a grid design, the maximum distance between the elements can be determined using equation 4.10.

$$d_{max} = \frac{\lambda}{1 + |cos(\theta_{initial})|} \tag{4.10}$$

Where, $\theta_{initial}$ is the angle at which the signal of the satellite should be picked-up, and λ is the wavelength of the signal. The maximum distance (d_{max}) is minimal when the pickup angle is 0°, resulting in a maximum distance of ± 55 cm when considering the downlink frequency. The maximum distance does not cause any problems since the system should fit into the mast. So the minimum distance between the elements is more critical. A minimum distance is necessary because otherwise the signal of each element would be relatively similar, which constrains the adjustment of the main beam in the antenna pattern. The minimum distance between the elements would be around $\lambda/10 \approx 10$ cm [33]. Since it is not advisable to approach this limit, the practical minimum distance can be set around 15 cm. Therefore the total size of the array can become relatively large with increasing number of elements. When considering a common monopole quarter wavelength antenna as the element used the size of a 3 by 3 array would be approximately 1 by 1 m. Thus it can be concluded that a phased array antenna would not meet the set size requirements. Therefore it will not be investigated for further development. If a higher frequency signal could be used, a phased array antenna would become feasible and be appealing because of the above mentioned benefits.

3. **Egg-beater antenna** The egg-beater antenna is a static antenna meaning it does not have active beam steering or a mechanical pointing system. Therefore the radiation pattern is configured such that it is omnidirectional around the vertical axis. Since the antenna has no steering, the peak gain of the antenna is lower because the radiation power is distributed in all directions. The low peak

gain results in a lower SNR, thus the ACM mode used is generally lower. Therefore the data rate is lower compared to a steerable high gain antenna. The main advantage is that steering is not necessary. The rocking of the submarine does not have a large influence on the perceived gain since radiation pattern does not have a large gradient. An example of an Egg-Beater antenna can be seen in figure 4.14.

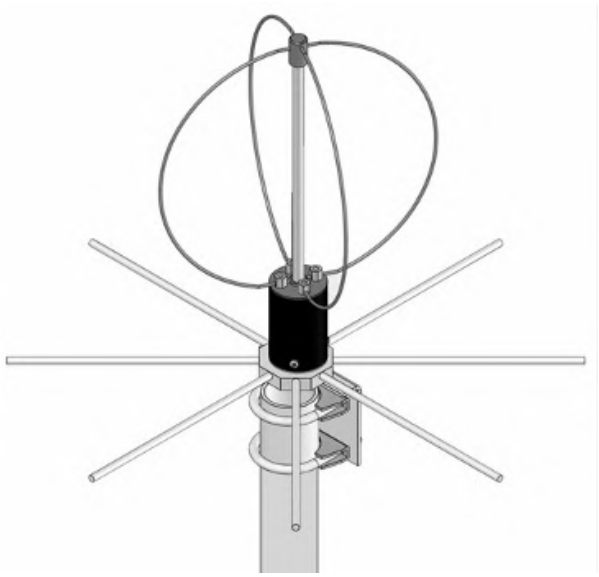

Figure 4.14: Egg-Beater antenna [5]

The diameter of two circles which form the antenna is depended on the wavelength of the frequency used, as circumference is equal to one wavelength. Using the downlink frequency, the diameter of the circle would be ± 37.5 cm, which is relatively close to the maximum diameter of 40 cm which is allowed by requirement RQ-P-2.1. Another factor to consider in satellite communication is the polarisation of the electromagnetic field as produced by the antenna. Often satellites are circularly polarised as this makes the exact orientation of the satellite with respect to the ground station less important since a match in polarisation with the ground station antenna can be achieved in any orientation. Therefore there are no polarisation mismatches, that would decrease the link budget and cause a lower data transfer rate [48]. The downside of having a circularly polarised antenna is that they are relatively expensive [55]. Therefore they are not so often used on small CubeSat like Brik-II. The Brik-II used two separate antenna for uplink and downlink. The uplink antenna is a dipole antenna, the downlink antenna is a monopole. Both of these are linearly polarised [50]. This information is important as the ground segment polarisation has to be adjusted to the polarisation of the satellite antenna. An Egg-Beater antenna is often used for satellite communication as it is circularly polarised. However, as Brik-II's antenna's are not circularly polarised this would make it less suited for the submarine communication system. A mismatch in polarisation causes a 3 dB loss, which would best be prevented [59]. As this loss is quit large in comparison to the tight link budget it was chosen to not investigate the egg-beater antenna further. Another factor which reinforced this decision is the lack of parameters which can be varied on the design. The only parameters which can be varied are the size of the ground plane and the distance to the ground plane. Therefore the egg-beater antenna does not leave much scope for customisation, that could yield better performance.

4. **Helical antenna** The last antenna considered here is the Helical antenna. It consists of wire which is shaped as a helix with a fixed diameter. An example of the helical antenna can be seen in figure 4.15. A helical antenna does not have any steering abilities. The radiation pattern of the antenna is fixed. A helical can be used in two different modes, depending on the circumference (C) of the helix in relative to the wavelength (λ) [45]:

1. **Axial mode:** Axial mode is possible when the circumference of the helix meets the following condition: $\frac{3\lambda}{4} \leq C \leq \frac{4\lambda}{3}$. In the axial mode main lobe of the radiation pattern in is the direction of the helix (perpendicular to the ground plane). It is relatively high gain but only transmits upwards. The signal is circularly polarised when in axial mode.
2. **Normal mode:** Normal mode is possible when the circumference of the helix meets the following condition: $C \ll \frac{\lambda}{4}$. In the normal mode the radiation pattern is closely related to a monopole. The maximum gain of the antenna is parallel to the ground plane. Perpendicular to the ground plane, the gain is generally the lowest. Also the peak gain in normal mode is lower compared to axial mode, as it has to be spread out over a larger surface. The wave emitted by the antenna is linearly polarised in normal mode, which matches the polarisation of the Brik-II antenna.

Figure 4.15: Helical Antenna [8]

Since the antenna can be designed to operate in two different zones, it would be interesting to investigate whether a design in the boundary of the regions would be possible. The normal mode is ideal for an omnidirectional radiation pattern, such that it can cover a large part of the satellite's pass. Furthermore it is linearly polarised. The downside of the normal mode is that the antenna right above the antenna is low. However the distance is also small at that point during the pass so communication would most likely still be possible. What the performance of the system is right above the ground segments. The axial mode would be perfect to compensate for this, as this would increase the gain in this area. Thus a combination of both modes would yield a favourable result.

The shape of the antenna is also desirable as it uses the allocated space in on-board the satellite perfectly. Since the antenna would operate in the boundary region, it has a circumference which

will be smaller than $\frac{3\lambda}{4}$, thus the diameter will be smaller than ± 26 cm. So the antenna would meet requirement RQ-P-2.1, as long as the length is less than 1m.

To see what design of helical antenna would result in the highest data transfer capability possible, an optimisation should be run. It would include the orbital characteristics as discussed in section 4.2, and the link analysis calculations as explained in section 4.1.

With the choice of the helical antenna, along with the information presented in chapter 3, an answers to sub-question 1 of the research questions as defined in section 1.1 can be given. The system will be placed in the communication mast on top of the sail of the submarine. The location is required as the UHF signal does not propagate through water [26]. To protect the system from sea water it will be placed inside a closed tube; the communication mast. The tube imposes size constraint to the antenna as defined by requirement RQ-P-2.1. The electronics of the system, which are assumed identical to the hardware used in the RRS, will be placed inside the submarine. The size constraints, as imposed by the communication mast, limit the possible types of an antenna suited. From the options considered, the helical antenna has been selected as the most optimal design. With this information it can be concluded that the physical design characteristics of the communication system have been identified.

4.4. Simulation Model

The helical antenna can have various form factors. To determine what design would be best suited a simulation model has been made. The goal is to calculate what design would have the largest amount of data throughput, and still meet all the requirements. In figure 4.16 the simulation model is represented in the form of a flowchart.

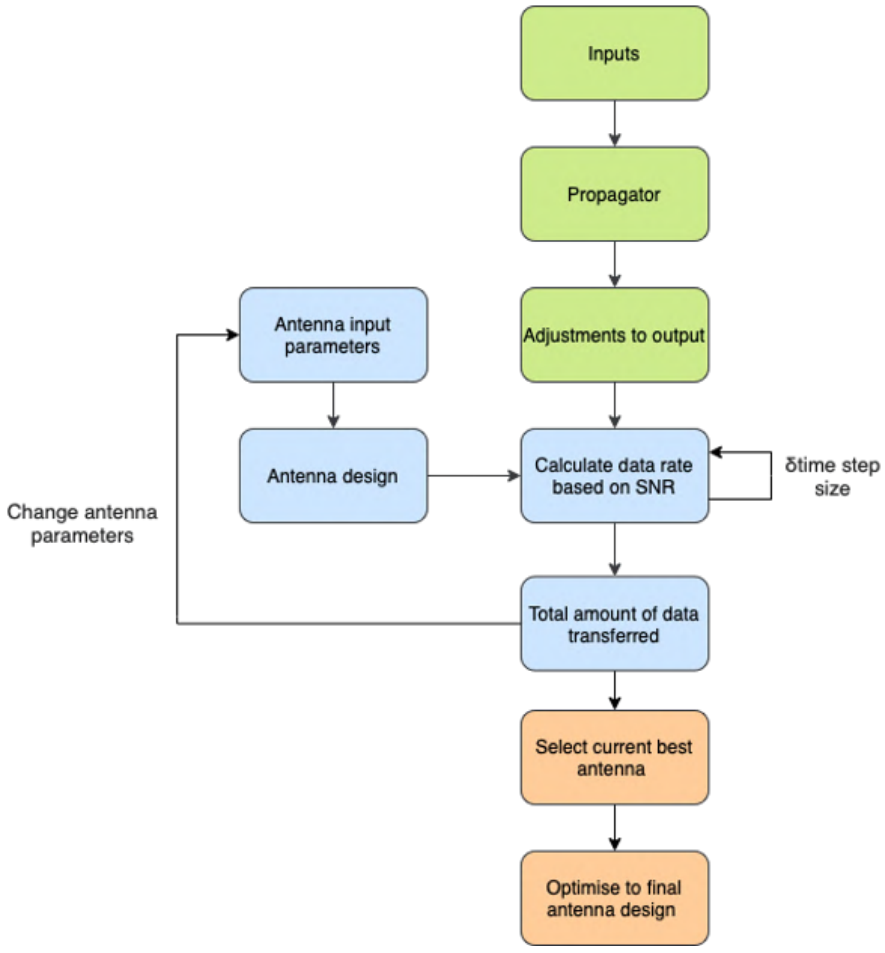

Figure 4.16: Simulation model flowchart

The first step in the model is to calculate the orbital propagation of the satellite over a set period. The selection of the period, location and step size corresponds to what is explained in section 4.2. The period was set to be 8 months, from August 2021 till April 2022. The location is Dongen, as the ground station is located there. The integration step size is 0.1 min, as derived from table 4.1. The propagation simulation will be performed once and the data will be used for the all link budget simulation. This is done to make sure that these results are consistent and can be compared.

The main goal of the simulation is to model the data transfer between the satellite and the ground segment. The ground segment consists of a helical antenna and the RRS hardware. The helical antenna design is variable, meaning that it can be changed to find the best design suited for the submarine application. The optimal design transmits the most data in a set propagation period. The total data transferred is calculate with an integration of the instantaneous data rate, as shown with the step size in figure 4.16. How the optimisation is performed is elaborated in the section 4.5, hereafter.

4.5. Optimisation

The optimisation of the antenna has the objective to optimise the antenna such that the total amount of data transferred in the set time period is maximal. The time period is defined in section 4.2.3. The radiation pattern of the helical antenna influences the instantaneous data rate. To obtain the radiation pattern a MATLAB toolbox is used to simulate a helical antenna. An example of an antenna simulated by the MATLAB toolbox can be seen in figure 4.17

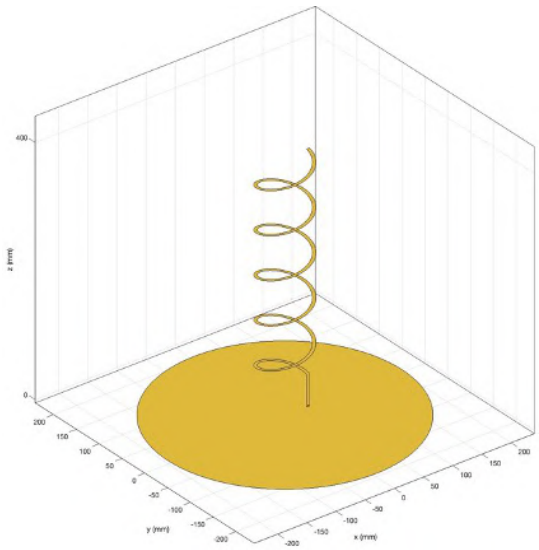

Figure 4.17: Basic helical antenna used as basic design

Variable Properties Antenna Design

The antenna design should be varied such that the radiation pattern changes. How the design influences the radiation pattern is calculated, and with that the performance of the antenna changes. There are four antenna parameters which can be varied to change the antenna design, and thus the radiation pattern. The four variables are depicted in the figures 4.22, and can be compared to the initial design in figure 4.17. The first variables is the spacing between the turns of the helix. The spacing between the turns can also be represented as the inclination angle of the helix. How this influences the design of the antenna can be seen in figure 4.18. The second variable is the number of turns of the helix, as shown in figure 4.19. An important limitation to the number of turns is the maximum length of ≤ 1 m, as dictated by requirement RQ-P-2.1. The third variable is the feed-height, so the distance from the ground plane till the start of the helix. An example of a antenna with no feed-height can be seen in

figure 4.20. The fourth variable is the diameter of the antenna. The diameter, in combination with the wavelength, dictates whether the antenna operates in the axial or normal regime of the antenna. The diameter of the antenna is also constraint by the size limitations, but this will not be a problem as explained in section 4.3.

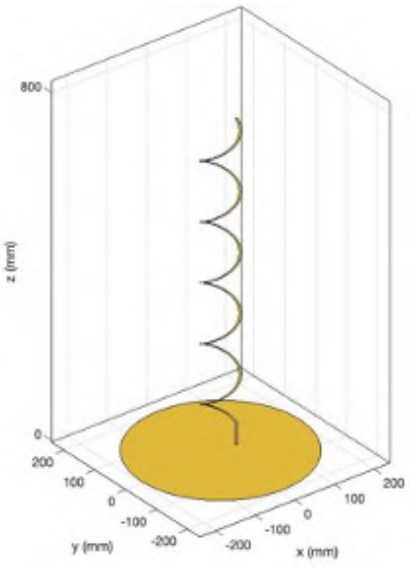

Figure 4.18: Spacing between turns

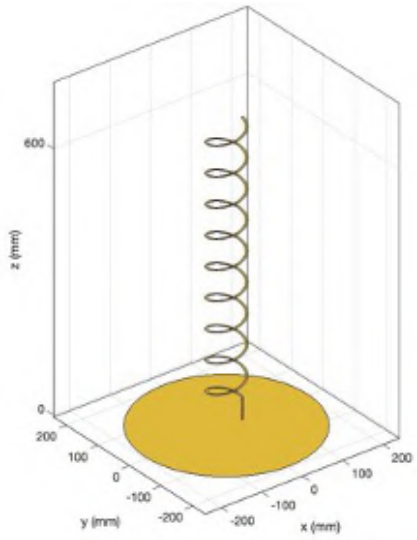

Figure 4.19: Number of turns

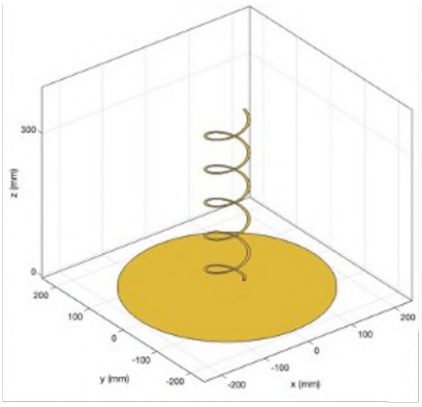

Figure 4.20: Feed-height of antenna

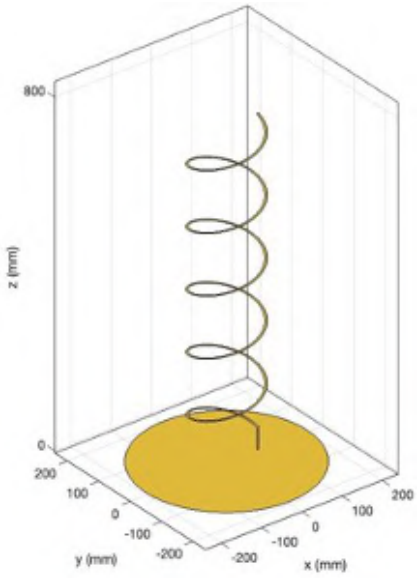

Figure 4.21: Diameter of antenna

Figure 4.22: Four variables helical antenna

The upper and lower bound for each of the variables during the optimisation can be seen in table 4.2. The boundary values have been determine in different ways. The spacing is set between a nearly flat to a steep helical shape. The maximum value corresponds to an inclination angle of 45°. The inclination angle is equal for the full helix, and is defined with respect to the ground plane. A larger spacing would result in a radiation pattern that is not symmetrical, which is not preferred. A omnidirectional pattern is needed to eliminate the influence of the orientation of the submarine antenna with respect to the satellite. If the radiation pattern is not omnidirectional the link strength can vary depending on the orientation, this would result in a varying amount of data transferred for the same pass. The minimum number of turns is also determined by the need for an omnidirectional radiation pattern, this required

at least one full turn. The minimum feed-height is based on the minimum cable length that would be required to feed the cable through the ground plane. The maximum is set at 50 cm, as this is half of the maximum length. The diameter boundaries are based on the wavelength multiplied by a variable factor. The diameter dictates if the antenna operates in axial or normal mode, as explained in section 4.3. The diameter can vary between full axial mode and normal mode with the set diameter boundaries.

	Spacing [cm]	**Turns [-]**	**Feed-height [cm]**	**Diameter [cm]**
Maximum	47.29	20	50	15.05
Minimum	1.58	1	1	5.02

Table 4.2: Boundary values for the variables in the helical antenna optimisation

The four parameters are not the only variables for the antenna design. The ground plane radius and the width of the wire are both also variable. The ground plane radius has been set to 20 cm, as this is the maximum value as dictated by requirement RS-2.1. The ground plane increases the possibility for the radiation pattern to reflect upwards. To investigate if this indeed increase the data throughput, the basic design from figure 4.17 has been simulated with varying round plane radius. The results have been normalised for the data throughput achieved with a ground plane radius of 20 cm. The results can be seen in figure 4.23 below.

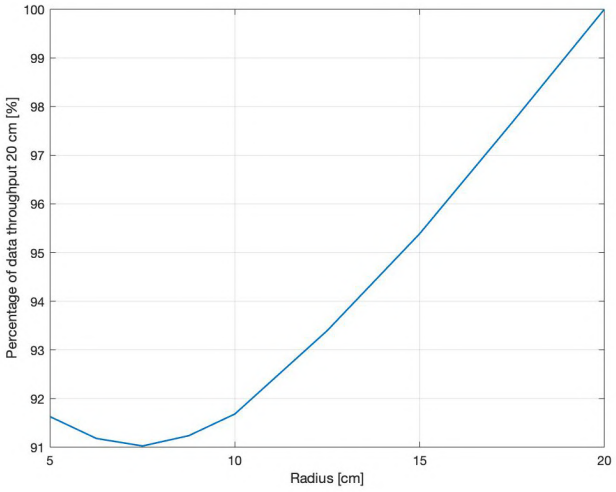

Figure 4.23: Data throughput for different ground plane radii

It can be observed that a larger ground plane radius results in a higher data throughput. Therefore a radius of 20 cm is chosen to achieve maximal data throughput. The next parameters that has to be determined before optimisation is the width of the antenna wire. The width is set to the diameter of normal electrical wire (14 Gauge), as this type of cable is readily available. It has surface area of 2.5 mm^2, that results in a diameter of 1.78 mm.

Boundary Conditions

Before the optimisation can be performed, a number of boundary conditions have to be set. The propagation conditions which have been selected in section 4.2 are used for the optimisation. Further boundaries conditions are listed below, along with an explanation.

- **Communication setup:** A critical requirement is RQ-P-1.1, the requirement that at least 1 MB of data should be transferred in a pass. The data transfer rate, and therefore subsequently the total data transferred, is dependent on the modulation scheme used. As explained in section 4.1.2, the modulation is dictated by the link strength. To change the modulation scheme with varying

link strength during a satellite pass, there has to be two way communication from submarine to satellite. In the case of a downlink transmission, the submarine has to inform the satellite that a higher modulation scheme could be used. To do this the submarine has to transmit a message. The downside of a transmission from the submarine is that it could be intercepted and used for locating the submarine by potential adversaries. This is also implied by requirement RQ-P-1.8. To prevent this, the system shall use the lowest modulation mode, ACM mode 1 for these situations. Since the ACM is now set the satellite can transmit information to the submarine without the need for two-way communication. The downside is that using a lower modulation mode reduces the amount of data transferred in a pass. Therefore the downlink with a set ACM mode is the critical case in which the 1 MB required has to be met. In the scenario of uplink or downlink with variable ACM modes, the 1 MB will easier achievable. Thus the optimisation will be focused on meeting the 1 MB requirement in a downlink situation with a set ACM mode. To get an idea of what data throughput possible, the simulation has been run using with basic antenna design as shown in figure 4.17. The resulting data throughput for different maximum elevation passes can be seen in figure 4.24.

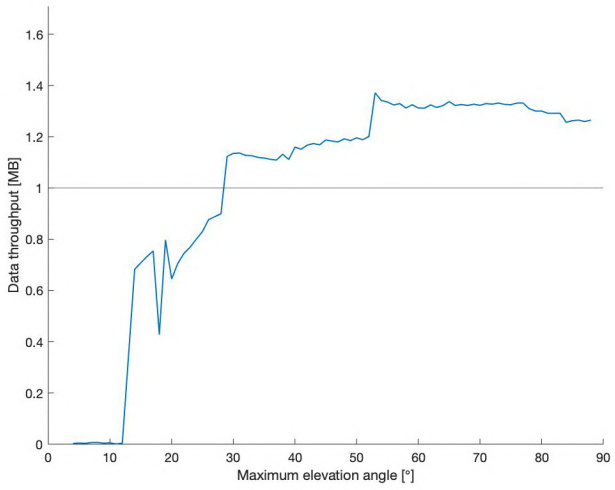

Figure 4.24: Resulting data throughput for passes with different maximum elevation angles

What is evident from figure 4.24 is that the 1 MB requirement is not met below 30° maximum elevation with the basic antenna design. The passes with an elevation below 13° don't have the ability to make contact. By trial and error it became evident that it would not be possible in the optimisation to get all the passes above the 1 MB level. The best results were achieved when the minimum elevation required during a pass was set at 20°, as will be shown in the results hereafter. The choice to eliminate the passes below 20° ensures that the optimised antenna will meet the 1 MB requirement for passes with an elevation above 20°.

- **Safety margin:** The safety margin used during the optimisation is 3 dB. The safety margin originates from two different factors. First of all the difference in polarisation between the helical and satellite antenna. The satellite is linearly polarised, the helical antenna is circularly polarised in the axial direction (i.e. straight above the antenna). In this situation there is a 3 dB mismatch due to the polarisation losses [59]. When the satellite is at low elevation angles, the polarisation losses are relatively small since the antenna is linearly polarised in the normal direction. The second factor which contributed to the safety margin is based on the ACM modes. In figure 4.2 it can be seen that the ACM modes are spaced approximately 1 to 1.5 dB apart, when $BER = 10^{-6}$ is considered. Thus a SNR surplus of 1.5 dB over the current ACM mode means that a higher mode is possible. However, in practise the SNR fluctuates, therefore there should be some extra overhead to ensure that the higher ACM mode is stable when switching [16]. These fluctua-

tions happen more often with increasing distance between the satellite and the ground segment. Therefore, the safety margin of 3 dB will compensate for polarisation losses at high elevation and increase the reliability at lower elevation angles.

Optimisation Strategy

The initial optimisation strategy used is a nonlinear gradient-based multi-variable method. This was chosen as the properties of the antenna cannot be linearized since the properties of the antenna do not linearly influence the data throughput of the system. Based on the gradient of the data throughput achieved, the step size of the next step is determined. The implementation of the optimisation in the simulation model has been done using the MATLAB optimisation toolbox, specifically using the ”fmincon” function. The method did not yield accurate results since different initial conditions yielded different maxima. The exact cause was could not be found but it was assumed to be caused by the large number of local maxima. A general scan of 10000 antenna through the boundary values, as defined in table 4.2, seems to reinforce the assumption. The results of the scan can be seen in figure 4.25.

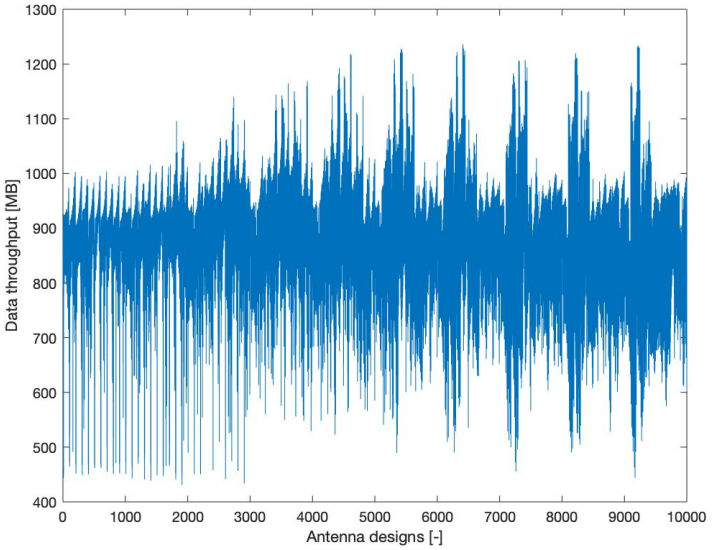

Figure 4.25: General scan antenna designs between boundary values

Therefore it has been decide to not use the gradient-based optimisation method. A different approach has been implemented to find the best antenna design. First the 100 antennas with the highest data throughput from the general scan are selected. Each of the 100 antennas are used as the initial location for a pattern search implemented using the ”patternsearch” function from the MATLAB optimisation toolbox. The results of the optimisation, using the pattern-search function, are detailed on the section 4.5.1 and 4.6 hereafter.

4.5.1. Results

Using the pattern-search function the 100 initial antennas converge red to 27 unique designs. These designs are deemed as optimal by the pattern-search function. This is due to the numerous local maxima. The antennas are close to the optimal design in term of data throughput, but have different design characteristics. The 27 antennas were not closely related in shape to each other. A selection has to be made from the 27 different antennas. All designs with more than 1% deviation of the best design’s data throughput, were not considered. Four different designs are within 1% deviation, and can be seen below in figure 4.26.

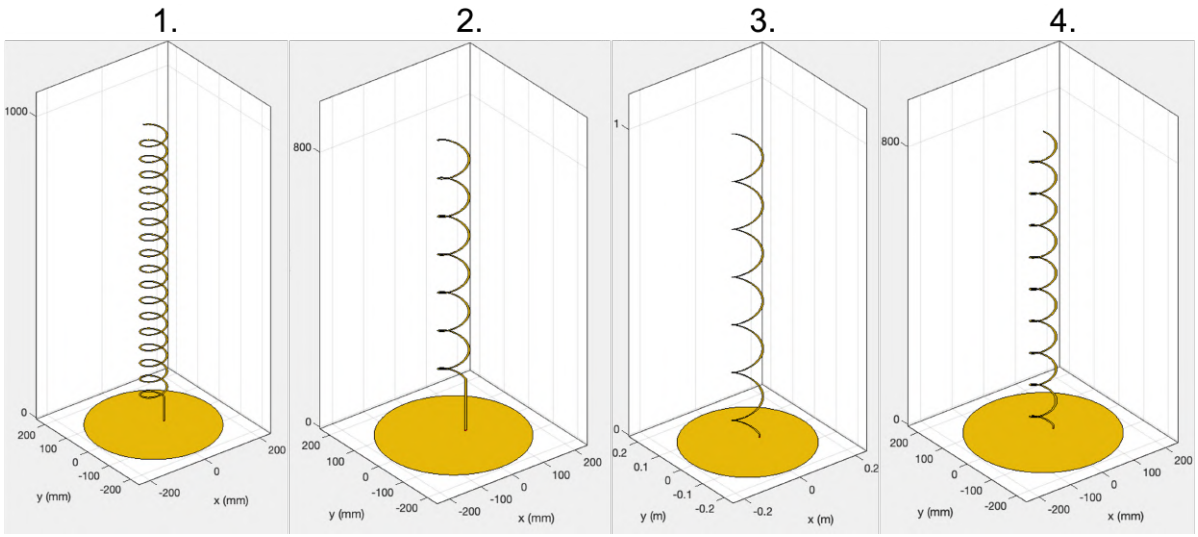

Figure 4.26: The four best antenna designs

As mentioned all the four designs are very similar in performance, however it can be seen in figure 4.26, that they have different in form factors. Two design come close to the maximum height of 1 m, these are the first and third antenna. Keeping in mind the space potentially required for mounting, cables and other electronic equipment the designs shorter than one meter are preferred. These are design two and four. The feed-height of the antenna is seen as part of the design that in theory does not influence the antenna radiation pattern. However, in practice it will influence the radiation pattern by emitting RF radiation, therefore antenna four was chosen as the final design.

The final design of the helical antenna chosen can be seen in figure 4.27. The antenna will be build and testing in the remaining part of the MSc thesis. The properties of the antenna can be found in table 4.3, along with a number of performance metrics.

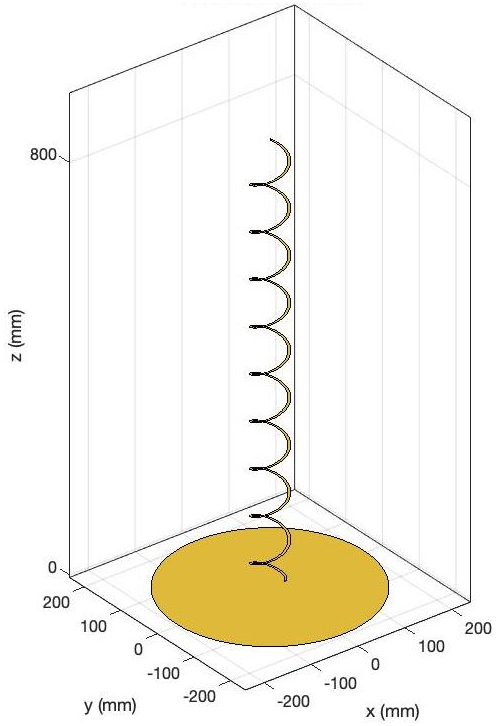

Figure 4.27: Final helical antenna design

Parameter	Value
Spacing	9.19 [cm]
Turns	9.1429 [-]
Feed-height	1 [cm]
Diameter	6.02 [cm]
Total data throughput (8 months)	1391.1 [MB]
Average throughout per pass (Downlink, ACM mode 1)	1.3612 [MB]
Half Power Beam Width	40°
Maximum gain	4.56 [dB]

Table 4.3: Final design properties and performance

4.6. Performance

The properties of the design as listed in table 4.3 provide a higher lever view of performance of the antenna system. To answer research sub-question 2, as defined in section 1.1, a more detail explanation of the system performance is required. This starts with the radiation pattern of the antenna, which is displayed in figures 4.28 and 4.29. On the left side in figure 4.28 the full radiation pattern is shown. It can be seen that the radiation pattern is omnidirectional. The highest gain is close to the horizontal direction, as confirmed by the vertical cut shown in figure 4.29. The Half Power Beam Width (HPBW) is 40°, with 20° above the horizon.

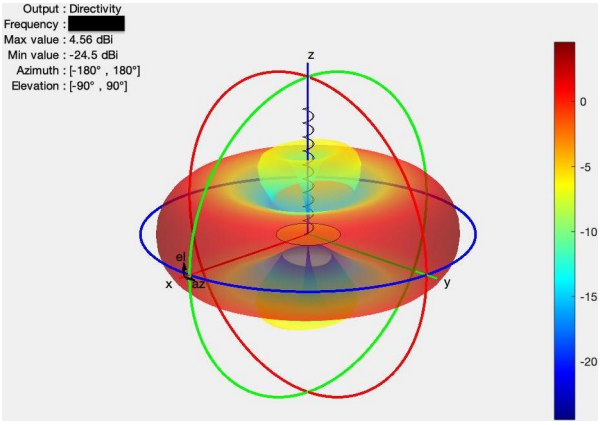

Figure 4.28: 3D radiation pattern

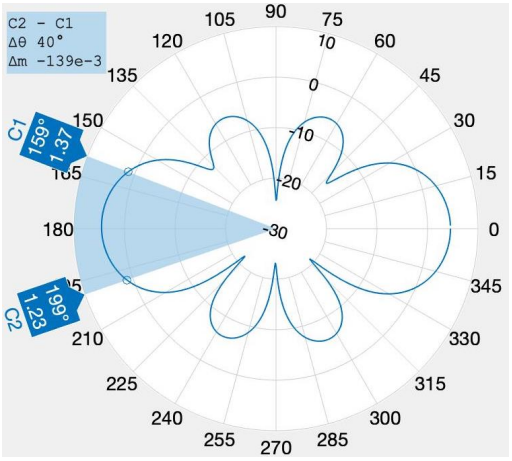

Figure 4.29: Vertical cut radiation pattern

The average data throughput per pass is more than 1 MB, as dictated by requirement RQ-P-1.1. In the total 8 months the orbital propagation has been done. When including all the passes with a maximum elevation above 20°, the total throughput is 1.391 GB. The basic design as shown in figure 4.17, has a total data throughput of 1.121 GB with an average of 1.0970 MB per pass. So the optimisation yielded a 24.41% improvement. One of the main requirements is that the antenna has the ability to communicate more than 1 MB during a satellite pass. Not all passes can meet the requirement, as passes with a very low maximum elevation only have a short contact time. As determined in the boundary conditions, the minimum elevation a pass should be 20°. To see if this condition has been met, the optimised design is compared to the basic design from figure 4.24, the result can be seen in figure 4.30.

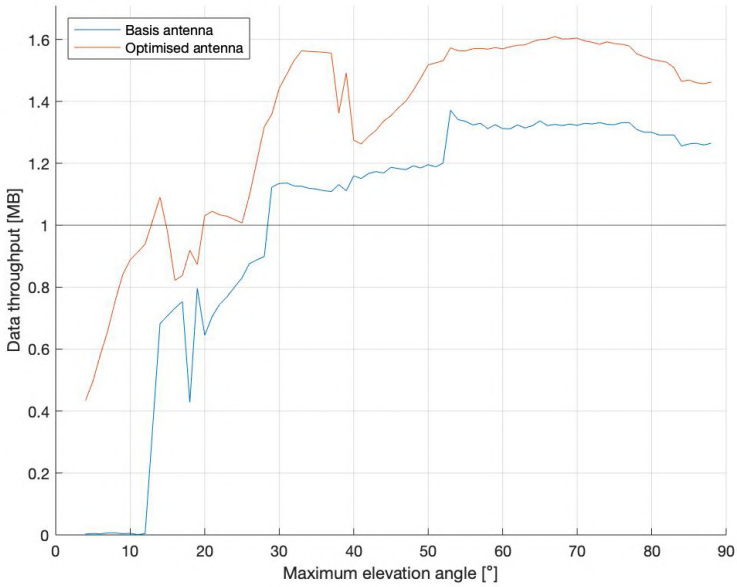

Figure 4.30: Average data throughput passes for maximum elevation angles

The antenna performance is significantly improved in comparison to the basic design. For all types of passes the total data throughput is higher compared to the basic design. Especially in the low elevation passes, <15° maximum elevation, a clear improvement is visible. As communication with the basic design would not have been possible for passes with a maximum elevation below 15°. When passes with a maximum elevation below 20° are included the data throughput of the optimised design is 1.98 GB, that is 31.0% better compared to the basic design. The requirements for the 1 MB is met for a passes with a maximum elevation above 20°. In case the maximum elevation is above 8° it could already be considered to surface since a throughput of 0.8 MB can be achieved. In the case of downlink with variable ACM modes total throughput is 4.46 GB, and the uplink with variable ACM modes has a throughput of 5.99 GB . The radiation pattern of the uplink is different from the downlink pattern, as can be seen in figure 4.31 and figure 4.32.

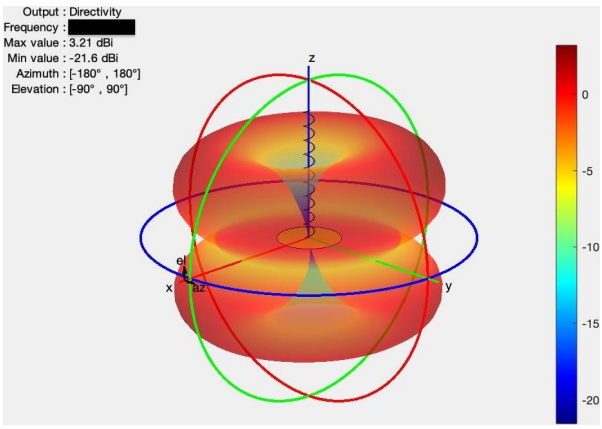

Figure 4.31: 3D radiation pattern uplink

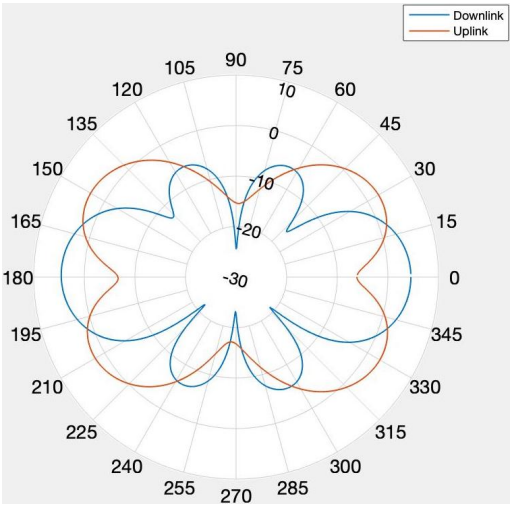

Figure 4.32: Vertical cut radiation pattern downlink and uplink

In figure 4.32 it can be seen that the maximum gain for the uplink is at higher elevation angles. The uplink pattern has not been considered in the optimisation. Therefore it has to be verified if uplink meets

the 1 MB requirement for all passes with a maximum elevation above 20°. For the simulation, the RRS hardware has been considered. If the data throughput should be increased, the RRS hardware can be adjusted to accommodate a higher power amplifier. How the downlink and uplink perform can be seen in figure 4.33.

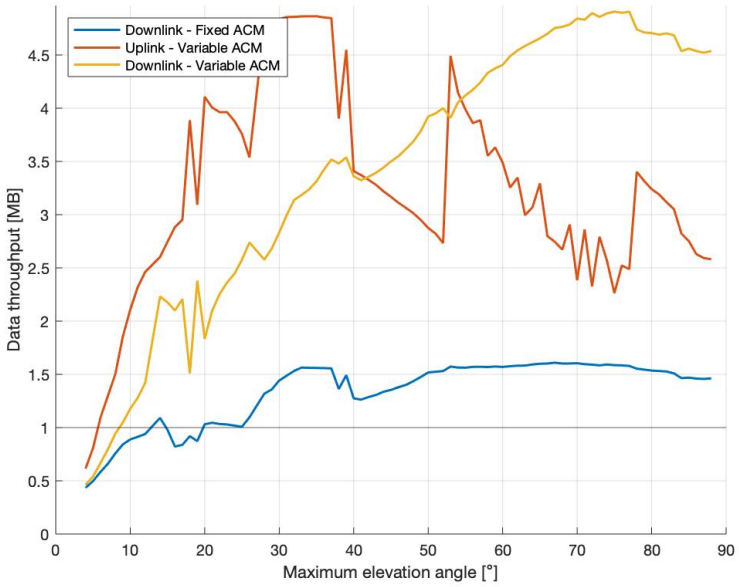

Figure 4.33: Average data throughput passes for maximum elevation angles

In both cases the requirements are met. The downlink with fixed ACM is shown to indicate the extra potential data throughput when the ACM mode is variable. Please note that the shape of the uplink is very different from the downlink due to the differences in radiation patterns for both the satellite and the submarine antenna. For the uplink, the radiation pattern of the ground segment is not adapted to fill the weak spots in the receiving antenna's radiation pattern. As can be seen for passes with a maximum elevation angle between 40° and 52°. However these pass can still transmit more than the required 1 MB, so no adjustments are necessary.

To provide a better overview of the performance of the submarine antenna the propagation time frame should be reduced, in this case 22-Sep-2021 00:00:00 till 23-Sep-2021 00:00:00 was chosen. Only passes with a maximum elevation higher than 15° are considered since the low elevation passes are not of interest The maximum elevation for the five passes remaining are 17.3°, 31.1°, 57.7°, 17.3°, and 74.4° as shown left to right in figure 4.34. Along with the elevation angles, the downlink data rate is shown, both for the fixed and variable ACM mode.

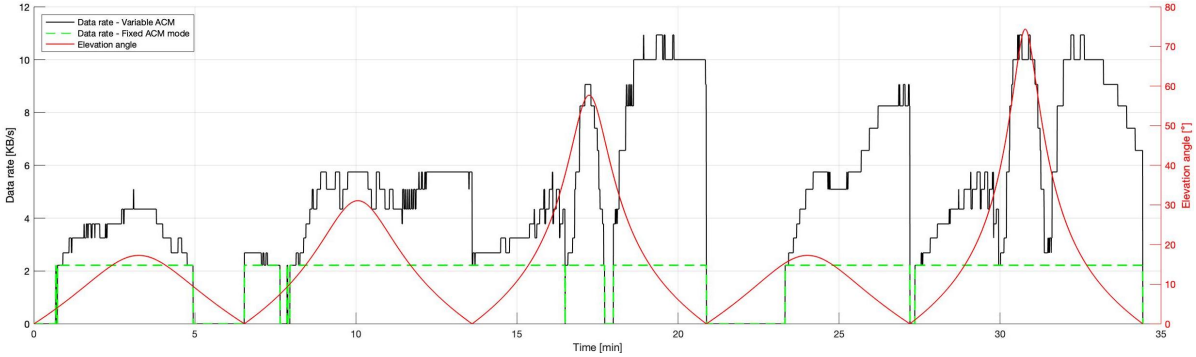

Figure 4.34: Data transfer rate for fixed and variable ACM mode along with elevation angle

It can be seen that the variable ACM mode often has a higher data rate, as the link strength is used to the full potential. Therefore the total amount of data transferred is higher. Pass number 1 and 4 have the same maximum elevation of 17.3°, however the transmission during the pass has a different shape. In pass 1 the transfer starts earlier in the pass compared to pass 4, while in pass 4 the transfer continues to lower elevation angles. If communication is possible depends on the SNR. To explain the differences between the passes, the SNR is shown in figure 4.35, along with the gain of the ground segment and satellite antenna.

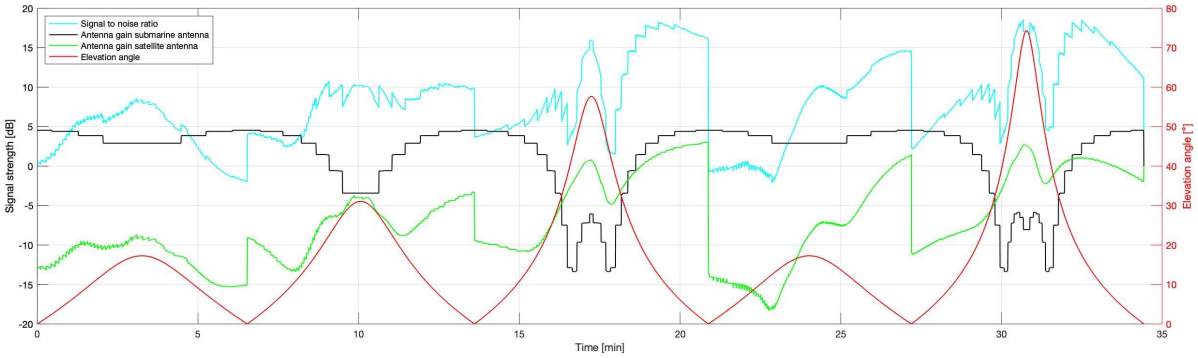

Figure 4.35: SNR, antennas gain and elevation angle over time

The SNR for pass 1 and 4 is not identical. The antenna of the submarine provides the same gain for both passes, however the antenna of the satellites provides different gain. The gain of the satellite's antenna is different for each pass due to the orientation of the satellite with respect to the submarine. Not all passes with the same maximum elevation angle have the same gain pattern as they can pass the submarine from a different cardinal point. How the passes are oriented with respect to the ground segment on-board the ground segment can be seen in figure 4.36.

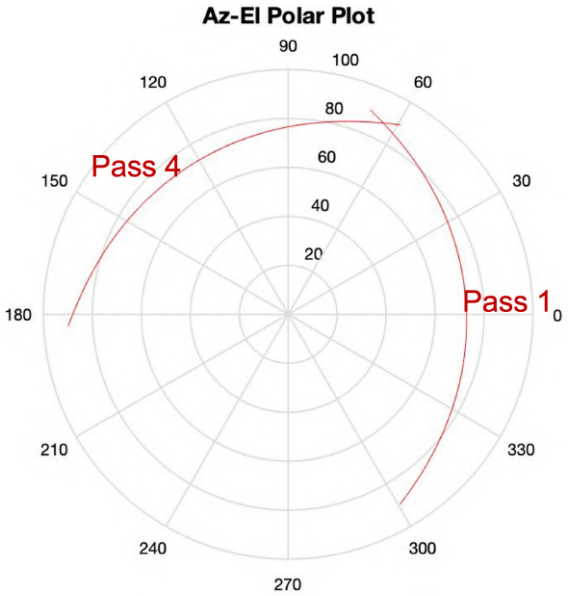

Figure 4.36: Pass 1 and 4 as seen from the ground segment

The performance of the system as simulated in this chapter is theoretical. To achieve the main objective of the thesis, and provide a thorough answer to research sub-question 2, the system performance has to be verified in real life. The verification should be performed by testing capabilities of the system. Before this can be done it should first be manufactured. The manufacturing process will be discussed in chapter 5 hereafter.

5

Antenna Manufacturing

In this chapter the manufacturing of the helical antenna design will be discussed. First it will be explained how the antenna is manufactured. Second, the building of the antenna along with the final result will be shown. Third the antenna will be adapted to match the impedance of the antenna to 50Ω resistance. The adaptions are required to prevent losses and achieve optimal performance.

5.1. 3D Design

The helical antenna is build up out of two main parts, the helix and the ground plane. The helix is made out of a conducting wire. The wire is the active part of the antenna and can be referred to as the hot or active side. The ground plane can be made out of different constructions, as long as it is seen as solid by the RF signal. If an object has a size $D \ll \lambda$, the object will not influence to the antenna radiation pattern. Therefore, the ground plane could have holes if it is with this condition. However, in the case of the prototype submarine antenna it was chosen to go with a metal plate since it was available and did not require additional tooling. If the mass of the antenna should be reduced, the ground plane can be perforated to meet the requirement. The helix is harder to manufacture as the shape is harder to achieve with tooling. Therefore it was chosen to use a 3D printer to create a mold that can be used as the supporting structure of the antenna. 3D printing was considered the simplest manufacturing technique for the prototype. The design can be seen in figure 5.1 below.

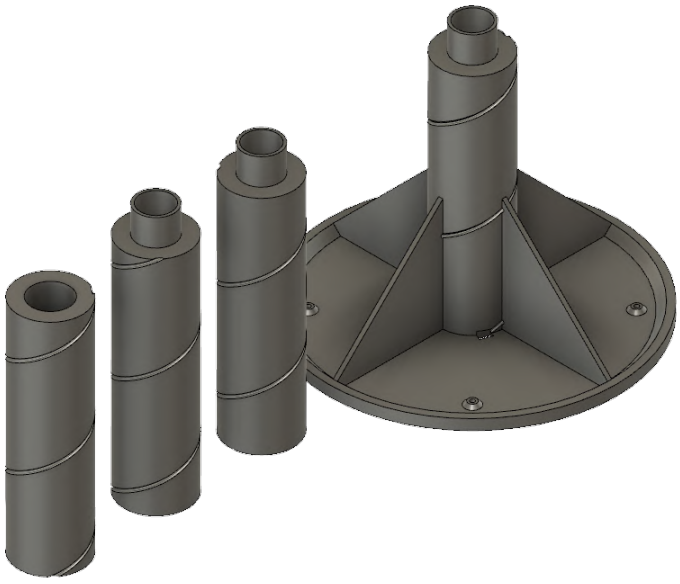

Figure 5.1: 3D model helical antenna mold

The structure was designed such that it can be 3D printed on the printer available at the 982 Squadron in Dongen. The four parts can be stacked to form the antenna. The grove on the side of the antenna can hold half of the active wire. The bottom part has a support structure such that the ground plane can be attached to the antenna. A number of characteristics of the 3D design can be seen in table 5.1 below.

Parameter	**Value**
Spacing	9.19 [cm]
Diameter	6.02 [cm]
Height	84.19 [cm]
Ground plane radius	20 [cm]
Radius antenna ground plane	13.64 [cm]
Cable grove diameter	3.5 [mm]
Screw size	M4

Table 5.1: Characteristics 3D print submarine antenna

The material chosen for the antenna mold is Acrylonitrile Butadiene Styrene (ABS). The material is waterproof and does not interfere with the antenna as it has a low dielectric constant, does not conduct electricity, and does not contain any metal [53]. ABS painted black should be avoided as it can contain carbon, which conducts electricity. ABS is cheap and relatively easy to print while being strong and only deform at higher temperatures [67]. The antenna will be connected to the rest of the system using a coax cable with a 50 Ω impedance. To connect the ground plane and the active helix a female N chassis connector is used. An example of such connector can be seen in figure 5.2.

Figure 5.2: Female N chassis connector [10]

The small pin on the right side of figure 5.2 is the connection for the helix. The active wire will be soldered onto the pin. The rest of the connector can be used to connect the ground plane. The connector will be attached using screws that screw into the tapped holes in the metal ground plane.

One of the tests that will be conducted after manufacturing is a radiation pattern test. To do the test more accurately and faster, it was chosen to attach the submarine antenna to the rotor of the RRS shown in figure 2.6. The rotor can achieve all angles required which ensures that the measurement is done correctly. To attach the antenna to the RRS rotor a connection arm had to be printed. The 3D render of the arm can be seen in figure 5.3. The arm will attach to the ground plane's middle point. In the next section the 3D printed design will be shown along with the assembled antenna.

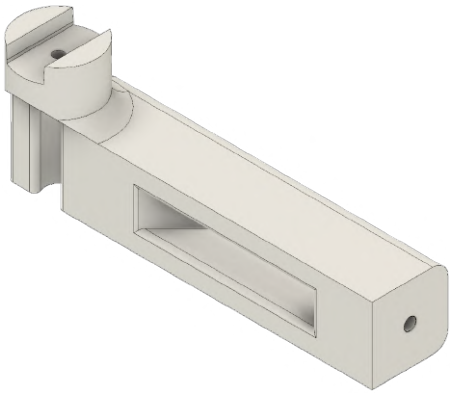

Figure 5.3: Arm to connect submarine antenna to RRS rotor

5.2. Antenna Assembly

The mold of the antenna has been printed successfully and can be seen in figure 5.4. The parts could be printed without the need of plastic support so no additional finishing was required. All the parts are glued together using superglue. The end result can be seen in figure 5.5. In figure 5.6 the opening left for the connector pin is shown. Here the connector can be soldered to the active helical antenna part.

Figure 5.4: The four 3D printed parts submarine antenna

Figure 5.6: Connector hole in antenna base plate

Figure 5.5: Submarine antenna assembled

The fully assembled antenna on top of the RRS rotor can be seen in figure 5.7. The connector for the coax cable can be seen in figure 5.8. The electrical tape applied to keep the cable in place does not interfere with the radiation pattern, as it not conductive and does not contain any metal [14].

Figure 5.7: Assembled antenna on RRS stand

Figure 5.8: Connector on underside ground plane

The antenna is now fully assembled. Before the test can be done the antenna's impedance should be changed to 50 Ω. How this is done and why it is necessary will be explained in the next 5.3.

5.3. Impedance Matching

The antenna impedance is the resistance of an electrical signal in the antenna. The impedance is measured at the connector of the antenna [46]. Connected electrical components should have the same impedance. If this is not the case losses will occur since part of the signal is reflected back. A schematic representation of an antenna system can be seen in figure 5.9.

Figure 5.9: Schematic of antenna system

To quantify the reflection in relation to inserted power (P_{in}) and the reflected power (P_{ref}), the Voltage Standing Wave Ratio (VSWR) is used. The VSWR can be defined as shown in equation 5.1.

$$VSWR = \frac{P_{in} + P_{ref}}{P_{in} - P_{ref}} \tag{5.1}$$

A lower VSWR corresponds to a better matched antenna, with the minimum being 1. Using the VSWR, the reflection coefficient (Γ) can be determined. With the reflection coefficient the mismatch loss (ML) can be determined. The equations used to calculate Γ and ML are 5.2 and 5.3, respectively [30].

$$\Gamma = \frac{VSWR - 1}{VSWR + 1} \tag{5.2}$$

$$ML = -10log(1 - |\Gamma|^2) \tag{5.3}$$

The mismatch loss should be as low as possible to ensure a strong signal transfer. Depending on which parameters is measured, the values as seen in table 5.2 should be achieved to get a good performing antenna. The VSWR cannot be higher than 3 since this would lower the data throughput such that the 1 MB requirement will only be met for all passes with an maximum elevation higher than 46°. Lower elevation passes will not always meet the 1 MB requirement. The increase to 46° would not be acceptable since the current limit is 20° minimum elevation as shown in figure 4.30. At a VSWR of 3 the data throughput is reduced with 7.01% compared to an ideal situation.

Parameter	Ideal	Minimal
Mismatch loss [dB]	0	1.25
VSWR [-]	1	3

Table 5.2: Ideal and minimal values mismatch loss and VSWR

The impedance of an antenna consists of a real (R) and imaginary part (j). The real part represents the resistance of the antenna. The imaginary part represents the reactive part of the impedance (e.g. capacitive or inductive, based on sign). The impedance is correlated to the mismatch loss of the antenna via the reflection coefficient. The reflection coefficient can be calculated using equation 5.2, however it can also be calculated directly from the impedance measured. To calculate the reflection coefficient from the impedance the characteristics resistance (Z_0) should be known. Most RF systems have a 50 Ω resistance, but different values are also common (e.g. 75 Ω). The reflection coefficient can be determined using the measured impedance as shown in equation 5.4. With the reflection coefficient the mismatch losses can be calculated using equation 5.3.

$$\Gamma = \frac{\sqrt{(R - Z_0)^2 + j^2}}{\sqrt{(R + Z_0)^2 + j^2}} \tag{5.4}$$

The impedance of the antenna is depended on the frequency of the input signal. Commonly the impedance is displayed in a Smith Chart. The impedance over the range from 250 MHz to 330 MHz is shown in figure 5.10. The yellow point is the impedance point for the uplink frequency, while the red point is the downlink frequency impedance. Please note that the figure is normalised around the characteristics resistance of $Z_0 = 50\ \Omega$.

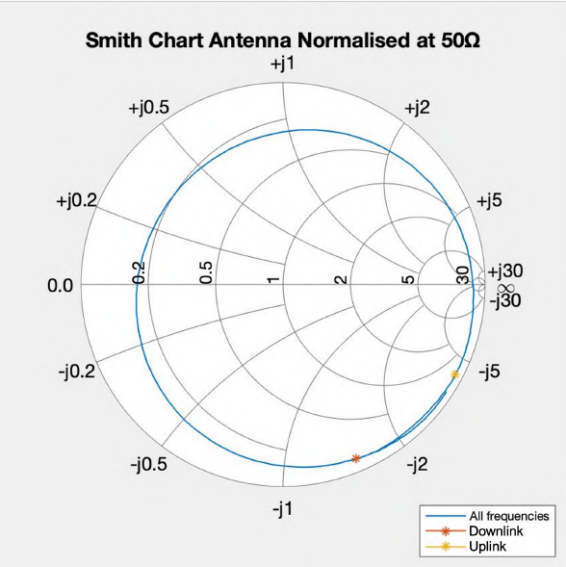

Figure 5.10: Smith Chart antenna before impedance match

For the downlink frequency the impedance is $18.0997 - 43.1022i\ \Omega$, for the uplink frequency the impedance is $42.5924 - 22.3068i\ \Omega$. To obtain a small as possible mismatch loss the ideal impedance of $50 - 0i\ \Omega$ should be approached. To see how much the current mismatch influences the performance of the antenna the VSWR should be measured. The result can be seen in figure 5.11.

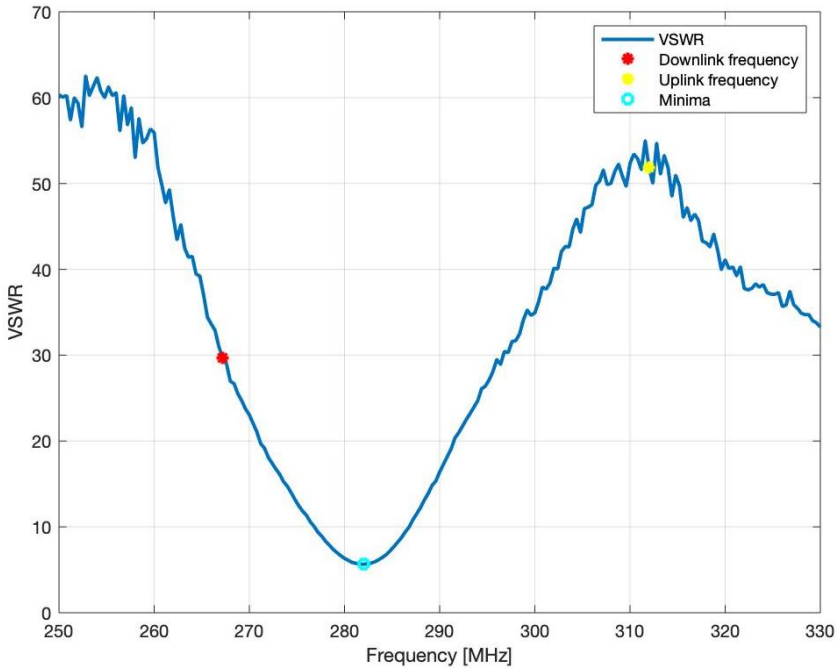

Figure 5.11: VSWR antenna before impedance match

It can be seen that the VSWR is too high for having a good power transfer. The maximum value should be 3, but even the lowest point is above 5.5. A VSWR of 5.5 yields a mismatch loss of 2.8 dB. Such losses are not acceptable as it would lower the data throughput with 18.58%. Furthermore it would increase the minimal elevation that is required to ensure that the 1 MB is met to 53°. Thus impedance matching is required to improve the performance of the antenna to an acceptable level, that would be the minimal value as provided in table 5.2. The impedance can be improved using a L-network. The best performance is achieved when the impedance is matched to $50 - 0i\ \Omega$ (i.e. the center of the Smith chart, as shown in figure 5.10).

5.3.1. L-Network

The impedance of an antenna can be changed by using a L-network. This type of network was chosen since it is relatively simple but still enables to match the antenna. The network can consist of one capacitor and one inductor and is placed between the connector and the antenna. Different types of L-networks can also consist of 2 inductors or 2 capacitors. The type of L-network that should be used is depended on the unmatched impedance of the antenna. In this case the imaginary part of the antenna is negative, so the antenna has capacitive properties. If the antenna has a impedance of 50 Ω it will be in the middle of the Smith chart. The impedance can be moved around the smith chart by a capacitor or inductor, as shown in figure 5.12.

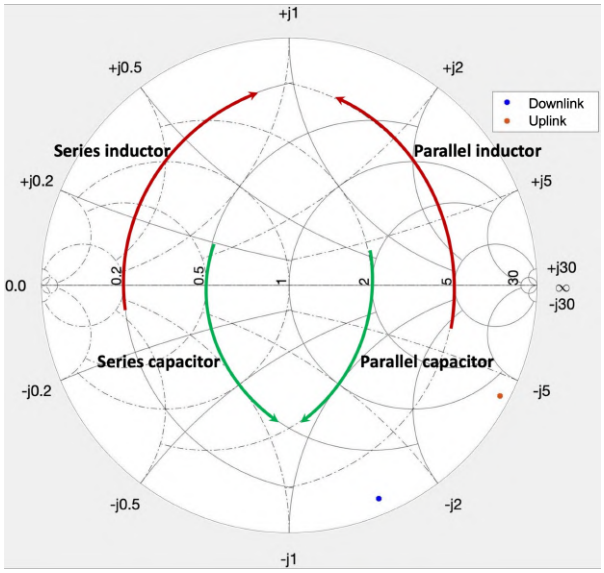

Figure 5.12: Moving in Smith chart

The dotted lines in figure 5.12 are a mirror of the impedance plot, named the admittance. Parallel components move along the admittance lines while series components move along the impedance lines. With the possibles moves along the lines a impedance point can be moved to the middle of the Smith chart [38]. The impedance of the uplink and downlink are both situated in the bottom right part of the smith chart. The type of L-network that should be used depends on the current impedance. For the submarine antenna, the matching network shown in figure 5.14 is used. The network can correct the impedance of an antenna that is outside the blue area in figure 5.13 [60]. The blue and orange dot are the downlink and uplink frequency impedance, respectively.

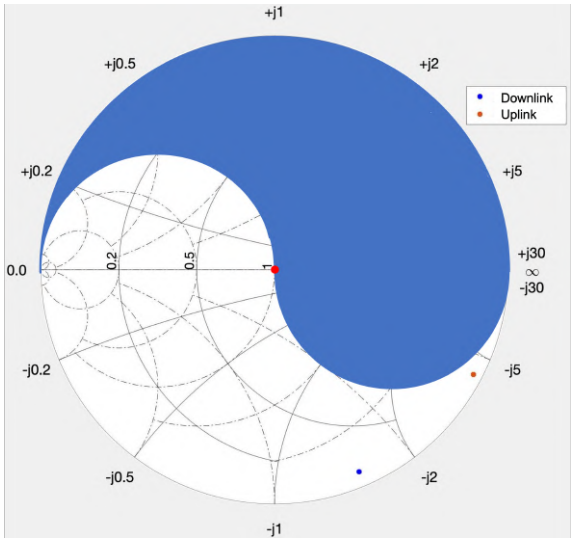

Figure 5.13: Section of Smith chart that can be match L-network

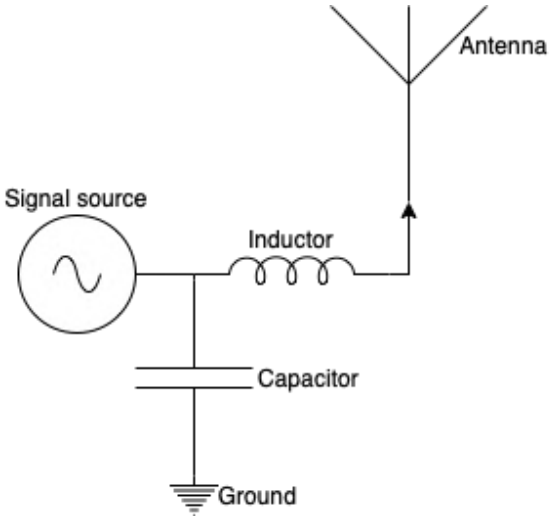

Figure 5.14: L-network used for impedance matching

Since both the uplink and downlink impedance are outside the blue area in figure 5.13, the L-network as shown in figure 5.14 is adequate. Now that the network is selected, the values for the inductor and capacitor have to be calculated. The values are frequency depended. Since the optimisation and has been done for the downlink situation this was chosen as the main frequency to match for the L-network. How well the uplink frequency is matched with this network will be investigated through measurements.

Equation 5.5 and 5.6 are used to calculate the capacitor and inductor characteristics respectively.

$$C = \frac{1}{2\pi f X_c} \tag{5.5}$$

$$I = \frac{X_l}{2\pi f} \tag{5.6}$$

How X_c and X_l are determined can be seen in figure 5.15.

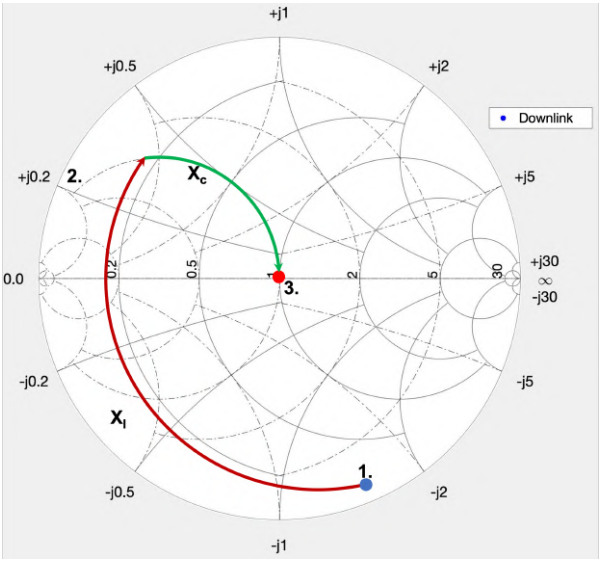

Figure 5.15: X_c and X_l impedance matching

X_l is the distance between point 1 and 2 as read from the admittance plot, which gives a value of $X_l = 3.7$. X_c is the distance between point 2 and 3 read from the impedance plot, which gives value of $X_c = 0.41$. Note that these values are normalised and have to be multiplied by 50. This yields the following values for the X_c and X_l as shown in table 5.3. With equation 5.5 and 5.6 the inductance and capacitance can be calculated. Please note that the exact values cannot be provided as this would provide the operating frequency. Therefore approximate values are provide in table 5.3.

	Capacitor	**Inductor**
Distance	22.5	185
Value	**27 pF**	**110 nH**

Table 5.3: Capacitance and inductance values

The inductor and capacitor used can be seen in figures 5.16 and 5.17 respectively. The capacitor is a variable trimmer that can be adjusted by turning the small screw. It was used such that an exact impedance match can be achieved since the initial impedance measured can vary. A deviation from the initially measured impedance will occur. The coil has been added between the antenna and connector, which influences the measured impedance. Furthermore the metal of the coil close to the antenna also influence the impedance measured at the connector. Therefore the variable trimmer is required since the system has to be tuned.

Figure 5.16: Coil used as inductor

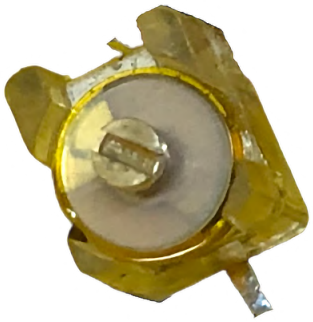

Figure 5.17: Trimmer capacitor

The inductor used was not designed to be easily adjustable like the capacitor. The inductance of the coil is varied by changing the distance between the turns. To reduce the number of turns without removing the coil from the antenna, two turns were shorted by soldering. To get an estimation of the coil inductance the following equation 5.7 can be used.

$$I = \frac{\mu_r \mu_0 N^2 \pi r^2}{l} \tag{5.7}$$

Where:

- μ_r | Relative permeability of the core [-]
- μ_0 | Permeability free space ($4\pi 10^{-7}$ [H/m])
- N | Number of turns [-]
- r | Coil radius [m]
- l | Coil length [m]

When matching the antenna, the final value for the coil was calculated to be 89.32 [nH]. The coil has the following parameters; $r = 7.5$ mm, $N = 2.75$, and $l = 12$ mm. The exact value of the coil can vary since the aforementioned number are not exact. The exact inductance of the coil should be verified for reproducibility of the design. The same should be done for the capacitor. The capacitance is not set since the trimmer was also used to fine-tune the impedance match. Both of the components were measured using a Vector Network Analyser (VNA), results are shown in table 5.4.

	Capacitor	**Inductor**
Predicted value	27 pF	110 nH
Measured value	**16.2 pF**	**94.55 nH**
Delta	**40 %**	**14 %**

Table 5.4: Predicted and measured component parameters

The variation of both values has the same causes. The first reason is that the measurement before impedance matching is not perfect. From the component values it can be calculated that $X_c = 36$ and $X_l = 160$, which is both shorter than expected. These are approximate numbers to prevent disclosing frequencies. The calculated values indicate that the initial impedance point moves. An estimation of where the impedance point is located can be seen in figure 5.18.

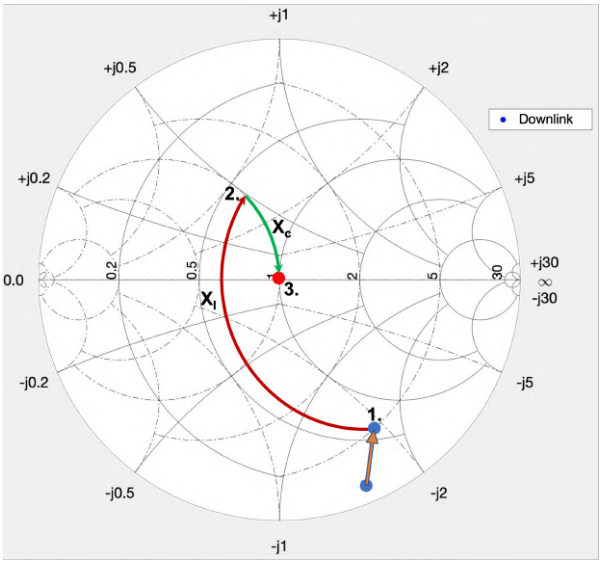

Figure 5.18: Estimation impedance antenna

There are multiple reasons why the point has moved. First, the added L-network itself moves the impedance of the system, before it is tuned. Thus the components needed to match the impedance are different. Furthermore the added metal close to the antenna changes the impedance of the antenna itself. Second, temperature differences can change the impedance of the antenna [66]. Since all the aforementioned procedures are not done in a single day this might play a role. The third reason the components are not exact has to do with the position of point 3 (seen in figure 5.18). In the calculations it is assumed that a perfect impedance match is achieved. However this is not necessarily the case. The end impedance at the downlink and uplink frequency can be seen in figure 5.19. It is not perfectly in the middle so there is still some mismatch loss. It was hard to fine tune the antenna to have a perfect impedance match. With components that allow for better fine tuning, an improvement should be easily achievable.

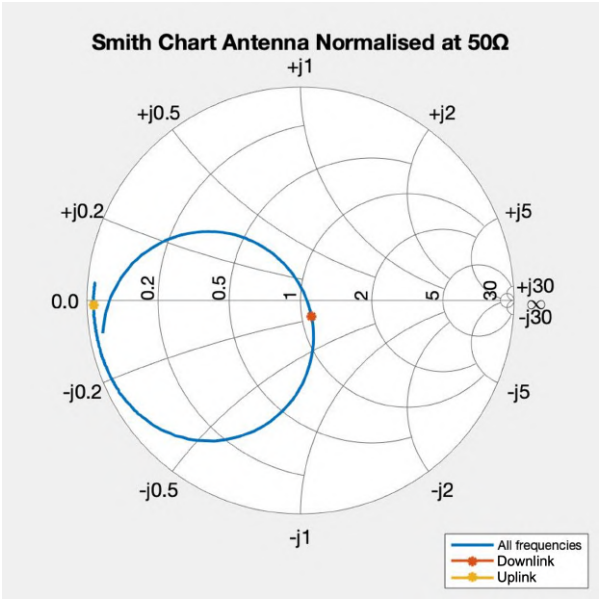

Figure 5.19: Impedance of antenna with tuned L-network

In figure 5.19 the uplink impedance with the L-network is also shown. It is far from a perfect match an therefore uplink will not be possible using the current L-network. There is no simple L-network

that can both match the uplink and downlink frequency simultaneously. A solution would be to use a duplexer [25]. Here two different matching networks are used that allow matching of both the uplink and downlink frequency. The implementation of a duplexer is more complex. It was not achievable within the time constraints of this MSc thesis. Since the antenna is matched for the downlink frequency the performance should be significantly improved compared to the figure 5.11. The VSWR of the matched antenna can be seen in figure 5.20. The VSWR around the downlink frequency can be seen in figure 5.21.

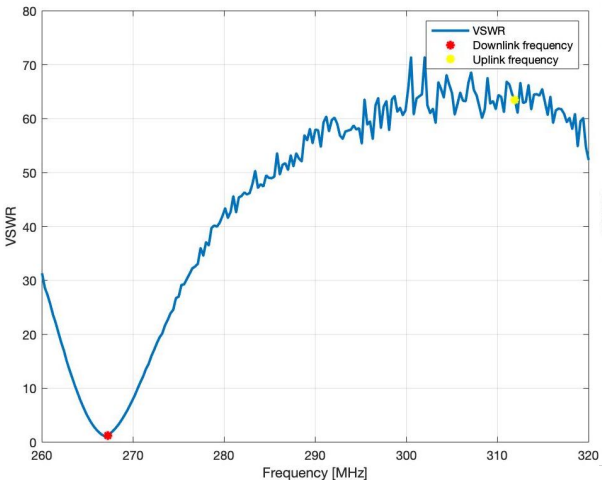

Figure 5.20: VSWR Antenna with L-network

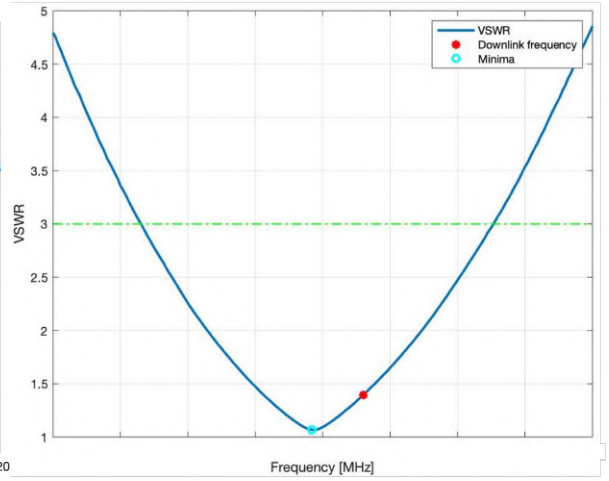

Figure 5.21: VSWR Antenna with L-network magnified around the downlink frequency

In figure 5.20 the VSWR for a large frequency range is shown. Since the VSWR should be below 3 to have a good functioning antenna most of the frequency range is not usable, only around the downlink frequency the VSWR is sufficiently low. In figure 5.21 the VSWR is magnified around the operating frequency. The frequency range with a VSWR below 3 is ± 2.55 MHz. The range is relatively small therefore the antenna has a small operating bandwidth. The VSWR at the downlink frequency is 1.3946. Converting this to mismatch loss yields 0.1196 dB. When the loss is taken into account in the SNR calculation, the resulting data loss is acceptable since the total data transferred, with parameters as defined in section 4.4, is 0.49% lower compared to a perfectly matched antenna.

6

Measurements

In this chapter the antenna test results will be discussed and a relation between test and simulation will be made. Furthermore it will provide an answer to the research sub-question as defined in section 1.1. The design of the antenna is based on the radiation pattern as calculated in the MATLAB simulation. It is important to verify that the simulation corresponds with reality. Do to this the radiation pattern of the antenna is measured and compared to the predicted radiation pattern. If the measured radiation pattern corresponds to the MATLAB radiation pattern, it can be assumed that the MATLAB simulation corresponds with reality. The second measurement is the verification the link budget calculations. To perform the test, the system should communicate with the satellite. The result of the measurement can then be compared to the predicted value.

6.1. Test set-up

In this section the test set-up of the two tests will be discussed. First the radiation pattern test in section 6.1.1, second the link budget verification in section 6.1.2 .

6.1.1. Radiation Pattern verification

The radiation pattern test has the objective measure the shape of the radiation pattern and show the gain of the antenna. To perform the test, one transmitting antenna is placed in the far-field radiation pattern of the submarine antenna. The far-field is the region where the radiation pattern is stable and takes its final shape [56]. The distance (r) from the antenna to be in the far field region of the radiation pattern is defined by the following condition:

$$r > \frac{2D^2}{\lambda} \tag{6.1}$$

Where D a characteristic length and λ is the wavelength. As the frequency is known along with the length of the antenna, the minimal distance r is ± 1.3 m. A schematic representation of the radiation pattern test can be seen in figure 6.1.

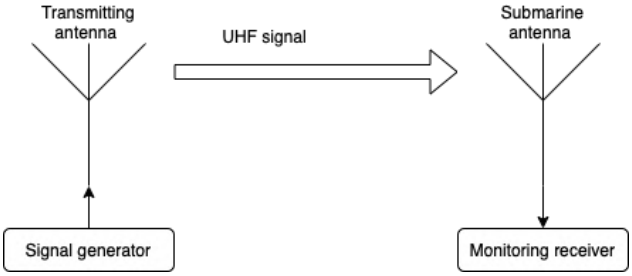

Figure 6.1: Radiation pattern test set-up

On the left side a transmitting antenna which is fed by a signal generator with a known input (P_{in}). On the other side the submarine antenna is situated with a receiver that indicated the received signal strength. Since the gain of the transmitting antenna is not an ideal antenna, the gain cannot be assumed. With a set-up of only two antennas only the relative gain can be calculated. To calculate the absolute gain a third antenna has to be used. The relative strength between each of the possible antenna pairs has to be measured. The measurement between each pair of antennas can be represented by equation 6.2, 6.3, and 6.4. The gains of the three antennas are the unknowns, these can now be determined since there are three equations.

$$P_{in} - FSPL_{1-2} + G_1 + G_2 - L = P_{1-2} \tag{6.2}$$

$$P_{in} - FSPL_{2-3} + G_2 + G_3 - L = P_{2-3} \tag{6.3}$$

$$P_{in} - FSPL_{1-3} + G_1 + G_3 - L = P_{1-3} \tag{6.4}$$

In the equations G_x is the gain of the respective antenna (e.g. $x = 1$). L are the losses induced in the system, such as cable losses. The cable losses will be quantified during the measurement. P_{x-y} is the signal strength received at the antenna y from the input power P_{in} at antenna x. FSPL is the attenuation of the signal due to the distance between the two antenna. A large distance will yield a larger FSPL resulting in weaker received signal that is more susceptible to disturbances. However, a large distance will increase the consistency of the signal as it further in the far-field region, as defined by equation 6.1. The FSPL can be calculated using equation 6.5.

$$FSPL = 20log_{10}(\frac{4\pi D}{\lambda}) \tag{6.5}$$

Where D is the distance between the antenna and λ the wavelength. To measure the radiation pattern the gain at all orientations with respect to the antenna should be measured. Therefore the angle between the submarine antenna and the transmitting antenna should vary. To perform the measurement accurately and consistent the RRS rotor will be used. A schematic representation of can be seen in figure 6.2.

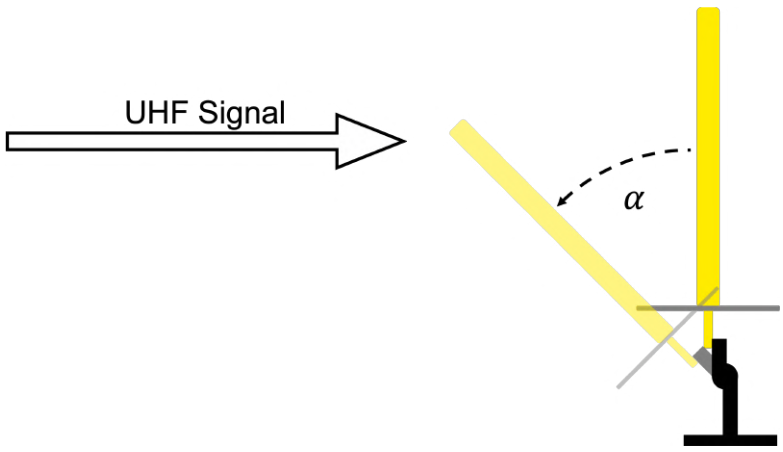

Figure 6.2: Schematic representation of submarine antenna orientation variation

With these parameters known, it is possible to calculate the gain at all orientations of the antenna, thus the radiation pattern can be constructed. The test should yield the radiation pattern that can be used to verify the working of the antenna based on the MATLAB radiation pattern simulation. How the measurements are conducted is elaborated in section 6.2.

6.1.2. Link Strength Verification

To verify if the performance of the antenna corresponds to the performance predicted by the link budget, a measurement has to be conducted. In an ideal situation a pass would be selected and the data

transferred over the whole pass would be measured. However as the measurements are on land, where there are buildings and threes that obstruct the signal, the measurement cannot be conducted under ideal conditions. To still verify the link budget, a different approach is required. A short section of a pass is selected where data transfer will take place. The segment should be selected such that a clear line of sight is possible. When using a Spectrum Analyser (SA) it is possible to measure the received signal strength. The measured strength can then be compared to the predicted signal strength from the simulation model. During the test, Brik-II has to send a carrier signal to the ground which can be picked-up by the antenna. A carrier signal is an unmodulated signal that has a narrow bandwidth. Therefore the signal strength is clearly visible and can be quantified. A modulated signal would spread out over a larger frequency range. Since the transmission power is the same, the peak of the unmodulated signal is higher compared to the modulated signal. Therefore the signal strength is easier to distinguish from the background noise. The SGP4 propagator will yield the orbital parameters of the satellite for the transmission period. The input should be the time and location of the test. Furthermore the test to measure the radiation pattern has been conducted. Therefore the actual gain of the submarine antenna is known. The measured pattern can be implemented into the link budget simulation. With the radiation pattern and orbital parameters, it is possible to simulate the link budget and compare it with the measured value. If the deviation is within expected margins, it can be concluded that the simulation is correct and the data rate should match the predicted rate.

6.2. Measurement execution

In this section the execution of the two measurements is discussed. First the radiation pattern test and thereafter the link strength measurement. Not only the measurement execution procedure is explained, but also possible issues and subsequent deviations are discussed.

6.2.1. Radiation pattern test

The radiation pattern test has been conducted twice. The first test was indoor in an anechoic chamber at the 982 Squadron in Dongen. The transmitting antenna for the first test is a circular polarised antenna. This was chosen as a part of the top part of the radiation pattern of the submarine antenna is circularly polarised. As explained in section 6.1.1 Here a reference antenna should be used. The three antennas used can be seen in the figure below. In figure 6.3 the circularly polarised transmitting antenna is shown. In figure 6.4 the linearly polarised reference antenna can be seen, and in figure 6.5 the submarine antenna.

Figure 6.3: Main transmitting antenna measurement 1

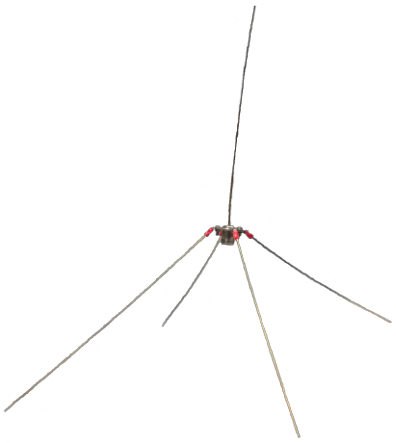

Figure 6.4: Reference antenna measurement 1

Figure 6.5: Submarine antenna

In the anechoic chamber, the transmitting and submarine antenna are placed on opposites ends of the room, as can be seen in figure 6.6. The circularly polarised antenna was placed on the wall and is connected to the signal generator. The transmitting antenna is attached to the wall using magnets, as

shown in figure 6.8. The submarine antenna is placed on a rolling plateau, such that all the sides of the antenna can be measured. In figure 6.7 the antenna is tilted towards the transmitting antenna as explained in section 6.1.1.

Figure 6.6: Anechoic chamber measurement 1

Figure 6.7: Submarine antenna during measurement

Figure 6.8: Transmitting antenna measurement 1

During the measurements the angle of the RRS rotor will vary from 25° till 90°. 90° is straight up, and 25° is nearly flat. A lower angle could not be achieved due to internal limitations of the stepper motor inside the RRS rotor. The other variation is the horizontal rotation of the plateau on which the antenna is placed. It is varied to check if the radiation pattern is omnidirectional and the same in each direction. The angles used for measurements are 0°, 90°, 180°, and 270°. When calculating the FSPL, the distance between the transmitting and receiving antenna should be determined. Here the difference in height is also accounted for in the calculation. Furthermore, when the antenna is tilted the distance is reduced. To determine the difference in distance the phase center of the antenna should be known. The phase center is the middle point of the radiation pattern's origin, and should therefore be used as the point from which the distance is calculated. The phase center is hard to calculate as the shape of the antenna is relatively complex [52]. Furthermore the phase center can also be located by measurements. However, this requires accurate measurement equipment that was not available. Therefore the phase center was estimated to be halfway up the antenna. The results of the measurements are discussed in the section 6.3.1.

The radiation pattern measurement has been conducted two times. The second measurement was done outside and over a larger distance. There are multiples reasons why the measurement was repeated:

1. The circularly polarised antenna does not match the satellite's polarisation. To see how the polarisation of the transmitting antenna influences the radiation pattern a second test is done with a linearly polarised transmitting antenna.

2. During testing in the anechoic chamber some variations in the radiation pattern were measured. To see if this was caused by the antenna or other disturbances in the chamber, the test procedure is repeated outside.

3. Since the phase center of the antenna cannot be determined, the variation in distance when tilting the antenna cannot be accurately taken into account. To lower the influence of this error, the distance between the antenna can be increased. In this case the distance error remains the same however its is a smaller fraction with respect to the total distance.

The antennas that are used in the outdoor test can be seen in figure 6.9, 6.10, along with the submarine antenna in figure 6.11. The transmitting and reference antenna are the same type linearly polarised antenna. In the calculation the two antennas are not assumed identical.

Figure 6.9: Main transmitting antenna measurement 2

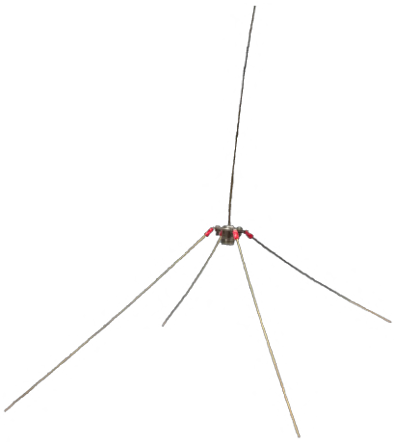

Figure 6.10: Reference antenna measurement 2

Figure 6.11: Submarine antenna

The measurement set-up for the outdoor radiation pattern test can be seen in figure 6.12, 6.13, and 6.14. The distance between the transmitting and receiving antenna has increased from 5.21 m to 13.87 m to reduce the influence of the phase center. If for both measurements the phase center deviates with 25 cm, the influences would be 1.21% and 0.36% for the 5.21 m and 13.87 m measurement, respectively. So increasing the distance results in a reduction of the possible error with a factor of ± 3.4. The signal generator was set at 9 dBm for the anechoic chamber measurement and 13 dBm for the outdoor measurement.

Figure 6.12: Radiation pattern measurement set-up outdoor

Figure 6.13: Radiation pattern measurement set-up outdoor

Figure 6.14: Transmitting antenna radiation pattern measurement outdoor

The outdoor measurement went well and the results are useful. The results of the measurements are discussed in section 6.3.1.

6.2.2. Link strength measurement

The location chosen for the measurement was Dongen, as this is the ground station location. It would allow for commanding the satellite during the pass and monitor the execution of the instructions. The build-in system of the ground stations can show the received signal strength over set bandwidth. In figure 6.15 the antenna can be seen along with the portable receiver. The 982 Squadron wanted to perform some measurement with the TacSat UHF antenna which is part of the RRS. The TacSat antenna can be seen on the right in figure 6.15. The set-up including the TacSat antenna can provide extra insight in the submarine antenna performance. Since the TacSat antenna has a more directional radiation pattern, the gain in the axial direction is higher, but the antenna gain is relatively low in other

directions.

Figure 6.15: Outdoor measurement set-up for link strength testing

During the measurements a number of issues were encountered that prevented collecting good data. Therefore, the measurements were inconclusive and no good conclusions could be drawn from the results. The issues are listed below:

1. **Brik-II:** The Brik-II satellite was unable to execute the command to transmit a carrier signal. Why the satellite was unable to do this was unclear to the satellite operators. One of the possible causes was that the satellite had been struck by a solar flare a few days prior. Therefore some systems were still disrupted and the system would fall back to safety mode. The time available during the measurement was not sufficient to mitigate the problem. Since the carrier signal could not be sent, it was chosen to transmit a modulated signal.
2. **Noise:** The goal of the measurement is to see the signal strength that can receiver. Since the test is outdoors, it was chosen to use a KEYSIGHT FieldFox as it is power by an internal battery. The fieldfox display can be seen in figure 6.16.

Figure 6.16: FieldFox receiver outdoor measurement

To detect the carrier signal it is important to lower the noise floor of the instrument. During the measurement, the noise floor was ± -120 dBm because the measured frequency range had a width of 2 MHz around the downlink frequency. The ”Res BW” as shown on the screen is the resolution bandwidth. It is the bandwidth of the filter that sweeps the set frequency range. Ideally the bandwidth should be as small as possible however the trade-off is sweep time. With the chosen bandwidth of 300 Hz the sweep duration, and therefore the update time, was around 1 second. When the filter measures the incoming signals, the power going through the filter is measured [2].

During the first pass allocated for testing, no signal was received by the antenna. The satellite was unable to transmit the carrier signal so no signal could be received. At that time it was unclear if the command was executed and nothing had been received or that the satellite didn't transmit. To verify that the measurement set-up was correct an indoor test has been done. A signal was transmitted using an available omnidirectional UHF antenna. The input signal was relatively low and ± 20 meters apart, but it could be received. The information displayed by the FoxField receiver during the indoor test can be seen in figure 6.17.

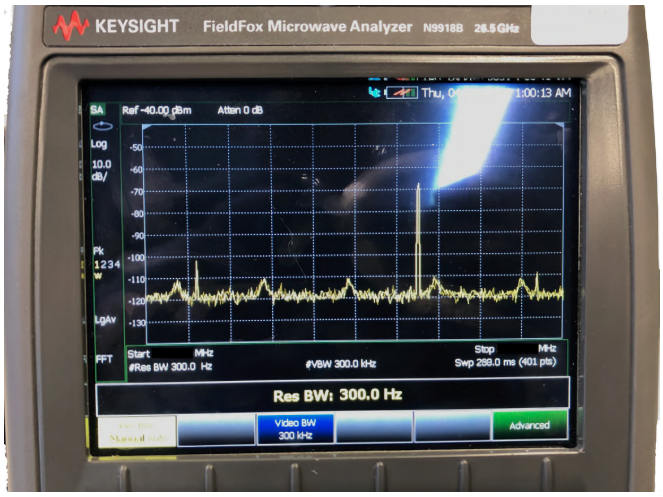

Figure 6.17: FieldFox receiver indoor measurement set-up test

It can be seen that a clear spike is visible at the downlink frequency. Therefore it was concluded that the system set-up was correct and the satellite transmission should be receivable. Before the satellite would pass again it was concluded that the carrier signal had not been transmitted. Therefore it was chosen to send a modulated signal instead of a carrier signal. Unfortunately the carrier signal could not be detected using the submarine antenna or the TacSat antenna. Therefore it was concluded that further investigation was necessary by the 982 Squadron as the TacSat antenna should be able to receive the signal. After further testing, it was concluded that the FieldFox would not have been able to receive the signal as the noise floor was too high. The peak of a carrier signal would reach around ± -120 dBm when using the TacSat. Therefore the carrier signal could not have been detected even if the satellite had performed the instruction correctly. The modulated signal has a lower signal strength as it spread out over a larger frequency range than the carrier signal and was therefore not detectable. The noise floor can be lowered using an external Low-Noise Amplifier (LNA) to make the signal more detectable. Using this, the signal should be receivable and communication should be possible. This is the case for both the TacSat antenna as for the submarine antenna design in the MSc thesis.

3. **Time:** Further testing was not possible due to the time constraints of the thesis. The LNA had to be ordered, tested and implemented before further measurement could be done. The 982 Squadron would also prefer to do further testing with the RRS since the necessity of a LNA also impacts the performance of the RRS. Therefore no further measurement could be done.

To conclude, the calculated link strength could not be compared to real-world measurement. Therefore, the link strength simulation could not be verified at this time. Future verification would be required to enable accurate data throughput predicted as requested by requirement RQ-P-1.1. Furthermore all requirements stating a quantified data throughput can verified.

6.3. Results

Now that the measurements have been conducted the results will be analysed. Possible deviations that are found will be investigated. Furthermore, the implications of the measurement result on the workings of the system will be discussed. First the radiation pattern measurements are analysed.

6.3.1. Radiation Pattern Measurements Results

The first step during testing is to measure all the distances between the antennas. Furthermore the input power from the signal generator should be known. The measurement parameters are shown in table 6.1.

	Anechoic chamber	Outdoor
Distance transmit-submarine antenna [m]	5.21	13.87
Distance reference-submarine antenna [m]	5.21	13.87
Distance transmit-reference antenna [m]	5.21	13.59
Power signal generator [dBm]	9	13

Table 6.1: Measurement parameters

The angles that have been considered when rotating the antenna around the upright axis are 0°, 90°, 180°, and 270°. The angle is also named the azimuth angle. An azimuth of 0 and 180° together are one slice of the radiation pattern. The same is applicable to the 90° and 270° azimuth angles. During the test the rotor system of the RRS was used, since this rotor system was designed to move a much lighter antenna there where some internal limitations in its movement while equipped with the Submarine antenna. It cannot tilt the antenna more than 65° from the upright position. Therefore, the elevation angles that can be measured are 0°, 10°, 20°, 30°, 40°, 60°, 65°. Using equation 6.2,6.4, 6.3 and the parameters from table 6.1 the gain of the antenna can be calculated for all angles. The results of the azimuth cuts can be seen in figure 6.18 and 6.19.

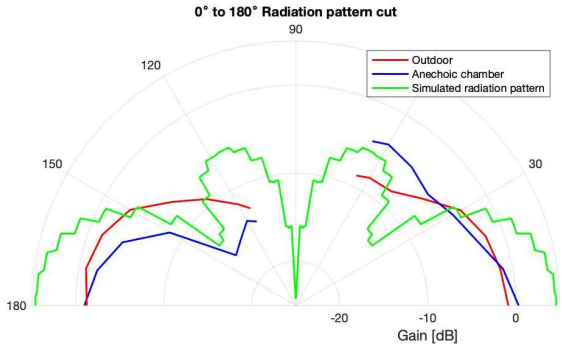

Figure 6.18: Radiation pattern slice 0°-180°

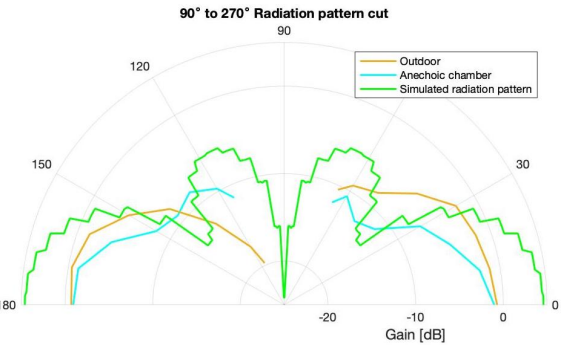

Figure 6.19: Radiation pattern slice 90°-270°

From the figures, it can be observed that the radiation pattern does not correspond with simulated radiation pattern. The absolute gain can be different due to losses since the ideal radiation pattern does not include any (e.g. cable losses, not perfect impedance match). However, the shape of the measured radiation pattern does also not match the simulated radiation pattern. Due to the losses, it is expected that the measured pattern is lower compared to the simulated pattern. This is the case in most of the pattern except around the 35° to 55° elevation range. The predicted radiation pattern has a significant dip in the gain. In the measured pattern it seems that this dip does not occur. Another observation is that the delta between the outdoor measurement and the anechoic chamber measurement

increases at higher elevations. This might be due to the fact that the submarine antenna is circularly polarised at the higher elevation angles, while at lower elevation angles the polarisation in linear. Since the anechoic chamber measurement uses a circularly polarised antenna to transmit a reference signal the polarisation mismatch is lower at higher elevations compared to the outdoor test where a linearly polarised antenna was used to generate a reference signal.

The next step was to identify the possible causes for the deviation in the shape of the measured radiation pattern. Therefore the dimensions of the antenna were measured, they were not a perfect match with the expected dimensions. The wire used for the antenna has a larger diameter than anticipated. Therefore it protrudes further from the grove made in the antenna. The diameter increases from 60.206 mm to 65.56 mm. The diameter of the wire used is a different, going from 2 mm to 2.05 mm. Also the feed-height has deviated, going from 10 mm to 7.75 mm. Even though these differences are relatively small, they have a significant impact on the radiation pattern of the antenna. The radiation pattern of the manufactured antenna can be seen in figure 6.20.

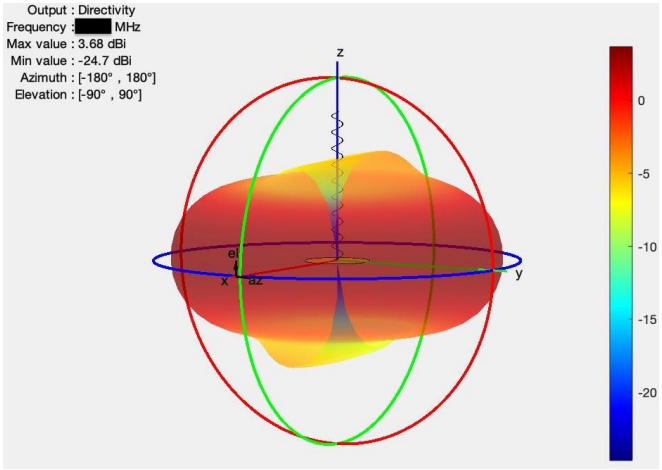

Figure 6.20: Radiation pattern manufactured antenna

The radiation pattern is very different compared to the theoretical design as seen in figure 4.28. It does not have the dip in the radiation pattern around the 35° to 55° elevation angle. Furthermore the pattern is not symmetric omnidirectional, as can be seen in figures 6.21 and 6.22.

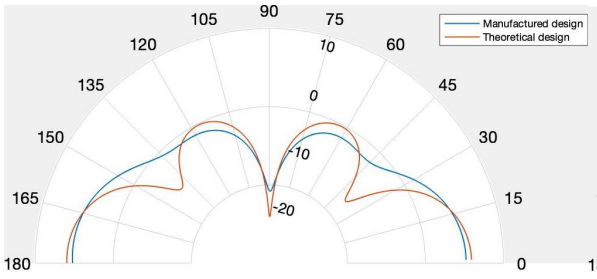

Figure 6.21: Radiation pattern slice 0°-180°

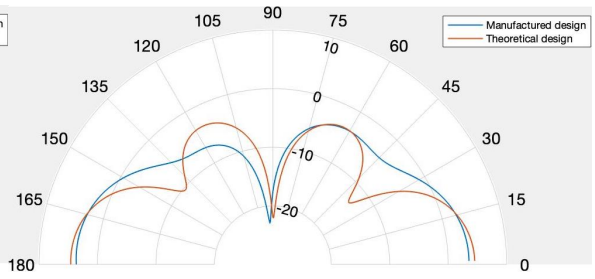

Figure 6.22: Radiation pattern slice 90°-270°

The radiation pattern slices are different from the theoretical design. The manufactured antenna has a lower gain at low elevation angles, while it has a higher gain in the 35° to 55° elevation angle range. Furthermore, the radiation pattern is not symmetrical at higher elevation angles. The asymmetry is particularly visible in figure 6.22, where the difference at 65° elevation is 3.58 dB. To see how much influence the differences between the theoretical and manufactured design have on the performance, the communication has to be simulated. The input parameters for the simulation are the same as used in section 4.5. The result is a data throughput of 1.367 GB which is 1.73% lower than the optimal design. So the impact of the manufacturing differences is limited.

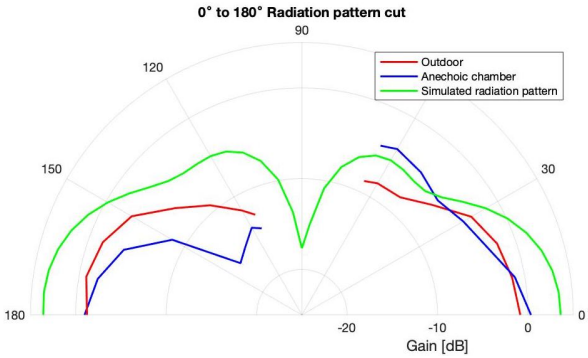

Figure 6.23: Radiation pattern slice 0°-180°

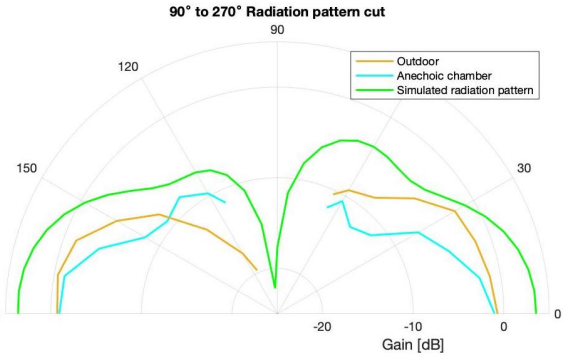

Figure 6.24: Radiation pattern slice 90°-270°

In figure 6.23 and 6.24 the radiation pattern is compared to the measurements results. The shape of the measured antenna radiation pattern corresponds better with the predicted shape of the radiation pattern, especially the outdoor measurement. The deviation seems to increase at higher elevation angles. The shape match is considerable better, however the absolute values still have a relatively high mismatch, often more than 4 dB. Therefore it was investigated what causes these differences. The effects that were identified are listed. These are all the losses that can be quantified with a certain accuracy.

1. **Cables:** The losses caused by the cables used during the measurements can be measured. A coupling is used to attach the cables together. The signal generator is attached and inserts a signal, the signal will be measured by the receiver. This is also done without the cables attached to create a baseline measurement. The difference in signal strength between the signal generator and receiver, minus the baseline reading, are the losses in the cable. The found value is 1.05 dB. The cables losses can be minimised by used better quality cables.

2. **Impedance:** The impedance of the antenna at downlink frequency is not perfectly 50 Ω. Therefore some losses are introduced into the system. In section 5.3.1 it has been determined that the losses are 0.1196 dB. The impedance losses can be reduced by achieving a better impedance match at the used frequency.

3. **L-network:** The L-network used to match the impedance also induced losses into the system. These losses are hard to measure. As these components are very small and need sensitive equipment. Another way to get an estimation of the losses is to make a simulation of the L-network and compare it with the ideal lossless system that is assumed in the radiation pattern simulation. Both systems can be seen in figure 6.25.

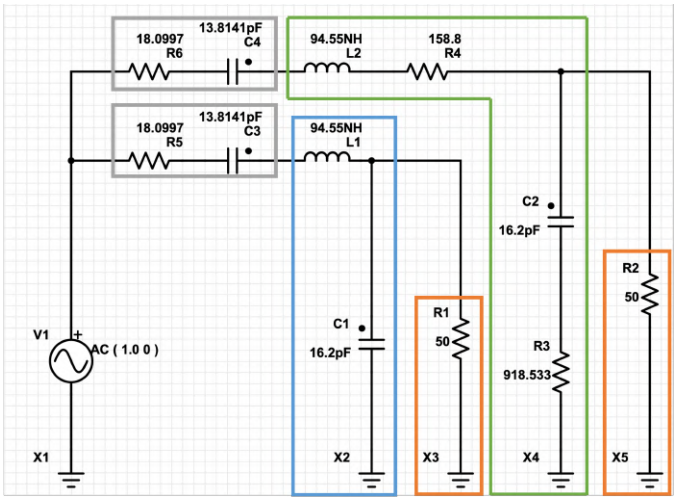

Figure 6.25: Schematic L-network to simulate losses

The orange colored rectangles are the antenna, and both have a real impedance of 50 Ω. In the blue rectangle the ideal L-network is build with the values from table 5.4. The ideal L-network will be compared with the green L-network that includes losses. The parasitic resistance of capacitor (C2) can be determined by calculating the Equivalent Series Resistance (ESR) by using equation 6.6.

$$ESR = \frac{tan(\delta)}{\Omega L} \tag{6.6}$$

Where:

- ESR | Equivalent Series Resistance
- Ω | Angular Frequency
- L | Capacitance capacitor
- $tan(\delta)$ | Loss tangent

The angular frequency can be calculated $\Omega = 2\pi f$, where f is the operating frequency. In an ideal situation the capacitor only has a negative reactance. However, in practice, the capacitor impedance also has a resistive part. The loss tangent $tan(\delta)$ is the angle between the resistive and negative reactants part of the capacitor impedance. The $tan(\delta)$ can be found in the spec-sheet of the variable capacitor used [15]. The worst case value allowed during production is $tan(\delta) = 25$. It can be assumed that in practise the loss tangent is lower. However, in the case of the L-network simulation, it is investigated how much the radiation pattern measurement can be affected by losses in the network. Therefore $tan(\delta) = 25$ has been used for the calculation, and yields $ESR = 918.533\ \Omega$. The resistive value of the capacitor can be calculated using equation 5.6, where X_l is the resistance, and yields $X_l = 158.8\Omega$. In the two grey rectangles the impedance of the antenna before matching is $18.0997 - 43.1022i\ \Omega$. Note that the impedance has a negative reactants part, therefore a capacitor should be added in series. The value of the capacitor can be calculated using equation 5.5, this yields $C = 13.8141pF$. The resistor is equal to the resistance of the impedance, 18.0997Ω. With all the component characteristics known a simulation can be done. Here the source signal generator applies a alternating current over the network. The frequency used is from 200 to 300 MHz. The input voltage is measured between the generator and R5/R6 in the network. Furthermore the output of the network at both antennas is measured. So the voltage is measured between L1 and R1 for the ideal network, an between R2 and R4 for the network including losses. Not the losses between the input and two outputs can be compared. The results are shown in figure 6.26

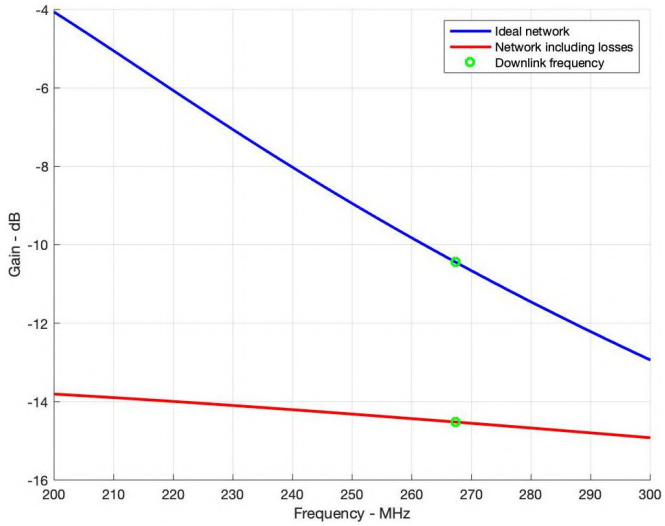

Figure 6.26: L-network simulated output

It can be seen that the output of the ideal network is higher than the network including the losses. The delta between the ideal network and the networking including losses, are the losses in the system. At the downlink frequency, the losses are 4.0872 dB. The losses due to the L-network can be improved using better components. A Surface Mount Device (SMD) capacitor of 15 pF would have a resistance of around $0.1\ \Omega$ [6] . That would decrease the losses in the L-network and improve the performance of the antenna. The inductor can also be found as a SMD component at 96 nH [7].

4. **Measurement equipment:** The equipment used for the measurement consists of the signal generator and the receiver. Both devices can have an error in the signal they generator or receive. According to the specification sheet the receiver has a typical error of +/- 1 dB in the UHF band [3]. The signal generator has an error of <0.5 dB according to the specification sheet [4]. Both the errors apply to all the values measured during testing, so the P_{x-y} in equation 6.2, 6.3, and 6.4 can each have a deviation of +/- 1.5 dB. The deviation also applies to the cables losses measured, as the same devices were used. The 982 squadron does calibrate the equipment regularly and therefore the deviation is most likely smaller. To visualise the uncertainty of the measurement induced by the equipment, an error range has been added. The range is represented by the dashed lines in figure 6.27 and 6.28.

When compensating for the aforementioned losses, and applying the error range, the radiation pattern is more similar in absolute gain as seen in figure 6.27 and 6.28.

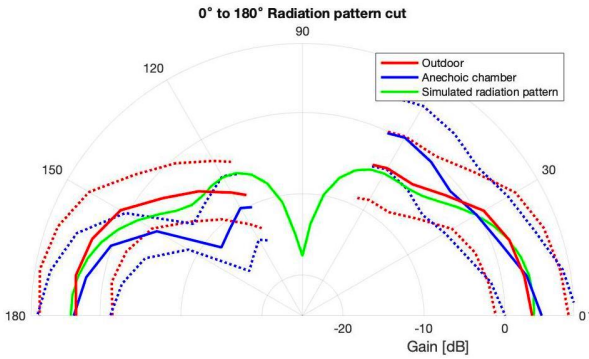

Figure 6.27: Radiation pattern slice 0°-180°

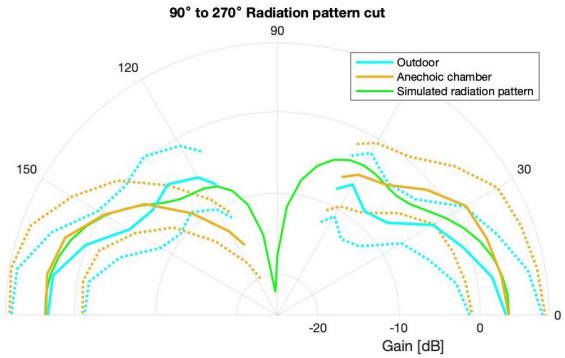

Figure 6.28: Radiation pattern slice 90°-270°

Overall, the match between the expected radiation pattern and the measured pattern is much better. The measurement in the anechoic chamber has a larger deviation compared to the outdoor measurement. On the left side in figure 6.28 the outdoor measurement has a large deviation at higher elevations, while at low elevation the match is nearly perfect. The outdoor measurement matches the expected radiation pattern the best. Therefore it was chosen for a data throughput simulation to see how much the deviation from the pattern influences the performance. The input parameters for the simulation are the same as used in section 4.5. It yields a data throughput of 1.3569 GB, which is 0.75% less compared to the ideal performance of the build antenna. It is 2.42% lower than the optimised antenna design that was selected. When the losses are not compensated the total data throughput is significantly lower, namely 1.0903 GB. That is a decrease of 21.80% compared to the design from the optimisation. To get a better idea of the performance difference between the measured radiation pattern compared to the predicted radiation pattern, the propagation period should be shortened. The same parameter are used as for figure 4.34. The data rate for downlink communication with fixed ACM mode is shown in figure 6.29. Here the radiation pattern of the manufactured antenna is compared to the measured radiation pattern. Doing this provides two possible insights, first the difference between the build system and the desired system. Second, it shows if the build antenna will be usable in practise.

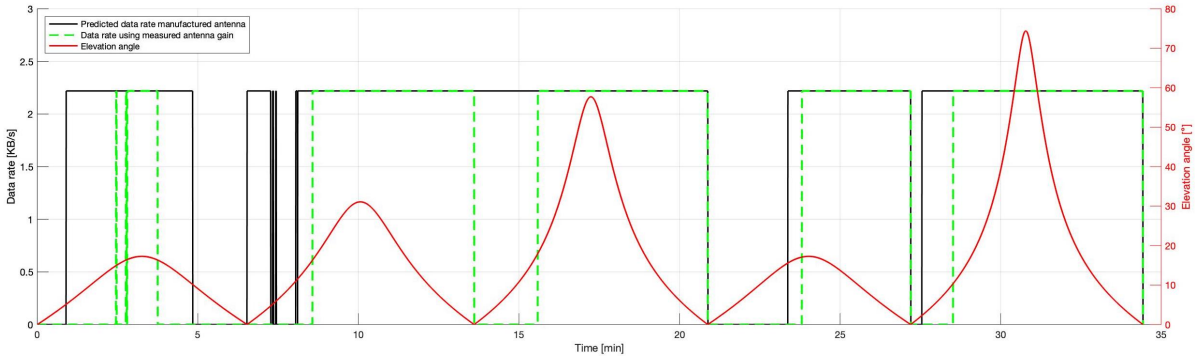

Figure 6.29: Data rate with fixed ACM mode for predicted and measured radiation pattern

It can be seen that the predicted radiation pattern enables communication more often compared to the measured radiation pattern. Mainly at the lower elevation angles communication is not possible since the SNR is not sufficient. The SNR and antenna gain can be seen in figure 6.30.

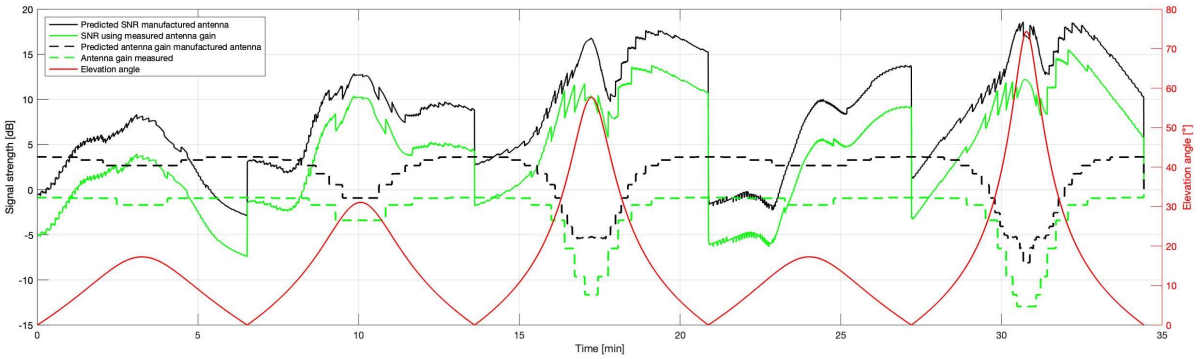

Figure 6.30: SNR and antenna gain for predicted and measured radiation pattern

Since the antenna gain of the measured radiation pattern is always lower than the gain of the predicted radiation pattern the SNR is also lower. What is interesting to see is that the measured antenna radiation pattern is close to predicted shape gain shape. Furthermore, it can be seen that the delta is SNR is lower around 30° elevation since the difference in antenna gain is also much lower. The predicted SNR is higher therefore, the data rate when applying variable ACM mode can be higher. The data rate for variable ACM mode can be seen in figure 6.31.

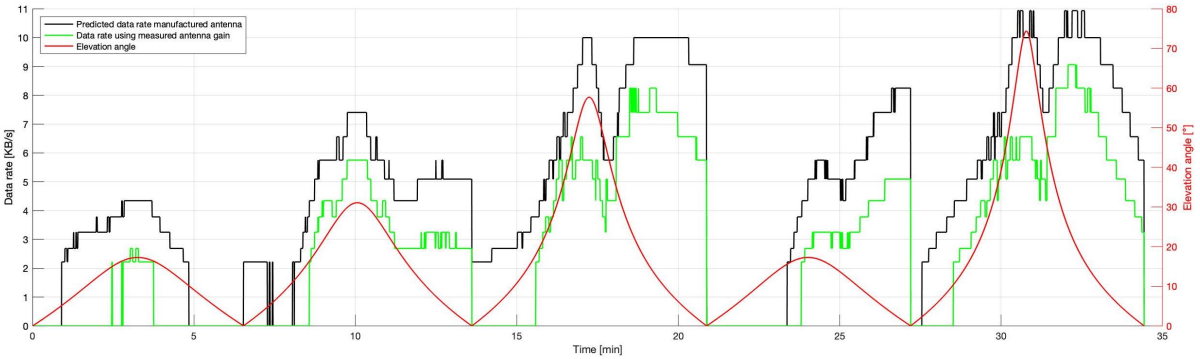

Figure 6.31: Data rate variable ACM mode for predicted and measured radiation pattern

The difference in data rate is larger compared to figure 6.29 as the ACM mode is higher. The total data throughput in figure 6.31 is 40.98% for the measured radiation pattern than for the predicted pattern.

From figure 6.31 it can be concluded that the measured gain has large implications on the capabilities of the submarine. The key performance requirement is the 1 MB that should be achieved during each pass with a maximum elevation above 20°. The most critical situation is the downlink with fixed ACM mode, as can be seen in figure 4.33. If the 1 MB can be achieved is shown in figure 6.32.

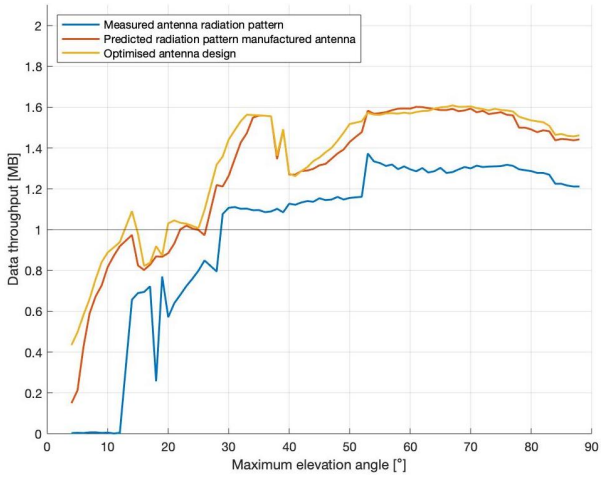

Figure 6.32: Average data throughput pass for different maximum elevation angles

It is evident that the predicted performance of the manufactured design is better than the measured performance of the manufactured design. Furthermore the performance of the simulated manufactured design is not as good as the optimised antenna design. The optimised antenna does not go below 1 MB for passes with a maximum elevation above 20°. For simulated manufactured design this does occur, but not as significant as for the measured design. The latter does not reach the 1 MB requirement for pass with a maximum elevation below 29°. Therefore the performance of the antenna does not meet requirement (RQ-P-1.1). However keep in mind that the gain of the measured radiation pattern can be improved. When the losses are compensated as show in figures 6.27 and 6.28, the performance difference is reduced. The different types of losses that have been considered are cables losses, impedance mismatch losses, L-network losses, and deviation to the measurement equipment. These are all influences that could be quantified. There are also number of factors that could not be quantified, but still have an influence on performance:

1. **Ground reflections:** During the measurement ground reflections have not been taken into account. The reflections influence the signal strength received at the antenna. Reflections can have an influence of ± 0.27 dB [39]. The influence of ground plane reflections depends on the distance between the transmitting and receiving antenna. The minimum distance (d) required to neglect the influence of ground reflections can be calculated by using equation 6.7 [65].

$$d \gg \frac{4\pi h_{Rx} h_{Tx}}{\lambda} \tag{6.7}$$

   Here h_{Rx} and h_{Tx} are height of the phase center above the ground for the receiving and transmitting antenna. During the outdoor measurement both antennas were place ± 1.45 m above the ground. Calculating the minimum distance yields ± 23.5 m. The distance between the antenna during measurement was 13.87 m. Therefore it can be concluded that ground reflections might have affected the measurement results.

2. **Influence plastic:** The ABS plastic used for the 3D printed material was assumed to not influence the radiation pattern. To research the impact of different materials close to a signal source the material used in radar domes are of interest. The ideal material used for radar domes is Telfon [11]. Telfon has the lowest dissipation factor $tand(\delta)$ and permittivity of the considered plastics. ABS has dissipation that is 25 to 95 times higher, being only 0.0050 to 0.019. However, when the distance to the antenna is small, as is the case with the ABS plastic, the effect on the radiation

pattern increases [31]. For future design it might be an option to 3D print the antenna from Teflon [61]. Another option would be to reduce the amount of ABS plastic used. Currently the antenna is quite sturdy and some plastic could be removed while still maintaining adequate rigidity. The amount of plastic could also be reduced by using a perforated design instead of a solid body.

3. **Positioning L-network:** The L-network is positioned above the ground plane of the antenna as can be seen in figure 6.33.

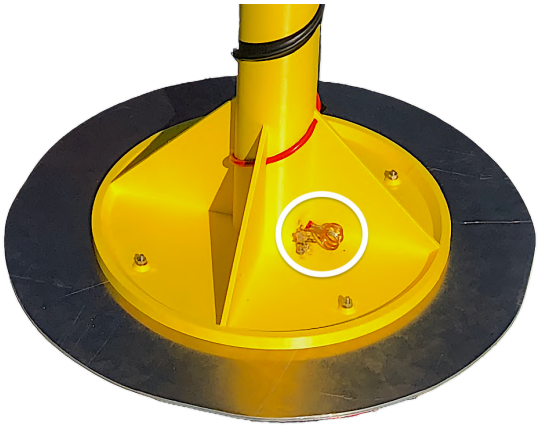

Figure 6.33: L-network location on submarine antenna

The placement here was chosen due to the lack of attachment options on the underside. Since the components of the L-network are conductive, they will influence the radiation pattern. In future iterations the L-network should be attached underneath the ground plane as this will prevent radiation to influence the radiation pattern of the antenna.

4. **Accuracy RRS rotor:** The accuracy of the RRS rotor has not been verified. Around the upright position the rotor can be unstable and sway a few degrees. Therefore the exact position of the rotor is not fully accurate so it can induce a small error in the measurement. The rotor system was not designed to take measurements. It was still used since it was the best option available.

6.4. Discussion

From the measurements a number of conclusions can be drawn. The shape of the radiation pattern is similar to the shape predicted in the MATLAB simulation. However, the absolute antenna gain is lower for most measurements compared to the predicted values. A number of possible causes, quantifiable and unknown, has been identified for the deviation. To improve the measurement and performance of the antenna, the impedance match should be improved. Furthermore, the losses in the L-network should be reduced by using SMD components. The smaller size of SMD components make it possible to move the components below the ground plane. These steps will likely improve the performance of the submarine antenna. Apart from the antenna, the measurement set-up should also be improved. The antenna should be measured in the anechoic chamber purposely build for antenna radiation pattern measurement and certified for the UHF frequencies used by the Brik-II. The equipment is selected to measure antenna gain, therefore it will allow for measurements with greater accuracy. Furthermore, the positioning equipment is more capable and accurate than the RRS rotor, thus the pattern can be measured at all angles and with greater accuracy. Lastly, the anechoic chamber would damp out all reflections which would allow for more accurate results. If all these improvements can be made a definitive conclusion on the radiation pattern simulation could made. As this is not the case for the current measurements set-up, it can be concluded that the possible discrepancies in the simulation cannot be identified.

The second measurement that has been conducted is the communication test with the Brik-II satellite. The purpose of the test, to verify the link strength simulation, could not be done since there were

a number of issues. Such as the satellite not executing commands correctly, too high noise floor, and time constraint. Therefore the link budget simulation could not be verified thus no accurate conclusion can be draw on the simulation results. So it is not possible to verify that the set requirements are met. It did however yield a valuable insight, namely that a LNA is required to lower the noise floor thus making the signal stand out more.

Concluding that, even though the workings of the MATLAB radiation pattern simulation cannot be fully verified, it can be seen that the measured radiation pattern is quite similar to the predicted patter. Furthermore, the measured radiation pattern should allow for communication between the submarine and the Brik-II satellite. The communication test could not confirm this due to a number of issues as mentioned above. To increase the accuracy of the radiation pattern test it should be performed in an anechoic chamber designed for radiation pattern testing. The link strength verification measurement could be redone once the LNA can be implemented. It can be concluded that a full answer to research sub-question 2 cannot be provided, as the full performance could not be verified. In the next section it will be investigated if the leading requirements set by the Navy are met.

6.5. Leading Requirements Verification

The three leading requirements as set in section 3.2.2 should be verified. These requirements induce a trade-off in the design process. The size constraints have influenced the type of antenna that could be incorporated into the design. Since the helical antenna selected is omnidirectional it induces restrictions on requirement RQ-P-1.8. To still enable downlink in critical operational situations, the systems is optimised to meet the 1 MB requirement (RQ-P-1.1) under these circumstances. Each of the leading requirement is discussed below.

- **RQ-P-1.1**: *The system shall provide a minimum link budget of >1 MB during a single pass under ideal conditions*
  The downlink with a set ACM mode was identified as the critical situation to meet this requirement. The system was designed such that a minimum of 1 MB could be transferred if a pass reaches an elevation of 20° or higher. The measured antenna radiation pattern performance is lower. To see how much the system deviates from the optimised antenna the propagation as defined in section 4.4 has been run with 3 different antennas. First for the optimised antenna. Second the antenna with the measured radiation pattern. Third for the measured radiation pattern antenna but the losses are compensated as listed in section 4.4. The results can be seen in figure 6.34.

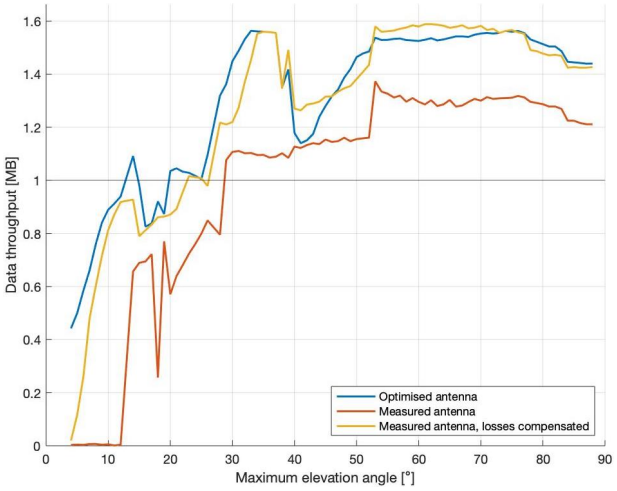

Figure 6.34: Average data throughput for passes with different maximum elevation angles

It can be seen that optimised antenna meets the requirements if a pass has an elevation higher

than 20°. Passes with an elevation of 20° or higher are 59% of all passes that occur in the propagation period defined in section 4.4. Please note that in the percentage calculated all passes are incorporated. Meaning that pass with a 1° elevation are considered for communication. Achieving the 1 MB for such low elevation passes cannot be considered feasible since the contact time is small. For the measured radiation pattern the minimum elevation angle required is higher, namely 29°. Passes with an elevation of 29°or higher occur 41%, which is 18% lower compared to the optimised antenna. If the losses identified in the antenna radiation pattern measurement are compensated the minimum elevation required decreases to 27°. Therefore the passes available would be 43%. So the manufactured design has a lower performance than the optimised design thus it will be less deployable than predicted. Furthermore the data throughput of the manufactured antenna is lower for all elevation passes as seen in figure 6.34. It can be concluded that it would be favourable to iterate on the manufacturing and build the optimised antenna according to the specification. Furthermore, precautions should be taken to ensure that the losses occurring in the current antenna are mitigated in the new antenna. This would ensure that the performance of the design is optimal.

- **RQ-P-1.8**: *The system shall only transmit high power signals in the direction of the satellite to limit detectability*
  This requirement was difficult to meet since all directional antennas were not viable options due to size constraints. Therefore an antenna with an omnidirectional radiation pattern had to be selected. The downside is that it transmits in all directions and cannot focus the signal towards the satellite. A phased array antenna would be able to meet the requirements. However, such system would not be technically feasible within the set size constraint, since the higher frequency is to0 low. So, the system is unable to limit high power signal transfers in all direction. Therefore the operational deployability is compromised. Meaning that the system should not transmit any signals if detection would have large consequences. During such circumstances the system should only be used to receive messages.

- **RQ-P-2.1**: *The system shall have a diameter <0.4 m and length of <1 m*
  The manufactured antenna has the following dimensions; Length 0.842 cm, diameter 0.4 m. Thus it can be concluded that the requirement is met.

7

Conclusion and Recommendations

This chapter presents the conclusions of this MSc thesis project. Section 7.1 will provide a recap of the work done. Section 7.2 will provide an answer to each sub-question, after which Section 7.3 will give the main conclusion of this thesis and check to what extend the main objective has been fulfilled. Hereafter, section 7.4 will discuss the recommendations and suggestions for future work.

7.1. Recap

The first step in this MSc thesis was to identify the problem that should be solved. Once identified the system requirements could be compiled in consultation with the Navy. From the requirements it was concluded that there are a number of similarities between the RRS and the submarine communication system. However, the antenna system installed on the RRS would not meet the size requirements. Therefore a new antenna systems had to be designed that would comply with the requirements. To find the optimal design for the antenna, a simulation tool for the communication between the submarine and Brik-II was developed. In the simulation different antennas were tested to find the optimal design. The helical antenna was selected as the basis for the optimisation. Once the optimal design was identified, a prototype antenna was manufactured using the 3D printing facilities at the 982 Squadron in Dongen. Hereafter, measurements were conducted to verify that the radiation pattern of the antenna corresponded with the radiation pattern predicted. The test showed a large overlap in the shape of the radiation pattern. However the absolute gain of the antenna did not correspond with the predictions. A number of reasons were identified that could explain the differences found as mentioned in section 6.4. Communication tests with Brik-II could not be performed due to commanding problems on the satellite's side.

7.2. Answer to Sub-Questions

At the start of the project a number of research question were set that should be answered. The questions have been defined in section 1.1. In this section each question will be discussed separately, starting with the first question.

> "**Sub-Question 1:** *What physical design characteristics does a satellite communication system have to meet to be deployable on-board the Dutch submarines?*"

The system will be placed in the communication mast on top of the sail of the submarine, as explained in chapter 3. This position is required since the UHF signal does not propagate through water [26]. To protect the system from sea water it will be placed inside a closed tube named the communication mast. This imposes size constraints on the antenna which rule out the use of a steerable directional antenna design, as elaborated on in section 4.3. Therefore an omnidirectional helical antenna design was selected. The exact design dimensions have been identified and are listed in table 5.1. The

electronics of the system, which are assumed identical to the hardware used in the RRS, will be placed inside the submarine.

> "**Sub-Question 2:** *What are the performance characteristics of the submarine satellite communication system?*"

The ideal performance characteristics have been identified after the optimisation of the antenna. The system would theoretically be able to achieve a 1 MB data throughput per pass if it has an elevation higher than 20°. The average throughput would be 1.3612 MB per pass, as shown in table 4.3. The results of the optimisation are discussed in more detail in section 4.5.1. From the radiation pattern measurements conducted it was concluded that the actual gain of the antenna is lower. Therefore the data throughput is 21.80% lower than the theoretical performance. The current performance should still enable satellite communication, but with a lower data throughput. A more detailed explanation is provided in section 6.3.1.

7.3. Conclusion

In the conclusion it will be examined if the objective has been achieved. The main objective of the project has been defined as seen below.

> "**Research Objective:** *To enable communication between a submarine and the Store and Forward payload of the Brik-II satellite by means of designing, manufacturing and testing an operationally deployable communication system for the submarines operated by the Royal Netherlands Navy.*"

A system has been designed that should be able to communicate with the Brik-II satellite. The choice was made to focus on the design of the antenna system. The electronics hardware that could be used is equal to that of the RRS. The first prototype of the system was manufactured, after which it has been tested to see if it matched the required performance. The current system is a prototype and is therefore not suitable for actual deployment on a submarine. A next iteration could be manufactured such that it can be used on-board. However, during the design and testing of the system two constraints on the deployability have been identified;

1. The performance of the manufactured antenna is lower than expected. The data throughput requirement of >1 MB can only be met for passes above 29°, which only occur for 41% of all passes. Therefore the deployability of the system is reduced.
2. The radiation pattern of the helical antenna is omnidirectional. Therefore the high power antenna signal is transmitted in all directions. The requirements indicate that such transmissions should be prevented, to limit the chance of detection. With the current size constraints it was not possible to design a system that would prevent this. The impact on the deployability is that no transmissions can be made if detection would have large consequences.

The first constraint is caused by losses in the system, as discussed in section 6.3.1. The losses can be mitigated with the next iteration of the prototype. The proposed solutions will be elaborated on in the section 7.4. The second constraint is more difficult to resolve; The helical antenna has been selected as the best antenna design in section 4.3. It is the best suited antenna type that is able to meet the size requirements. Another alternative for the SATCOM system would be to utilise a grid phased array antenna. However, a grid array is not possible since it would not meet the size requirements due to the relatively low UHF band. A phased array antenna consisting of two vertically stacked egg-beater antenna could be considered as a viable alternative, as it would lower the high power signal transmission in directions other than the satellite. However, it would not completely mitigate the transmission constraint as the egg-beater antennas still have an omnidirectional radiation pattern. Therefore it can be concluded that with the current size requirements it is not feasible to fully resolve the constraint. Thus the constraint should be included in the operational considerations that are made during a mission.

Currently MOD is in the process of awarding contracts regarding the design and manufacturing of new submarines [35]. The impact of the size requirements on the design, and thus deployability of a UHF SATCOM system, can be useful information. The new submarine could be designed to accommodate a UHF phased array system that would enable steerable transmission to decrease the chance of detection.

It can be concluded that the prototype system will provide added value to submarine operations. Further iterations on the current design should be conducted to provide adequate data throughput and thus increase the deployability. What future work should be done to ensure the deployability of the SATCOM system is discussed in section 7.4 hereafter.

7.4. Recommendations and Future Work

In this section the required future work, along with a number of recommendations, will be discussed. The recommendations are divided into two categories: possible hardware changes to the antenna, and recommendations on testing and verification. First the hardware recommendations are listed.

- **Size deviation:** After manufacturing it was discovered that the antenna does not fully match the optimised design. To build the antenna as specified by the optimisation, the groove in the 3D design should be enlarged to accommodate the larger diameter of the wire. Furthermore, the amount of ABS used should be reduced to decrease the influence on the radiation pattern. Another option would be to consider different materials (e.g. Teflon) as the support structure material. Remanufacturing the antenna should lead to an improvement in performance as it will be closer to the optimised radiation pattern.
- **Reduce losses L-network:** The losses in the L-network are predicted to have a large influence on the antenna gain (i.e. upwards of 4 dB), as explained in section 6.3.1. The losses in the L-network can be mitigated using components with less internal resistance. It would be suggested to use SMD components and accommodate the L-network on a printed circuit board.
- **Position L-network:** The position of the L-network on the topside of the antenna ground plane disturbs the antenna radiation pattern. Thus the intended performance of the system is affected. It is suggested to relocate the L-network to the bottom side of the ground plane.
- **Duplexer:** Currently, the L-network is only capable of adjusting the impedance for a single frequency, in this case the downlink frequency. The uplink frequency differs from the downlink frequency. Therefore, uplink to Brik-II is currently not possible. Thus it is suggested to install a duplexer as this will enable bidirectional communication using a single connection. Therefore the impedance for both the uplink and downlink frequency can be matched.

The next part of the recommendations are the tests that should be conducted to reach the objective. The aforementioned hardware changes should be implemented before doing the recommended measurements. Otherwise the measurement and their associated conclusion are not valid.

- **Radiation pattern:** The radiation pattern measurement yielded inconclusive results. Since the radiation pattern is of great importance to the performance of the system, it should be characterised in more detail. The best way to measure the radiation pattern is by using an anechoic chamber. Because of the signal dampening material reflections are reduced, specifically ground reflections. Furthermore, in the conducted radiation pattern measurements the pattern was measured with steps of 10° in elevation, and 90° in azimuth. Using smaller step sizes should yield better insight into the radiation pattern. Since these facilities are designed for accurate antenna gain measurements, the equipment used is specifically made for this task. So the deviation due to measurement equipment inaccuracy is lower. With the measured radiation pattern a prediction can be made on the communication capabilities of the system. Furthermore, the MATLAB simulation used to optimise the antenna design can be verified.

- **Communication with satellite:** The strength of the signal received from the satellite should be measured. As discussed during in section 6.2.2 a LNA should be implemented. The received signal strength can be compared to the expected signal strength calculated by the simulation tool. If the signal strength corresponds to the predicted value, the assumption can be made that the tool provides an accurate simulation of reality.
- **Assembled system communication with satellite:** After the aforementioned validation tests, the submarine antenna should be combined with the RRS hardware. The assembled system should be subjected to full system functionality tests. The main goal is to characterise the communication capabilities of the submarine system with the SFP. This should be done by testing up and downlink data throughput for different passes. The operational deployability should be validated based on of the set requirements. Furthermore the test should help identify the limitations of the system.

Appendix 1

ID	Requirement	Explanation
RQ-P.1	The system shall be able to transmit and receive messages from the Brik-II satellite using the UHF band	
RQ-P.1.1	The system shall provide a minimum link budget of >1 Mb during a single pass under ideal conditions	The 1 Mb is set as a value which provide enough reason for the submarine to surface
RQ-P.1.2	The system shall provide an estimation of the link budget during a pass	
RQ-P.1.3	The system shall predict the chance of establishing contact during a certain period afloat (based on; The duration of submerging, the latest TLE information, and the time the submarine can stay afloat)	Since the submarine can be submerged for a long time the accuracy of the prediction can vary. To enable the submarine personnel to make an informed decisions if they want to surface, this information should be provided
RQ-P.1.4	The system shall be able to maintain communication capability for at least 3 months after last contact	The system should still be usable after being submerged for a relatively long period
RQ-P.1.5	The system shall be able to receive and sent message when afloat	
RQ-P.1.6	The system shall be able to contact the Brik-II satellite under swaying conditions of less then 10 °/s	
RQ-P.1.7	The system shall be able to operate in a frequency range of 250 to 340 MHz	The extra frequency range is required to provide flexibility.
RQ-P.1.8	The system shall only transmit high power signals in the direction of the satellite to limit detectability	The submarine can be located by the interception of transmitted signal. Therefore the system should limit the necessities of transmission
RQ-P.2	The system shall be design such that it shall fit on the sail in a temporary arrangement	The manual deployment ensures that the prototype can be tested and used quickly without full integration.
RQ-P.2.1	The system shall have a diameter <0.4 m and length of <1 m such that it can be carried up through the stairwell and hatch	
RQ-P.2.2	The system cables that connect the outdoor system to the indoor system shall run through the hatch and stairwell when the system is installed on the sail	The cables can not run through the pressure hall since this required further verification which will not be done for the prototype
RQ-P.2.3	The system shall be powered by the 110V system according to the MIL-STD-1399	
RQ-P.2.4	The system shall have a 19 inch server rack form factor with a limited depth of 40 cm	
RQ-P.2.5	The system shall consume less than 250 W of power during operations	
RQ-P.2.6	The system shall be a stand along system and will not interact with the on-board communication systems	On-board system are not allowed to interacted since this product will not be verified for communication with the submarine's systems
RQ-P.2.7	The system shall be integrated without the removal or reduction in operational functionality of other systems on-board	Multiple communication systems can be located within the communication mast. The current systems have to remain functional
RQ-P.2.8	The system shall not interfere with other communication systems installed	If other systems operate in the same frequency domain, they cannot communicate simultaneously
RQ-P.2.9	The system shall be removed from the sail and stored inside when submerged	
RQ-P.2.10	The system shall design such that it can be set-up within 5 minutes after surfacing	To ensure a short duration of surfacing as this is a vulnerable situation for the submarine The period is longer than the final system since the prototype has to be deployed by hand
RQ-P.3	The system shall have a Human Machine Interface	
RQ-P.3.1	The system shall have a screen to display information	
RQ-P.3.2	The system shall provide the satellite position, system status, GPS information, orbit information, possible system warnings, and contact status	
RQ-P.3.3	The system shall provide an interface from which a file can be selected for transmission	
RQ-P.3.4	The system shall consume less than 20 W of power during standby	
RQ-P.3.5	The interface shall be set-up such that it can be operated by an employee without an engineering background	
RQ-P.3.6	The system shall be rebootable within 5 minutes	
RQ-P.3.7	The system shall be able to store orbit parameters, file for transmission, error messages	
RQ-P.4	The system shall not be fully shock and water. The system shall posses minimal water resistance against precipitation.	As there might be spray from the waves or light rain
RQ-P.5	The system shall have a mass of less than 20 kg	The weight has been lowered since it would not be possible to carry a heavier system
RQ-P.6	The system shall be able to operate between a temperature of 0° to 45° Celsius	
RQ-P.7	The system shall be able to perform in light to medium sea conditions	The sea conditions are calmer since it deployment is not possible in heavy conditions
RQ-P.8	The system shall storable by hanging from the ceiling	

Table 7.1: System requirements prototype

Bibliography

[1] Ettus Research - USRP B205mini-i. Ettus Research, https://www.ettus.com/all-products/usrp-b205mini-i/, Visited: 23-08-2021.

[2] VBW and VBW Averaging. Keysight Technologies, https://rfmw.em.keysight.com/wireless/helpfiles/89600b/webhelp/subsystems/PowerSpectrum/Content/ps_VBW.htm, Visited: 26-10-2021.

[3] Monitoring Receiver Military and civil monitoring from 9 kHz to 3 GHz ITU-compliant measurements, . Rhode & Schwarz, https://www.valuetronics.com/pub/media/vti/datasheets/Rohde%20and%20Schwarz%20ESMB.pdf, Visited: 01-11-2021.

[4] SMA100A Signal Generator Specifications, . Rhode & Schwarz, https://scdn.rohde-schwarz.com/ur/pws/dl_downloads/dl_common_library/dl_brochures_and_datasheets/pdf_1/SMA100A_datsw_en_5213-6412-22_v0700.pdf, Visited: 01-10-2021.

[5] Satellite Eggbeater Antenna, 70cm band M2 Eb-432/rk70cm. Ham Radio Antenna, https://ham-radio-antenna.net/satellite_eggbeater_anttena_70cm_band_m2_eb_432_rk70cm.htm, Visited: 22-08-2021.

[6] MuRata Capacitor Data Sheet, . Murata Manufacturing, https://www.farnell.com/datasheets/2731080.pdf, Visited: 23-10-2021.

[7] LQW15CN96NJ00D - MuRata - Wirewound Inductor, . Farnell, https://nl.farnell.com/murata/lqw15cn96nj00d/inductor-96nh-5-choke/dp/2219315?st=murata%20rf%20coul%2096nh, Visited: 23-10-2021.

[8] FPV 5.8G 11dbi RHCP Polarization Helical Antenna. Ofvende, https://www.fvendedor.top/index.php?main_page=product_info&products_id=556849, Visited: 22-06-2021.

[9] Technical Considerations for Enabling a NATO-Centric Space Domain Common Operating Picture (COP). NORTH ATLANTIC TREATY ORGANIZATION STO TECHNICAL REPORT.

[10] Chassisdeel N (female) met flens. AmateurRadioShop.nl, https://www.amateurradioshop.nl/webshop/connectoren/rf-connectoren-en-adapters/detail/135/chassisdeel-n-female-met-flens.html, Visited: 11-10-2021.

[11] Material Selection In Radomes Design & Properties. Poly Fluoro LTD, https://polyfluoroltd.com/blog/polymer-radomes-radar-enclosures/, Visited: 04-10-2021.

[12] Vlooteenheden. Ministery Of Defense, https://www.defensie.nl/organisatie/marine/eenheden/schepen, Visited: 13-10-2021 .

[13] Onderzeeboten. Ministery Of Defense, https://www.defensie.nl/onderwerpen/materieel/schepen/onderzeeboten, Visited: 13-10-2021 .

[14] Everything You Need To Know About Electrical Insulation Tape. RS Components B.V, https://nl.rs-online.com/web/generalDisplay.html?id=ideas-and-advice/electrical-insulation-tape-guide, Visited: 27-09-2021.

[15] Vishay Variable Trimmer Capacitor 2 → 18pF 300V dc PTFE. RS Components, https://nl.rs-online.com/web/p/variable-trimmer-capacitors/0380236, Visited: 22-10-2021.

[16] Application of propagation predictions to Earth/space telecommunications system design. *Propagation Effects Handbook for Satellite Systems Design*, 1981. National Aeronautics and Space Administration, Chapter 7.

[17] Latitude, Longitude and Coordinate System Grids, 2001. GISGeography, https://gisgeography.com/latitude-longitude-coordinates/, Visited: 06-09-2021.

[18] TacSat-4 (Tactical Satellite-4), 2013. European Space Agency, https://earth.esa.int/web/eoportal/satellite-missions/t/tacsat-4, Visited: 22-08-2021.

[19] Grondslagen van het maritieme optreden, 2014. Ministry Of Defense, https://www.defensie.nl/binaries/defensie/documenten/publicaties/2014/02/13/grondslagen-van-het-maritieme-optreden-nederlandse-maritiemmilitaire-doctrine/GMO+digitaal.pdf, Visited: 12-10-2021.

[20] Verkenner onderwater; Het belang van de onderzeeboot als inlichtingensensor, 2016. Militaire Spectator, https://www.militairespectator.nl/thema/operaties/artikel/verkenner-onderwater, Visited: 12-10-2021.

[21] Minister van Defensie, 2021. Ministerie van Defensie, https://www.defensie.nl/organisatie/bestuursstaf/minister, Visited: 18-10-2021.

[22] List of VLF-transmitters, 2021. Military-History, https://military.wikia.org/wiki/List-of-VLF-transmitters, Visited: 16-09-2021.

[23] Mission Tubular Bells: Part One, 2021. Virgin Orbit, https://virginorbit.com/tubular-bells-1/, Visited: 16-10-2021.

[24] Aantallen personeel, 2021. Ministerie van Defensie, https://www.defensie.nl/onderwerpen/overdefensie/het-verhaal-van-defensie/aantallen-personeel, Visited: 18-10-2021.

[25] Sherif H. Abdelhalem, Prasad S. Gudem, and Lawrence E. Larson. Tunable CMOS integrated duplexer with antenna impedance tracking and high isolation in the transmit and receive bands. *IEEE Transactions on Microwave Theory and Techniques*, 62:2092–2104, 2014. ISSN 00189480. doi: 10.1109/TMTT.2014.2338271.

[26] G.P. Bouten. Literature Study Royal Netherlands Air Force Section Space, 2021. TU Delft.

[27] *SCCC—SUMMARY OF DEFINITION AND PERFORMANCE*. Consultative Committee for Space Data Systems, Washington, DC, USA, ccsds 130.11-g-1 edition, 2019. CCSDS Secretariat, National Aeronautics and Space Administration.

[28] Damon DeLuca. SGP4 Orbit Propagator with GUI, 2018. MathWorks File Exhange, https://www.mathworks.com/matlabcentral/fileexchange/55179-sgp4-orbit-propagator-with-gui, Visited: 26-08-2021.

[29] Kiruthika Devaraj, Matt Ligon, Eric Blossom, Joseph Breu, Bryan Klofas, Kyle Colton, and Ryan Kingsbury. Planet High Speed Radio: Crossing Gbps from a 3U CubeSat. *Small Satellite Conference*, 8 2019. https://digitalcommons.usu.edu/smallsat/2019/all2019/106.

[30] S.W. Ellingson, R. Browder, and A. Walz. *Electromagnetics, Volume 1*. Virginia Tech University Libraries, 2018. ISBN 9780997920185.

[31] E. E. Weaver E. F. Duffy F. L. Cain, B. J. Cown. EFFECTS OF NEAR-FIELD OBSTACLES ON FAR-FIELD ANTENNA PERFORMANCE CHARACTERISTICS. 1975. doi: 10.1109/ISEMC.1975.7567868.

[32] United States Space Force. About the Unites States Space Force, 2019. https://www.spaceforce.mil/About-Us/About-Space-Force/, Visited: 02-11-2021.

[33] L.E. Frenzel. HOW PHASED ARRAY ANTENNAS WORK, 2018. Nuts and Volts, https://www.nutsvolts.com/magazine/article/how-phased-array-antennas-work, Visited: 06-09-2021.

[34] C. Fuchs, C. Schmidt, F. Moll, Dirk Giggenbach, and A. Shrestha. System aspects of optical LEO-to-ground links. *SPIE*, 10562:105625N, 9 2017. ISSN 1996756X. doi: 10.1117/12.2296054.

[35] Nathan Gain. Latest Update On The Netherlands' Walrus-Class Submarine Replacement Program, 2021. NavelNews, https://www.navalnews.com/naval-news/2021/05/latest-update-on-the-netherlands-walrus-class-submarine-replacement-program/, Visited: 06-12-2021.

[36] V.K. Garg. *Wireless Communication & Networking*. Elsevier Inc, 2007.

[37] A. Goldsmith. *Wireless Communication*. Cambridge University Press, first edition, 2005. ISBN 9781520837063.

[38] Dr. Anitha Govind. Antenna Impedance Matching – Simplified. Abracon, https://abracon.com/uploads/resources/Abracon-White-Paper-Antenna-Impedance-Matching.pdf, Visited: 08-10-2021.

[39] Leland H. Hemming and Raymon A. Heaton. Antenna Gain Calibration on a Ground Reflection Range. *IEEE Transactions on Antennas and Propagation*, 21:532–538, 1973. ISSN 15582221. doi: 10.1109/TAP.1973.1140538.

[40] *Allowable short-term error performance for a satellite hypothetical reference digital path*. International Telecommunication Union (ITU), Place des Nations 1211 Geneva 20 Switzerland, s.2099-0 edition, 2016.

[41] *Attenuation by atmospheric gases and related effects*. International Telecommunication Union (ITU), Place des Nations 1211 Geneva 20 Switzerland, p.676-12 edition, 2019.

[42] Kaya Kanemaru and Hirohiko Masunaga. A Satellite Study of the Relationship between Sea Surface Temperature and Column Water Vapor over Tropical and Subtropical Oceans. *Journal of Climate*, 26:4204–4218, 6 2013. ISSN 0894-8755. doi: 10.1175/JCLI-D-12-00307.1.

[43] J. Karremann. Wat zijn de taken van onderzeeboten?, 2011. Marineschepen.nl, https://marineschepen.nl/onderzeeboot-taken.html, Visited: 13-10-2021.

[44] J. Karremann. Walrusklasse onderzeeboten, 2021. Marineschepen.nl, https://marineschepen.nl/schepen/walrus.html, Visited: 13-10-2021.

[45] John D. Kraus. The Helical Antenna. *Proceedings of the IRE*, 37:263–272, 1949. ISSN 00968390. doi: 10.1109/JRPROC.1949.231279.

[46] Dun Wei Liao, Xin Yi Wang, Bo Zhou, and Feng Wei. A novel impedance matching method of helix antenna. *undefined*, 2:771–773, 11 2016. doi: 10.1109/ICMMT.2016.7762437.

[47] Fernando Aguado Marcos Arias. *Small Satellite Link Budget Calculation*. International Telecommunication Union (ITU), 2016. International Telecommunication Union (ITU).

[48] Adam Narbudowicz, Suramate Chalermwisutkul, Ping Jack Soh, Mohd Faizal Jamlos, and Max J. Ammann. Compact UHF Antenna Utilizing CubeSat's Characteristic Modes. In *2019 13th European Conference on Antennas and Propagation (EuCAP)*, pages 1–3, 2019.

[49] Karen Northon. Record Number of Americans Apply to Be An Astronaut at NASA, 2016. NASA, https://www.nasa.gov/press-release/record-number-of-americans-apply-to-beanastronaut-at-nasa, Visited: 23-11-2021.

[50] H.Y. Oei. Brik-II S/C Antenna measurement campagne, 2020. ISIS - Innovative Solutions In Space.

[51] B.A. Oving. Store & Forward Ground-Space (RRS-SFP) Interface Control Document. Logistiek Centrum Woensdrecht 982SQN T&MO.

[52] Enrique G. Plaza, German Leon, Susana Loredo, and Luis F. Herran. Calculating the Phase Center of an Antenna: A Simple Experimental Method Based on Linear Near-Field Measurements. *IEEE Antennas and Propagation Magazine*, 59, 10 2017. ISSN 10459243. doi: 10.1109/MAP.2017.2731209.

[53] B. Podsiadły, A. Skalski, B. Wałpuski, P. Walter, M. Słoma, B. Podsiadły, A. Skalski, B. Wałpuski, P. Walter, and M. Słoma. Electrically conductive acrylonitrile butadiene styrene(ABS)/copper composite filament for fused deposition modeling. *SPIE*, 10808:1080856, 10 2018. ISSN 1996756X. doi: 10.1117/12.2501546. https://ui.adsabs.harvard.edu/abs/2018SPIE10808E..56P/abstract.

[54] Mark L. Psiaki, Brady W. O'Hanlon, Jahshan A. Bhatti, Daniel P. Shepard, and Todd E. Humphreys. GPS Spoofing Detection via Dual-Receiver Correlation of Military Signals. *IEEE Transactions on Aerospace and Electronic Systems*, 49(4):2250–2267, 2013. doi: 10.1109/TAES.2013.6621814.

[55] Ashaad Rambharos. *Satellite Communications*. Intelsat, 2014.

[56] Edward J. Rice. Multimodal Far-Field Acoustic Radiation Pattern Using Mode Cutoff Ratio. *https://doi.org/10.2514/3.60984*, 16:906–911, 5 2012. ISSN 00011452. doi: 10.2514/3.60984. https://arc.aiaa.org/doi/abs/10.2514/3.60984.

[57] Sayan Roy, Sayeed Sajal, and Benjamin D. Braaten. A phase correction technique based on spatial movements of antennas in real-time for designing self-adapting conformal array antennas. *Microwave and Optical Technology Letters*, 59:3002–3010, 12 2017. ISSN 10982760. doi: 10.1002/MOP.30861.

[58] Jairam Sankar. Different Types of Radio Antennas. Electronicsforu, https://www.electronicsforu.com/resources/radio-antennas-types, Visited: 07-08-2021.

[59] John S. Seybold. Introduction to RF Propagation. *Introduction to RF Propagation*, pages 1–330, 9 2005. doi: 10.1002/0471743690. https://onlinelibrary.wiley.com/doi/book/10.1002/0471743690.

[60] Tolga Soyata, Lucian Copeland, and Wendi Heinzelman. RF Energy Harvesting for Embedded Systems: A Survey of Tradeoffs and Methodology. *IEEE Circuits and Systems Magazine*, 16: 22–57, 02 2016. doi: 10.1109/MCAS.2015.2510198.

[61] Kerry Stevenson. 3M Enters 3D Printing Market With Printable PTFE Service. Fabbaloo, hhttps://www.fabbaloo.com/2019/11/3m-enters-3d-printing-market-with-printable-ptfe-service, Visited: 07-10-2021.

[62] G.J.TH. Netjes U.N. Berrevoets. Militaire Satellite Communicatie, 2015. Ministry Of Defense, https://vovklict.nl/intercom/2014/3/46.pdf, Visited: 24-11-2021.

[63] David Vallado. Astrodynamics Software, 2020. CelesTrak, https://celestrak.com/software/vallado-sw.php, Visited: 08-08-2021.

[64] D.B. Verhaard. System design document. BRIK-II: Remote Radio Station. Logistiek Centrum Woensdrecht 982SQN T&MO.

[65] B.A Vvedenskij. On Radio Communications via Ultra-Short Waves. *Theoretical and Experimental Electrical Engineering*, page 447–451, 12 1928.

[66] Ravindra Kumar Yadav, Ravindra Kumar Yadav, Jugul Kishor, and Ram Lal Yadava. Effects of Temperature Variations on Microstrip Antenna. *International Journal of Networks and Communications*, 2013:21–24, 2013. doi: 10.5923/j.ijnc.20130301.03. http://journal.sapub.org/ijnc.

[67] Z. N. Yin and T. J. Wang. Deformation of PC/ABS alloys at elevated temperatures and high strain rates. *Materials Science and Engineering: A*, 494:304–313, 10 2008. ISSN 0921-5093. doi: 10.1016/J.MSEA.2008.05.039.

[68] Victor Zakharov, Yury Yasyukevich, and Mari Titova. Effect of magnetic storms and substorms on GPS slips at high latitudes. *Cosmic Research*, 54:20–30, 2016. doi: 10.1134/S0010952516010147.